ASSESSMENT OF THE USE OF GROUNDWATER FOR IRRIGATION IN THE SOUTHERN PART OF LAKE NAIVASHA, KENYA.

Richard Oppong-Boateng

February 2001.

ASSESSMENT OF THE USE OF GROUNDWATER FOR IRRIGATION IN THE SOUTHERN PART OF LAKE NAIVASHA, KENYA.

By

Richard Oppong-Boateng

Thesis submitted to the International Institute for Aerospace Survey and Earth Sciences in partial fulfilment of the requirements for the degree of Master of Science in Groundwater Resources Evaluation and Environmental Management

Degree Assessment Board

Prof. Dr. A. M. J. Meijerink, Chairman (Head, WRS Division)

External Examiner: Prof. Dr. G. P. Kruseman, TNO, Delft.

Supervisor: Drs. Robert Becht (ITC, Enschede)

Member: Drs. D. Kovacs (ITC, Enschede)

INTERNATIONAL INSTITUTE FOR AEROSPACE SURVEY AND EARTH SCIENCES

ENSCHEDE, THE NETHERLAND

CHAPTER 1

1 INTRODUCTION

1.1 GENERAL

Groundwater plays a vital role in the economy of Kenya. The demand for this resource in the field of agriculture, energy and other purposes has been on ascendancy, as it acts as the major source of water for the country's over-increasing agricultural industry as well as the rural population domestic use.

It has been a major concern coupled with growing economic development, to ensure that water is made available in any form being surface or groundwater for agriculture and other purposes for which it is intended.

This led to the establishment of an Irrigation Development Plan called 'The National Water Master Plan' by the Kenyan Government in the 1980's to tap its abundant groundwater resources for its over-increasing agricultural industry which contributes 20% of its Gross Domestic Product (GDP). Kenya is estimated to have total irrigation potential of 352,400 hectares but only 625 hectares (representing about 1%) of the total water managed area of 73,025 hectares are irrigated from groundwater, with the remaining areas supplied with water from streams and storage reservoirs.

Having proposed to develop 1000 hectares of smallholder irrigation schemes annually, the objectives of the 'Water Master Plan' could not be achieved and on average managed between 200-300 hectares per year, leading to under-utilising of groundwater resources and irrigation land potential. However, of the 19% of the potential areas equipped for irrigation, the greater part is located along the Lake Naivasha basin, where irrigated agriculture with modern and sophisticated irrigation systems are being used to pump water from the Lake and shallow wells along the basin.

The groundwater outflow which is in the order of $56*10^6$ m^3/yr (Ase et. al., 1986) from the Lake towards the southern part of the basin. This could therefore be harnessed for irrigation to reduce the Lake water abstraction and its subsequent negative impacts on the dynamism between the Lake and the shallow groundwater flow system.

Groundwater development schemes for irrigation in the south of the lake Naivasha are being undertaken even though the source and amount of replenishment to the underlying aquifers having been ascertained.

In conclusion, the use of groundwater for irrigated agriculture can be effectively evaluated, harnessed and sustained by assessing the groundwater flow pattern, geochemistry, water balance as well as the interaction between the freshwater lake and shallow groundwater system in the study area.

1.2 PROBLEM FORMULATION

The use of groundwater for irrigation in the south of the Lake Naivasha requires to a greater extent the understanding of the water movement in the sub-surface in terms of the relationships between the lake and groundwater flow system and quality of groundwater in the study area.

This has been the cause of the major setbacks or problems that have persisted over the years in evaluating and assessing the use of the groundwater in the south of the lake for irrigation.

The outflow from the lake to the south has been estimated to be in the order of $56*10^6$ m^3/yr, but the flow pattern and quality for irrigation have still not been clearly established to warrant the usage of groundwater in the area for irrigated agriculture.

It has been revealed from previous studies that the use of the lake water for Irrigated agriculture has contributed immensely to the decline in the level of the lake Naivasha. One key issue is the effect of water abstraction on the lake levels with the area under irrigation steadily increasing since 1980.

Environmental Science of Australia (1992) in an Environmental Impact Assessment Study in the area, estimated that about $59*10^6 m^3$/yr of water is taken from the Lake for irrigation, which is far above the quota of $30*10^6 m^3$/yr. This withdrawal, it concluded as being approximately twice the outflow value of $34*10^6 m^3$/yr McCann (1974) and equivalent to other values postulated by other researchers from the Lake Naivasha to the southern part.

Detailed studies into the use of groundwater in the southern part for irrigation purposes have not been effectively conducted and as such, the resources have not been fully evaluated and harnessed to supplement the surface and groundwater irrigation schemes along shoreline of the lake Naivasha.

1.3 IMPORTANCE OF STUDY

The growing importance of groundwater for irrigation cannot be over-emphasised. Its optimal use requires the development of this sub-surface system of the hydrologic cycle and to identify the sources of recharge as well as the quality.

By integrating the use of groundwater into irrigated agriculture in the southern part of the basin, there will always be water available in quantity and quality in case of drought, which often results to some extent failure and inefficiencies in most surface-water irrigation schemes, as was experienced recently.

With most of the water users having reached their quota of $30* 10^6 m^3$/yr (ESA, 1992) of the lake water and having a great deal of land for agriculture, supplementing this with groundwater is seen as the only possible means to keep their agricultural activities functioning.

This will go a long way to replenish the decrease in water availability for agriculture owing to rapid industrialisation and ever-increasing municipal needs of the lake water and also safeguard the overall irrigation efficiency to meet all year round crop water requirements.

To meet this challenge, it was envisaged that detailed studies be conducted to evaluate the use groundwater for maximising crop production without affecting the groundwater flow patterns and dynamism between the lake and shallow groundwater system.

The outflow from the Lake Naivasha having been estimated to be in the order of $46\text{-}56*10^6$ m^3/yr it is therefore expedient to make use of this underground seepage, rather than concentrating all the massive and sophisticated agricultural activities within the vicinity of the lake Naivasha. For irrigated agriculture to be sustainable in the south of the lake, it is expedient that the location of the source of recharge, flow direction, quantity and quality of the subsurface outflow from the lake should be ascertained.

This could be useful for the management of underlying aquifers to meet the increasing demand of the groundwater resources and address environmental issue which often leads to over-exploitation of the lake water resources by the change of the groundwater chemistry and flow pattern.

To meet these challenges, hydrogeological, hydrochemical and isotopic studies are therefore necessary for a viable long-term assessment and development of the sustainability and suitability of the groundwater for irrigated agriculture. These give in-depth knowledge into the identification of the recharge source, quantities and flow direction of the groundwater flow system.

In conclusion, striking a balance between groundwater and Lake Water use for all year round agricultural activities or cropping requires thorough assessment of the groundwater flow system, recharge and hydrogeochemistry of the groundwater resources.

1.4 OBJECTIVES OF RESEARCH STUDY

1.4.1 MAIN OBJECTIVE

The main objective of the study is to evaluate the sustainability and quality of groundwater for irrigation.

1.4.2 SPECIFIC OBJECTIVES

The specific objectives are:

- To determine the flow direction and source of recharge of the shallow groundwater system.
- To determine the characteristics or properties of the underlying aquifers.
- To determine the amount of recharge to the groundwater system.
- To determine the quality of groundwater.
- To characterise the quality of groundwater based on their chemistry into irrigation water quality.

1.5 RESEARCH APPROACHES

Four approaches were adopted to meet strictly the objective of the study and they are elaborated as follows:

1.5.1 HYDROGEOLOGICAL APPROACH

- To determine the Properties of underlying aquifers from Aquifer test pumping analysis.
- To quantify the contribution of groundwater as potential source of water for Irrigation.
- To estimate recharge of groundwater from climatic data.

1.5.2 HYDROCHEMICAL APPROACH

- To assess the quality of groundwater based on their chemistry.
- To characterised groundwater based on their chemistry into irrigation water standards with emphasis on sodium absorption ratio (SAR), Exchangeable sodium ratio (ESR) and other parameters.
- To assess the impact of the water with high TDS, SAR, ESP, CEC etc on the soils structure.

1.5.3 ISOTOPIC APPROACH

- To assess the flow pattern of groundwater through the underlying aquifers.
- To determine the origin of the shallow groundwater system.
- To determine the extent of mixing and residence times of groundwater.

1.5.4 STATISTICAL AND GEOSTATISTICAL APPROACHES

- To determine the extent of correlation between the chemical variables.
- To determine the chemical pattern of groundwater by interpolation in GIS environment.

1.6 LITERATURE REVIEW

Research study on Lake Naivasha and it's environs dates back to about 60 years ago. Since that time, numerous studies have been executed by various researchers into the hydro-geological and hydrological aspects of the basin as well as the groundwater quality in the vicinity of the Lake.

However, the studies that have been conducted so far did not lay much emphasis on the use of the groundwater resources in the south of the Lake Naivasha for Irrigation in terms of the sustainability and quality but mainly touched on its use for Geo-thermal energy generation by KenGen. These studies were undertaken in collaboration with the Kenyan government and the Governments of the Consulting agencies on the other hand as a result of a memorandum of understanding between the two bodies.

The University of Leicester groups with counterparts from the University of Nairobi investigated into the groundwater chemistry of the shallow aquifers and indicated that boreholes in the vicinity of the lake have different characteristics from the lake water. They also concluded that the major ions of groundwater reflect the complex volcanic geology of the Naivasha area.

Morgan (1998) in her study on Groundwater chemistry in the Naivasha area, explained that the quality of groundwater has deteriorated due to high level of nitrate from agricultural activities as well as high level of fluoride.

Melack and Gaudet (1981) in the study on Major ion chemistry in the tropical African basin (Naivasha) area estimated the amount of water loss by seepage from lake Naivasha as 5 (1973), 11(1974) and 20%(1975) of the total water loss. In terms of chemical composition, they postulated the waters to be of predominantly sodium, calcium, and bicarbonate, chloride, Magnesium and total dissolved solids. With direct measurements of seepage in near shore shallows, they indicated that water enters the lake via groundwater seepage in the North and leaves the lake in the southern portion.

The Environmental Science of Australia (1992) in an Environmental Impact Assessment Study in the area estimated that about $59*10^6 m^3$/yr of water is taken from the lake for irrigation which is far above the quota of $30*10^6 m^3$/yr. This withdrawal it concluded as been twice ($34*10^6 m^3$/yr by McCann, 1974) the outflow from the lake to the southern part of it and equivalent to values postulated by other researchers.

Darling, Allen and Armannsson (1989) used stable isotopes to indirectly detect the subsurface outflow. The stable isotope data confirmed that much of the steam used by the Olkaria geothermal power station is derived from the lake water but from simple balance they stated that the decline in the lake level cannot be attributed to the steam use at the Olkaria Geothermal Plant.

Darling et al (1990) and Darling, Gizaw and Arusei (1996) used stable isotopic techniques to evaluate the Lake-groundwater relationship and fluid-rock interaction in the rift valley. They indirectly determined the directions of subsurface outflow from the lake and traced the lake water to a distance of about 30km South of the Lake at the Suswa volcano.

The Ministry of energy and the British geological survey in joint studies used isotopic techniques to estimate groundwater recharge and chemistry in deep well for geothermal power. Also KenGen scientists (Omenda et. al.) based at the Olkaria geothermal continue investigations into the relationship between the shallow water resources and the deep geothermal field.

Ojiambo (1992,1996) in his studies indicated that the main subsurface outflow originates from the intersection of Oloidian bay and estimated the outflow from the lake to be ranging from $18*10^6 m^3$ to $50*10^6 m^3$/yr. He found out that the stable isotope concentrations of the geothermal reservoir fluids to be lighter than that of Lake Naivasha but heavier than precipitation and groundwater. Likewise, the mixing of deep geothermal waters with shallow groundwater and Lake Naivasha was found to be the recharge source of the Olkaria geothermal reservoir.

Further outflow studies suggest the following: (Sikes, 1953) came out with an outflow of $43*10^6 m^3$/yr. from estimates of monthly and annual water budget for the lake based on river gauging and

evaporation rate measurements. (Ase et. al., 1986) quoted a value of 46-56*10^6 m^3/yr using underground seepage theory and (Mecca, 1974) estimated the outflow to be 34*10^6 m^3 /yr. from water budget studies and finally (Mmbui, 1998) estimated outflow rate of 4.6*10^6 m^3/month in his M.Sc research study.

1.7 BACKGROUND DATA

- Groundwater analysis of boreholes and wells by the University of Leicester 1996.
- Groundwater analysis of boreholes and wells from the Ministry of Land Reclamation, Regional and Water Development-Water Resources Division, Nairobi 1943-1995.
- Isotope data analysis of Lake Naivasha, geothermal well and boreholes by the British Geological Survey 1996.
- Isotope data analysis by Ojiambo (1992,1996)
- Aerial photographs 1:50000 and 1:12500
- Topographical map 1:50000
- Geological map 1:10000
- Landsat image: bands 3,4 and 5 taken in January 1996.
- Landsat image: bands 1-6 taken in June 2000.
- Exploratory soil map 1:1000000 in 1980.

1.8 METHODOLOGY

The methodology is in three stages and was executed in line with the objective of the research. It is elaborated in details below:

1.8.1 PRE-FIELDWORK

- **Identification and analysis of available information prior to fieldwork.**
  - ♦ Selection of appropriate wells and their parameters.
  - ♦ Consulting with isotope centres for isotopic analysis.
  - ♦ Extraction of information from previous works (Literature review).
  - ♦ Image processing and information extraction using GIS methods.

1.8.2 FIELDWORK

- **Field observations and data collection.**
  - ♦ Hydrogeological data collection and mapping to verify wells locations and elevations with GPS.
  - ♦ Measurement of physical parameters such as pH, Ec and water level in wells.
  - ♦ Water sampling and analysis for chemical constituents (Alkalinity, Total hardness and Chloride).
  - ♦ Groundwater sampling for isotopic analysis.

1.8.3 POST FIELDWORK

- **Data analysis and Conclusions.**

♦ Hydrogeological assessment on groundwater sustainability.

♦ Hydrochemical assessment of the quality of groundwater.

♦ Isotopic analysis and assessment of groundwater recharge and flow pattern.

♦ NETPATH mixing and hydrodynamic modelling.

♦ Interpretation of results and conclusions.

♦ Recommendations, if any.

1.9 RESEARCH QUESTIONS

1.Will isotopic hydrogeochemistry provide sufficient evidence and insight into the flow pattern, direction and origin of the shallow groundwater system in the south of the Lake Naivasha?

2. Is the groundwater in the south of the lake Naivasha of good quality for irrigation?

3.Will the use of groundwater for Irrigation in the south of the Lake Naivasha conflicts the dynamism between the lake and shallow groundwater flow system?

4.Will the over-increasing demands of groundwater for Irrigation give rise to the sustainable use of the groundwater resources?

1.10 OUTLINE OF THESIS

Chapter 1: This is the introductory chapter. In this chapter, the Problem formulation, Importance, Objectives of the research study and Literature review are elaborated.

Chapter 2: This focuses on the Description of the study area (National and Local settings) in terms of Basic information such as Location, Climate, Geomorphology, Geology and Hydrogeology.

Chapter 3: This chapter deals with the hydrogeological aspects based on pumping test evaluation, groundwater flow from piezometric map and Thermodynamics. The estimation of groundwater flux to the underlying aquifer as well as geophysical investigations into the extent of underlying aquifers has been discussed. Various cross sections have been constructed to verify the possible subsurface flow from the Lake Naivasha into the shallow and deep groundwater system.

Chapter 4: This chapter deals with the Hydrogeochemistry and emphasises on the suitability of groundwater for irrigation from the perspective of sodium absorption ratio (SAR), electrical conductivity (Ec) hazards.

Chapter 5: This focuses on the use of Statistical and Geostatistical methods to determine respectively the correlation and spatial variability of the chemical variables. The end product of statistic method was used to determine the coefficient of correlation amongst the various chemical variables. Indicator Variograms were plotted in GIS environment using Ilwis software program.

Chapter 6: It deals with isotope geochemistry into the origin of the shallow groundwater in the study area using stable and radioactive isotope of Oxygen, Hydrogen and Carbon of five datasets. The various plots of Deuterium and Oxygen-18 have been constructed and used to extensively determine the origin or recharge source of groundwater south of the Lake Naivasha.

Chapter 7: This deals with the NETPATH mixing and hydrodynamic modelling, to estimate the contribution of Lake Naivasha to the groundwater flow system as well as the residence time of groundwater into the shallow wells and deep geothermal wells.

Chapter 8: This chapter incorporates the conclusions and recommendations based on outcome of all the findings envisaged in all the analysis.

CHAPTER 2

2 DESCRIPTION OF STUDY AREA

2.1 REGIONAL SETTING

2.1.1 LAND AREA AND IRRIGATION POTENTIAL

Kenya is situated on the East Coast of Africa and has a total land area of 580370km^2. Cultivable land is estimated at about 57 million hectares, which is 98% of the total land area. However, only about 10 million hectares are classified as high to medium potential land. The cultivated area was estimated to be 3.7 million hectares in 1989,which is 38% of the high to medium potential cultivable land and made up of 6.4% of the area of the country.

The total population is 30 million (1999 statistics) and the leading sector in the national economy is agriculture which accounted for 30% of Gross Domestic Product, GDP (1988).

Area of country	580370 km^2
Total population	30,000,000
Population density	52 inhab/km^2
Rural population	47 inhab/km^2
Cultivable land	9936000 ha
Cultivated land	3738105 ha

Table 1: Basic statistics on Kenya.

2.1.2 SURFACE AND GROUNDWATER RESOURCES

The internal surface water resources have been estimated at 20.2km^3 per year from the 5 main drainage basins: Lake Victoria, the rift valley, Athi river, Tana River and Ewaso Ngiro. There are 17 major dams with a total storage capacity of 4.06km^3, 660 small dams and 41 subsurface dams with an estimated storage of 0.0047km^3. The potential yield from groundwater has been estimated to be 0.315km^3 per year and 68% of this yield is ascribed to shallow wells.

2.1.3 TROPICAL CLIMATE OF KENYA

Kenya lies within a semi-arid and arid climatic region in the eastern horn of Africa. Approximately 80% of the land are classified as semi-arid or arid .The difference in climate is quite distinct. The movement of the inter-tropical convergence zone (ITCZ) provides two rainy seasons, which is followed by a dry season.

The first rainy season starts from March till May and the second from October to November thus for three (3) months duration each, with the first season considered long and intensive rainy season while the second is short and less intensive.

The rainfall is considerable but more than 1500mm/year at the edges of the rift valley and decreases rapidly to under 200mm/year in the valley bottom. The dry seasons occur intermittently between the two rainy seasons from January to February and from July to September.

2.2 LOCAL SETTING

2.2.1 LOCATION OF STUDY AREA

The study area lies in the Eastern Kenyan rift valley province and located in the Naivasha Division of Nakuru District at approximately 100km from Nairobi, the capital city of Kenya. It lies within the UTM zone 37 and coordinates:

X_{max} =221000, X_{min}=190000

Y_{max}=9934000, Y_{min}=9907000

Thus, it is bounded by latitude 0°49′ S and 0°52′ S and longitude36°18′ E and 36°21′ E. The study area is located in the central portion of the rift floor at a mean altitude of 1885m above mean sea level. It is surrounded by the Lake Nakuru-Naivasha highlands, with decreasing altitude from the North towards the South. The location of study area is depicted in figure 2.

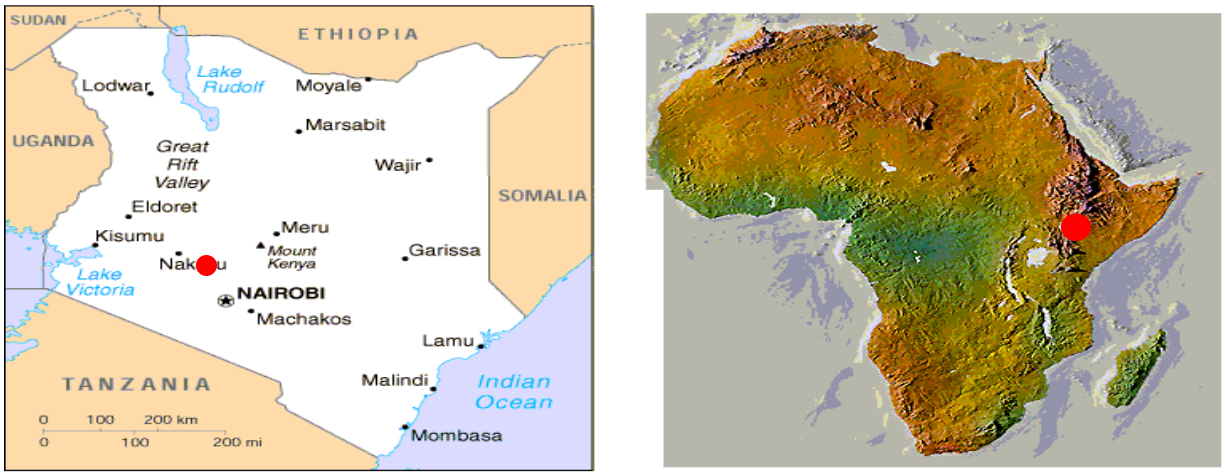

Figure 1: Location maps of the study area (National and Continental).

2.2.2 RAINFALL PATTERN

There are primarily two periods of rainfall per year, being seasonal and the pattern is similar to other parts of the country. The long term average annual rainfall shows variation in descending order from 1279mm/year in the first period (March-May) to 598mm/yr in the second period (October-November). Annual values of precipitation in the hilly areas are high, ranging from 1250mm to 1500mm with similar or lower rates of evapo-transpiration while the lower rainfall values average 430mm at Magani and 930mm at Nakuru for the valley floor (Clarke et al 1990).

The highlands surrounding the drainage basin receive more rain than the lake and valley floor and provide most of the water that maintains the lake. The average annual rainfall is estimated to be about 667mm/year and 650mm/year for the period of 1931-1960 by (Lars-Eric, 1986) and (Wiberg, 1976) respectively.

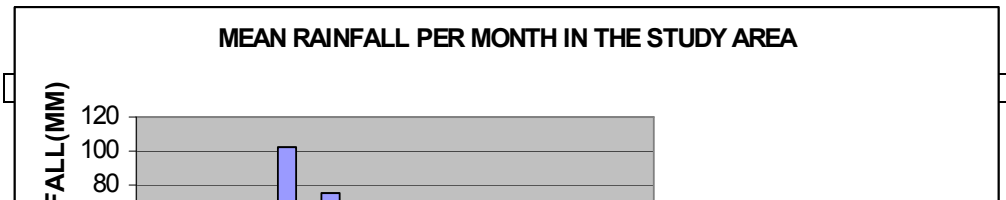

Figure 2: Bar chart of Mean Monthly Rainfall in the study area.

2.2.3 TEMPERATURE AND EVAPORATION

The temperature in the vicinity of Nakuru is relatively stable, with the mean maximum monthly temperatures varying between 17°C and 20°C. The warmest periods are from January to March with the mean maximum of 29°C recorded in February. The coldest periods are from the months of July to August and the mean minimum temperature of 10°C recorded in January. The mean annual temperature of 18°C is often recorded.

Due to hot, dry and windy climate in the Naivasha section of the Gregory rift rains, evaporation increases each month after April. This is responsible for the annual evaporation loss exceeding the rainfall by a factor of two. Low relative humidity and an average daily maximum temperature of 25°C tend to cause annual potential evaporation of 1500-1900mm/yr (Ase et al., 1986) far in excess of rainfall.

There is therefore very little spatial variation but this often differ seasonally where at times potential evapotranspiration is highest during the dry periods and lowest in the rainy periods. This is due to the fact that rainy periods are characterised by high relative humidity.

Evapotranspiration is notably higher in areas where there is little soil cover and low rainfall and less in dense thick vegetation and higher rainfall areas.

Month	Jan	Feb	Mar	Apr	May	Jun	Jul	Aug	Sep	Oct	Nov	Dec
Evapo(mm)	188	185	193	138	131	122	123	128	139	131	119	155

Table 2: Monthly evaporation data from 1955-1990 (Nakuru).

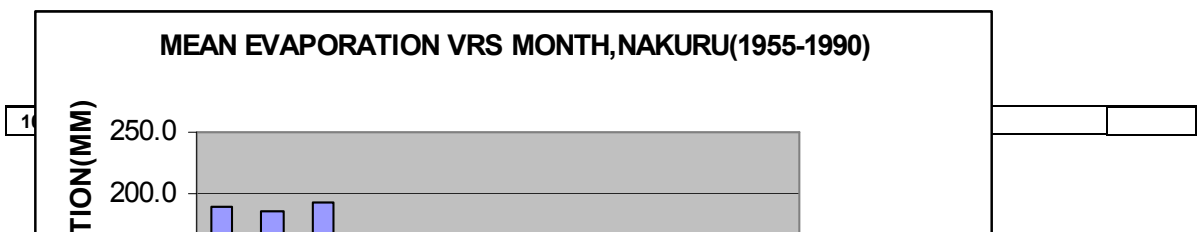

Figure 3: Bar chart of Mean Monthly Evaporation (1955-1990).

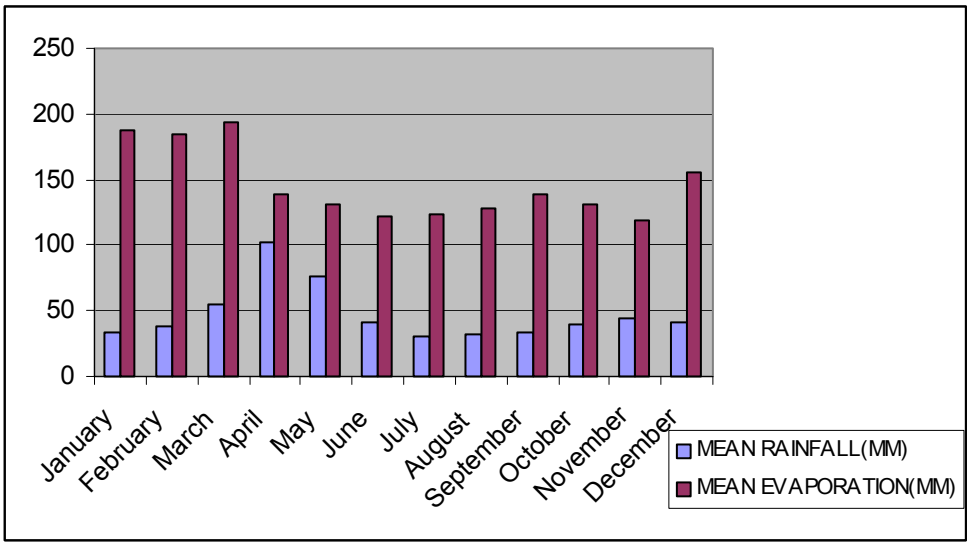

Figure 4: Bar chart of Mean Rainfall and Evaporation.

2.2.4 DRAINAGE NETWORK

There are a lot of rivers that discharge into the Naivasha basin. The main rivers are the Gilgil (420km^2 watershed), Karati and Malewa (1750km^2 watershed). The rains on the Aberdare mountains and Kinangop plateau maintains the perennial flow in the Malewa River. The Malewa and Gilgil drain from the northern part of the catchment whiles the Karati River drains from the northeastern part. Flow in the Karati River and other streams are seasonal and at times do not reach the lake as surface water.

The Malewa River accounts for about 90% of the river discharge into Lake Naivasha. There are also small streams that flow westwards and develop into four main tributaries, the Mugutyu, Kitiri, Makungi and Turasha. The later is the most important tributary and joins River Malewa at approximately 8km east of Gilgil. The tributaries of the Malewa river form a very dense dendritic drainage pattern and but have a radial pattern in the Kipipiri area as a result of the conical shape of the volcano in the vicinity. Streams in the western part of the basin disappear in the rift before reaching the Lake.

2.2.5 VEGETATION

The vegetation in the flat areas are mainly bushes and savannah. However, due to the diversity within the lake Naivasha basin all sorts of vegetation are found within the vicinity. The northern parts of the basin near the source of the Malewa River are boarded by tropical evergreen forest. Along the slopes of the rift valley is tropical grassland, which ranges into bushland typical of the rift floor.

The vegetation within the rift having a semi-arid character and high potential rangeland for grazing purposes. The exceptional case is recognised in mountainous areas where tropical rain forests are prominent. Engulfing the lake Naivasha are acacia trees, woodland with trees which are as high as 35m tall and the drainage basin serve as polders for grazing.

2.2.6 SOILS

Soil surveys have extensively been carried out in the area with each having fairly different level of detail. The soils are derived basically from weathered volcanic and basement rock system and occupying the floor of the rift valley in Naivasha (Ongweny, 1973) as light grey or brown to pinkish non-calcareous soils.

In the high areas of the catchment, there are non-calcareous black or grey soils overlying yellow-brown compact sub-soils with iron concretion. The soils in the Aberdare mountains, Kinangop plateau and the source of the Malewa river are young soils with predominantly morillonite clays (Rachillo, 1977). At the edges of the lake, the soil is less alkaline and more liable to crack during drying (Gaudet, 1977) whiles those along the north shore above the lake are generally high in exchangeable Na^+ and K^+ (Makin, 1967).

2.3 GEOLOGICAL AND HYDROGEOLOGICAL SETTINGS

2.3.1 GEOLOGICAL SETTING

The geology of the area is generally made of volcanic rocks and lacustrine deposits. In the basin are complex geological structures, which have been subjected to several tectonic processes leading to varying structural features. The volcanic rocks consist of basalt, trachytes, ashes, tuffs, and agglomerates and acid lava.

There are four major periods of volcanic activity (V1-V4) and faulting (F1-F4) which resulted in the present situation (Baker et al, 1988). The bed of the lake composed mainly of volcanic material and subsequently deposited pyroclastics and organic matter produced locally. The sediments are composed of sand, pebbles as well as gravels made up of rounded pumice clasts (Studdard et. al.1995).

The southern part lying within the catchment of the lake falls within the Greater Olkaria volcanic complex which are made up pyroclastics which includes lacustrine sediments. Craters, fumaroles, Hot Springs and steam vents are found in several places in the south-eastern and south-western regions.

Martin (2000) of the University of Postdam, Germany stated during a geological excursion that there exist regions, which are geologically very young with all rocks and structure having been formed during the past 4 Ma due to rifting in the parent geology. He further indicated that the Lake sediments are between 150-60,000years old and the volcanic lie on the Lake sediments. Towards the Olkaria the volcanic is made up of pumice and obsidian, which are in the form of flow.

The bed of the lake have previously been described to compose mainly of volcanic material and subsequently deposited pyroclastics and organic matter produced locally. The sediments are composed of sand; pebbles as well as gravels made up of rounded pumice clasts (Studdard et al.1995).

The southern part lying within the catchment of the lake falls within the Greater Olkaria volcanic complex which are made up pyroclastics which includes lacustrine sediments. In the beds of the gorge

spring are pumice that have been turned into Chur through geothermal activities. They are the hardest rock types in the study area. There are also Kedong valley tuffs at the slopes of the gorge as well as pronouncement of Lake sediments at the upstream of gorge. Further south of the Gorge is rhyolite but not pumice which is less than 60,000years old (Martin, 2000).

Yellow tuff
Kedong valley tuff
Tuff
Lava flow

Figure 5: Stratigraphy of Olkaria Volcanic complex (Martin, 2000).

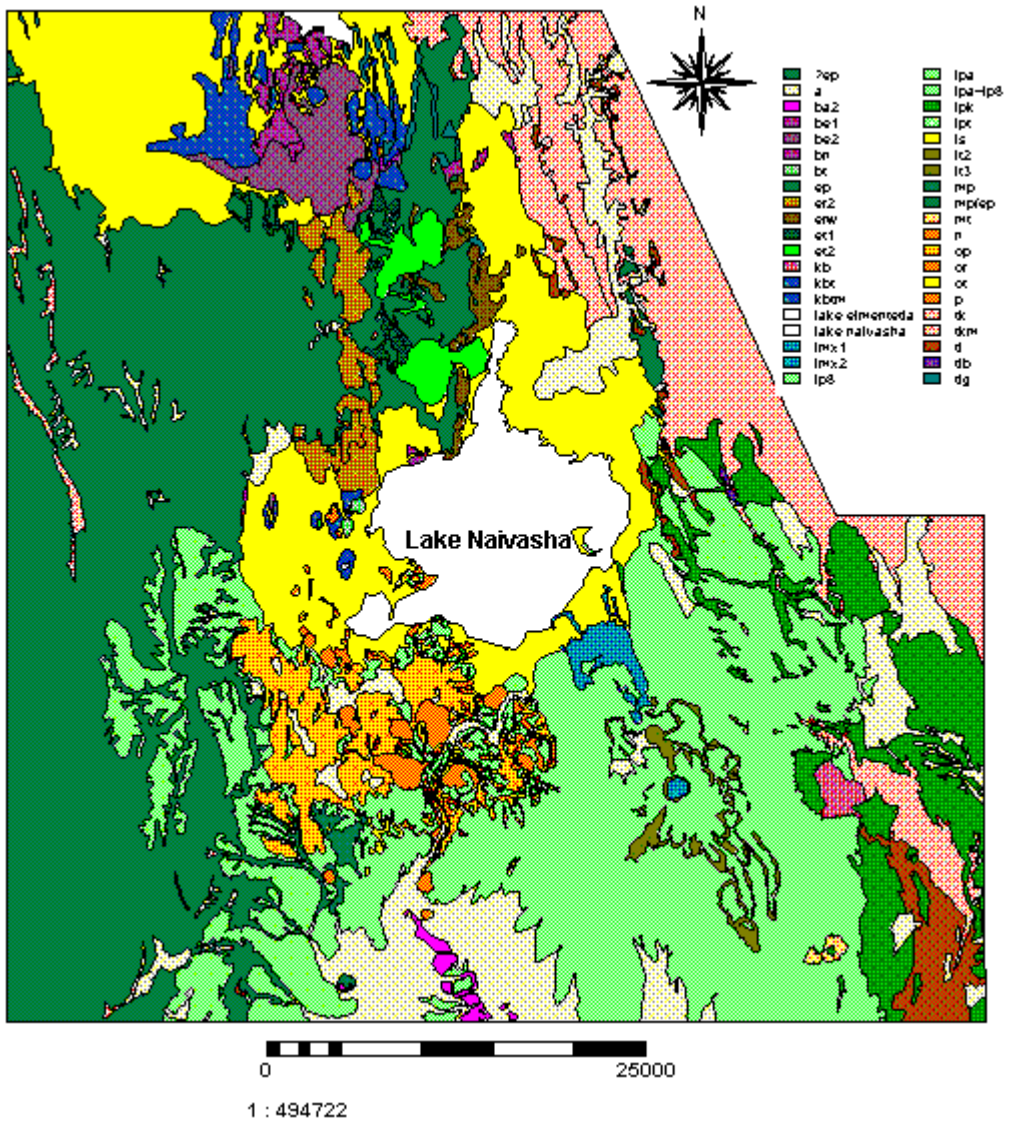

Figure 6: Geology map of the study area.

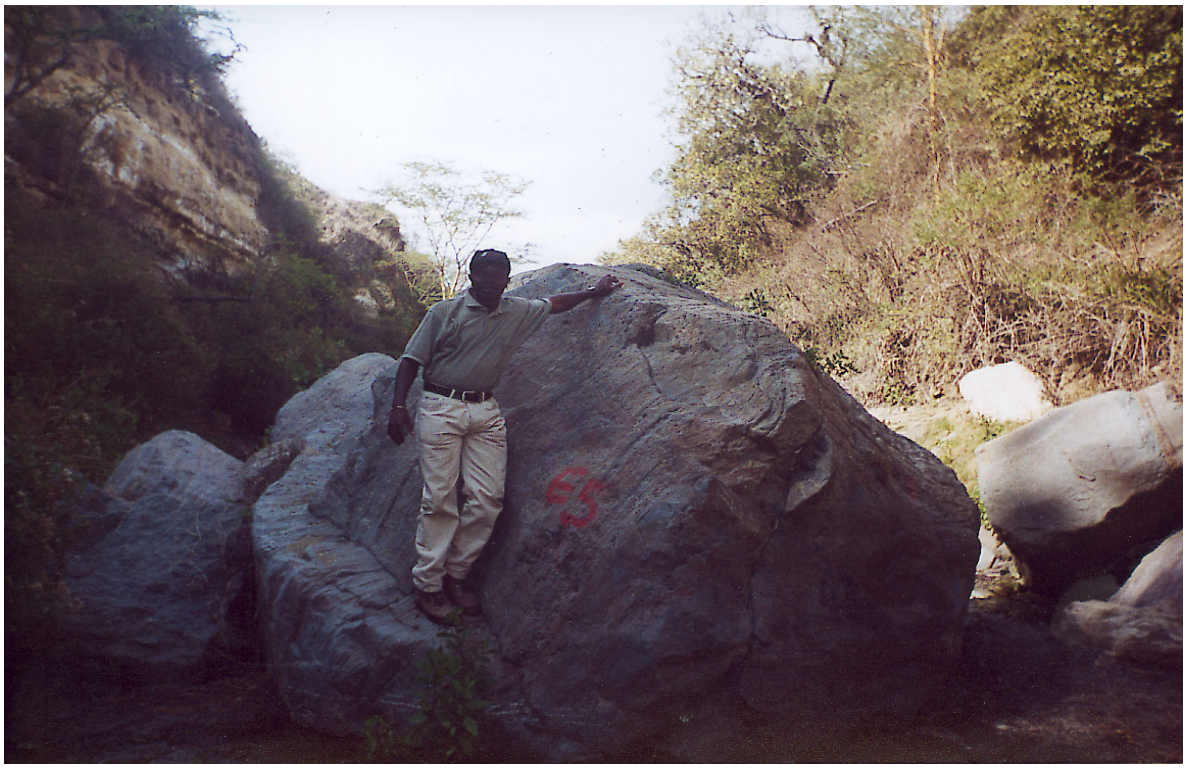

Plate 1: Olkaria volcanic unit in the Gorge near Hell's gate.

EPISODE	ACTIVITY	UNITS	AGE RANGE
V4	Late quaternary to recent salic volcanoes	Longonot, Eburru, Olkaria, Clementia, Ndabibi and Alkira	0.4-0 Ma
D4	Extensive minor faults of the rift floor	Volcanic groups, fluvio and lacustrine sediments	0.8-0.4Ma
V3	Quaternary flood lava of the rift	Gilgil trachytes, Kijabe	1.65-0.9Ma
D3	Renewed faulting of the rift margin	Hill formation	1.7Ma
V2	Early Quaternary flood trachytes	Limuru trachyte,karati	2.0-1.8Ma
D2	Formation of steep faults (narrowing of grabens)	Basalt formation	3.0-2.0Ma
V1	Pliocene volcanic ash flows	Kinangop tuff	3.7-3.4Ma
D1	Major faulting of Eastern rift margin	Mau tuff formation	4.0-3.0Ma

Table 3: Major volcanic and deformation episode (adopted from Clark et al, 1990).

2.3.2 HYDROGEOLOGICAL SETTING

Hydrogeology is greatly influence by the geology, topography and climatic factors that pertain in the area. Topography in the vicinity creates two different hydro-geological environments, which affects significantly the Hydrogeology. In the localised highland areas, there exist deep groundwater tables as well as steep groundwater gradient. This environment is often associated with high rainfall values, which are sources of groundwater recharge if all conditions are fulfilled.

The high hydraulic gradient accounts for the outflow of groundwater from the lake to the south as well as some infinitesimal outflow towards the north. Structural features such as faults, often optimise storage, transmissivity and recharge with the significant of these occurring in places that are adjacent to or within a surface drainage system. In the valleys, shallow groundwater table, low precipitation and low values of recharge are often envisaged.

Aquifers are normally found in fractured volcanic rocks and at times along weathered contacts between different lithological units and they are often confined or semi-confined with low storage coefficient.

The main aquifer is lacustrine volcanic and sedimentary which are often weathered between the lithological units. Permeability is generally low in the rift but there exist some variations locally as a result of some formations. Clark et al (1990) estimated by inventory of boreholes and envisaged that the lake sediments have permeability of 12-148m/d.

However, aquifers with relatively high permeability are found in sediments covering parts of the rift floor and are often unconfined with high specific yield (Stuttard, 1995). Data from existing boreholes and wells reveal complex hydrogeological conditions and depth to water varies throughout the basin but it is generally ranging from 1.3m to about 240m. Estimated hydraulic conductivity average 10m/d and well yield on average is 3 l/s/m. Tuffs in the east of the lake are reported to have high conductivity (average 0.8m/d) and trachytes to the Southeast and in the west have conductivity of 1.1m/d.

Plate 2: Stratigraphy of the Olkaria volcanic complex in the Gorge.

Unit	Description
?ep	Eburru pumice, pantellerite; trachyte pumice, ash fall deposits
a	Alluvial deposit
ba2	Alkaria basalt, basalt and hawaiite lava flows, pyroclastic cones
be1	Older elementetia basalt, hawaiite lava flows, pyroclastic cones
be2	Younger elementetia basalt, basalt, hawaiite and mugearite / benmoreite lava flows and pyroclastic cones
bn	Ndabibi basalt, hawaiite lava flows, pyroclastic cones
bt	Surtseyan / strombolian ash cones
ep	Eburru pumice, pantellerite and trachyte pumice, ash fall deposit
er2	Eastern eburru pantellerite, lava flows, pyroclastic cones
erw	Waterloo ridge pantellerite, welded and unwelded pyroclastics
et1	Older eburru trachyte, lava flows and pyroclastics
et2	Younger eburru trachyte, lava flows and pyroclastic cones
kb	Kijabe hill basalt
kbt	Surtseyan tuff cones
kbtm	Surtseyan tuff cones with laterally equivalent fall tuffs
Imx1	Lower longonot mixed basalt/trachyte lava flows and pyroclastic cones
Imx2	Upper longonot mixed basalt/trachyte lava flows and pyroclastic cones
Ip8	Longonot ash
Ipa	Longonot alkaria pumice
Ipa+ip8	Longonot ash and alkaria pumice
Ipk	Kedong valley tuff, trachyte ingimbrites and associated fall deposit
Ipt	Longonot volcanice, pre-caldera welded pyroclastics and lava flows.
Is	Lacustrine sediments
It2	Lower longonot trachyte, lava flows and pyroclastic cones
It3	Upper longonot trachyte, lava flows and pyroclastic cones
Mp	Maiella pumice, trachyte, pantellerite pumice and ash fall deposits
Mp/ep	Maiella pumice/eburru pumice
Mt	Magaret trachyte, unwelded and welded pyroclastics
N	Ndabibi comendite lava flows, domes and pyroclastics
Op	Olkaria comendite, pyroclastics (include pre-Ipk lacustrine sediments, reworked pyroclastics in ol Njorowa gorge)
Or	Olkaria comendite, lava flows and domes (include ol Njorowa pantellerite lava and welded pyroclastics)
Ot	Olkaria trachyte, lava flows
P	Ndabibi pantellerite lava flows
Tk	Kinangop tuff (eastern rift margin)
Tkm	Mau tuff (western rift valley)
TI	Limuru trachyte
Tlb	Karati and ol mogogo basalt
Tlg	Gilgil trachyte

Table 4: **Description of Legend of Geology map.**

2.4 GEOMORPHOLOGY

Three main geomorphologic units are found in the study area. In the western part lies the Mau Escarpment, the Kinangop in the east and the rift valley plain that the lake basin forms a part.

- **Mau Escarpment**

This forms the western part of the rift valley. The maximum elevation is more than 3000 meters above mean sea level and decreases in height in both north and south direction. It consists basically of soft and porous volcanic ashes and tuffs and stretches to a distance of about 36km within the map area. It is drained by river Marmonet and without surface watercourse into the lake except that it recharges the alluvium in the Ndabibi plain.

- **The Kinangop Plateau**

It forms the eastern margin of the study area and rises to an elevation of about 2750 meters above mean sea level. Its western margin has very steep scarp, broad flat plain and ranges in height from an elevation of 100m to 240m but at its extreme portion is buried with young pyroclastic rocks. It is deeply incised deeply by the tributaries of Malewa River. In relative terms, the crest is between 500 and 600meters to the rift floor but it is clearly distinguished from the floor by a lot of faulted basements. The plateau is composed basically of soft volcanic rocks.

- **The Rift floor Plains**

This is an area of moderate altitude that resulted from the time of formation of the rift. The highest elevation is about 2000m and is found in the vicinity of the Naivasha basin. The basin is largely covered with sediments derived from erosion of the surrounding volcanic rocks of the rift margins. They were deposited in the lacustrine environment during the Gamblian stage of the Pleistocene period and are usually referred to as the Gamblian lake sediments.

Surprisingly, the lake sediments are not thick and barely exceed 30meters (Thompson et. al, 1963).

The Naivasha basin is covered partially by quaternary alluvial sediments and composed of mainly sand, pebble beds and gravel having rounded pumice clasts (Stuttard et al, 1995).

2.5 HYDROLOGY AND MORPHOLOGY OF LAKE NAIVASHA

Lake Naivasha is a freshwater body located at an elevation of 1886m amsl. The total surface area is of the lake is about 200km^2 of which 139km^2 and 64km^2 are made up of open water and swamp respectively (McCann, 1974). It is shallow with an average depth of about 5 meters and the deepest part is 8 meters found near the Hippo point. However, barometric profile of the lake bottom shows the central portion to be flat with the two deepest parts in the Oloidian bay (11.5 meters) and the Crescent Lake (18 meters).

The level of Lake Naivasha has been fluctuating during the past century. Since that time the lake level fluctuated in the order of an incredibly 9.5 meters. This natural dynamism has called for a lot of studies to really ascertain the cause of this phenomenon. This has been attributed to the different use of the lake water for agriculture and domestic water supply to the inhabitants in the Naivasha and its environs.

2.6 GROUNDWATER OCCURRENCE IN THE STUDY AREA

Groundwater occurrence is greatly determined by the geological conditions as well as the available water for storage. Fresh volcanic rocks tend to be compact with no primary porosity although secondary porosity may be well developed. These rocks underlying the rift valley therefore have low permeability though there are at times considerable variations where layers with poor hydraulic conductivity may be overlain with layers of good hydraulic properties.

In places where rivers are the most important component of the geological formation /environment, abundant alluvial deposits form the aquifers. These areas are expected to have better hydraulic properties compared to areas where volcanic formation is the geological history. These areas have low values of transmissivities and as such have poor hydraulic properties.

2.7 IRRIGATION SYSTEMS IN THE STUDY AREA

There are three different types of irrigation systems being employed by small to large-scale commercial farms in the study area. The irrigation systems range from Sprinkler and Drip in the small-scale farms to Pivot irrigation systems on the large-scale farms.

Plate 3: Pivot irrigation system in the study area.

CHAPTER 3

3 HYDROGEOLOGICAL ASSESSMENT OF GROUNDWATER FLOW SYSTEMS

3.1 INTRODUCTION

This chapter is to determine the direction of groundwater flow and to estimate groundwater flux from hydrogeological, geoelectrical and hydrogeochemical perspectives. The sustainability of groundwater is largely dependent on the mentioned perspectives.

Groundwater flow is largely controlled by three factors: the distribution and quantity of recharge to the flow system surface topography and the hydraulic conductivity of the material through which the groundwater flows.

A key starting point to ensure a sustainable future for groundwater system involves a comprehensive hydrological assessment of the properties of the underlying aquifers, which controls the movement of groundwater in the subsurface environment. The properties include the storage coefficient, hydraulic conductivity and transmissivity of the confined or unconfined aquifers.

These properties in the study area vary from one point to the other with the wells close to the lake having good hydraulic properties. Whiles some areas have absolutely very high transmissivities of order of 5000m2/d, others have values as low as 0.01m2/d.

3.2 METHODOLOGY

The X and Y co-ordinates defining the position of the wells and boreholes were used to verify the distributions of wells in the areas of interest. A point map was created and overlain onto the Tm image of June 2000 and the wells that are located in the four areas namely, Oserian &Sulmac, Longonot and Eburru were identified and selected for the hydrogeological assessment.

Hydrogeological data collection was conducted from 7th September 2000 and continued till 2nd October 2000. During the period, reconnaissance survey was conducted to identify the location and elevation of the wells in the areas of interest in the southern part of the lake and supported with few in the north and other areas with the Global positioning system (GPS) fitted with an Altimeter.

The preliminary hydrogeological data collection included mapping and levelling of the 25 shallow wells selected for the studies. Their locations and elevation were measured with GPS fitted with an altimeter and the elevations as well as locations of some of the wells that were doubtful were measured with ordinary level instrument with reference to the National datum and Multi-satellite GPS respectively.

The depth to water level in the wells were measured where possible with a Dipper fitted with a beeper and light which gave a signal any time the instrument came into contact with the water in the wells. The static water level was determined as the difference between the elevation of the wells (contour values) and the depth to water level (surface water levels in the wells).

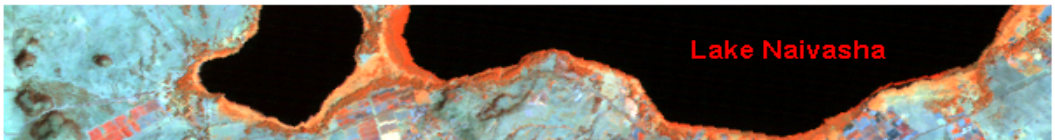

Figure 7: False colour composite (bands 4, 5,7) Tm images (1996), south of Lake Naivasha.

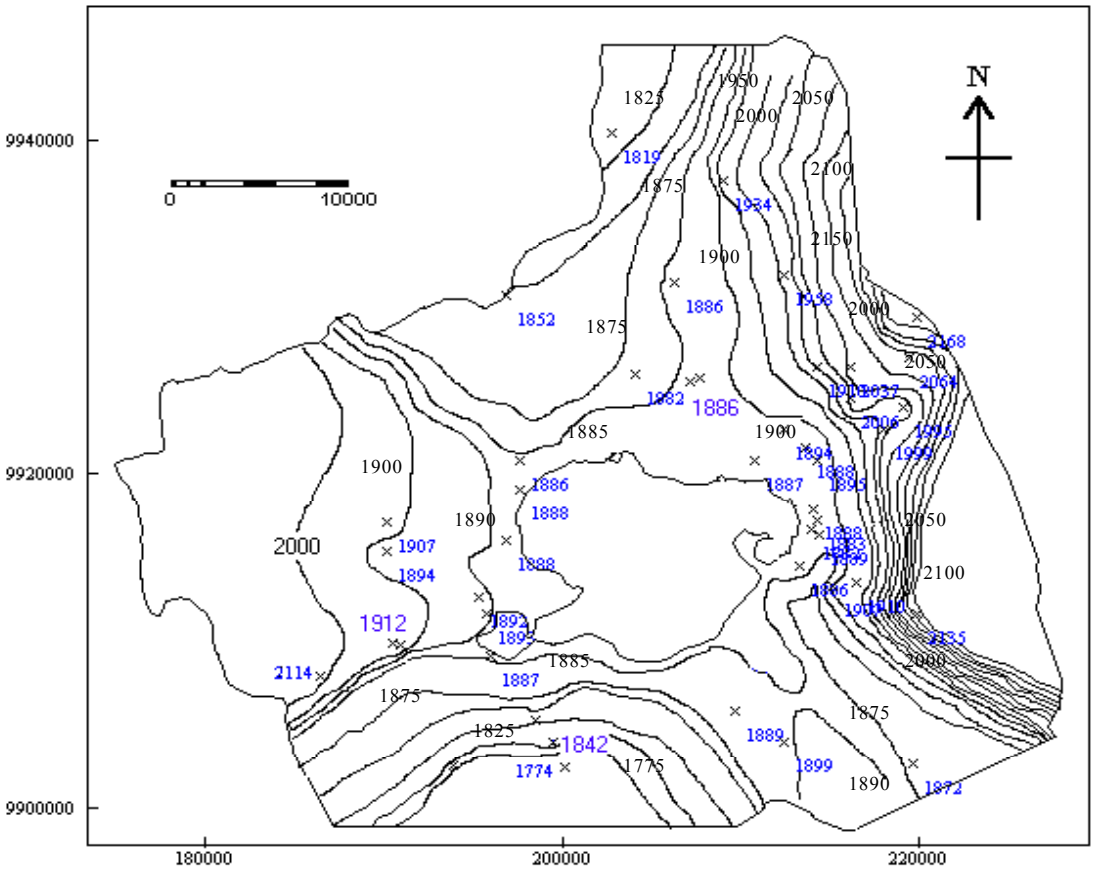

Figure 8: Piezometric surface of the area under the natural setting during 1980 period. Source: Owor, 2000.

3.3 GROUNDWATER FLOW PATTERN FROM PIEZOMETRIC MAP

The piezometric surface map from the static water level provides in-depth understanding of the subsurface flow trend and is depicted in figure 7. The groundwater elevation in the study area controls the direction and mode of the subsurface flow as postulated by various researchers. The flow is from regions of increasing heads to that of decreasing head as groundwater flows from higher energy levels towards lower energy environment if the energy is essentially the result of elevation and pressure (Davis and DeWiest, 1966).

There exist two prominent piezometric highs that are recognisable in the areas of interest. The first is in the south-eastern of static water level of about 2200ma.s.l and second in the south-western parts with static water level of 2000ma.s.l. The entire area can be said to be made up of a series of rise and fall in water level elevation. The piezometric map suggests that the direction of groundwater movement are from the flanks and the Lake Naivasha which recharge the shallow wells along the Lake and wells further south (figure 7).

These areas south of the lake can therefore be characterised as discharge points and the lake Naivasha and other wells on higher elevations in the vicinity as recharge areas. These suggest that the subsurface environment in the southern parts have the highest potential for groundwater and the subsurface flow of groundwater tilts away from the Lake towards the southern wells in the study area. It is to be considered that the direction of flow to some of the wells might have been reversed recently due to over-pumping for irrigation, typically in the north-eastern part of the study area.

Faults and stratigraphic seals may at times constraint or enhance the flow of groundwater. These are evident in the Olkaria fields where there exist numerous fault lines mainly controlled by the WNW-ENE (observed during geological excursion as part of fieldwork in September 2000). The flow directions are confirmed using chemical data and discussed in details in Chapter 4.

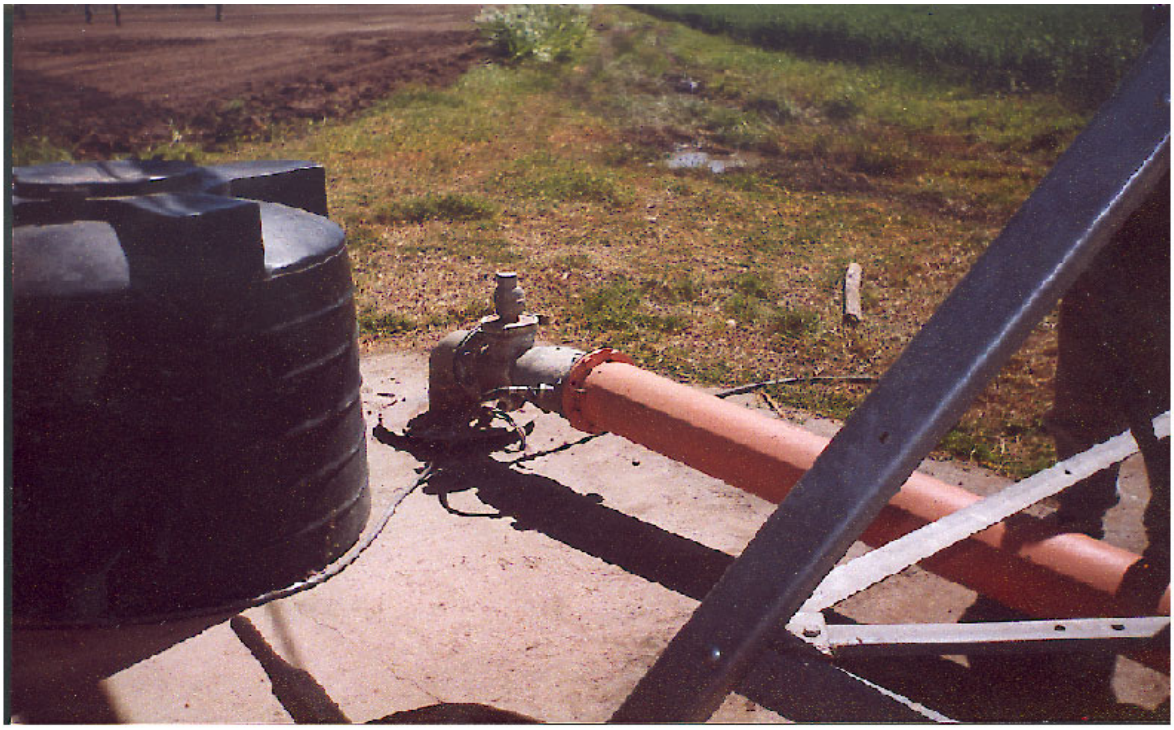

Plate 4: Borehole with Pump-intake fitted in Three Point farm.

3.4 GROUNDWATER FLOW THROUGH AQUIFERS

The flow of groundwater through the aquifers to the south of the Lake was evaluated by constructing profile through the aquifers. The sections were drawn for the ground level, water level and elevation

of the bottom of the wells. Three scenarios of cross sections were considered and are elaborated below:

- Cross section or profile taken from the Sher farms to Sulmac, Kedong and finally to Heather farms (figure 8).
- Cross-section from well C2071 into well 630D close to the Olkaria field (figure 9).
- Cross-section from Ngodi well to Moi Ndabi well 1 and finally to Kongoni wells (figure 10).

The water levels from the cross sections in 2 scenarios are below the Lake Naivasha level (1886m amsl) recorded during fieldwork in September 2000. The Kedong C210, Sulmac, C2071, UW1 and C630D have the water levels below the Lake Naivasha level (figures 8 and 9). These wells are therefore in the vicinity of the Lake Naivasha outflow and therefore receiving substantial amount of recharge from the Lake Naivasha.

The reverse is observed in scenario 3, where the water levels in the south-western wells are above that of the Lake level. The Ngodi and Moi Ndabi 1 wells located on piezometric highs at an elevation more than 2000 meters a.m.s.l and have their water levels at about 1900masl, which is above the Lake level of 1886 (present level recorded). The groundwater flow from these wells tends to converge into the Kongoni well and perhaps recharge the Lake Naivasha. The Ngodi and Moi Ndabi 1 wells can therefore be said to be one of the recharge sources of Lake Naivasha (Figure 10).

The inflow and outflow areas are recognisable on the piezometric map and cross sections (figures 8-11). There is decreasing piezometric contours towards the southern wells (figures 8 and 9) and decrease /increase in piezometric contours towards the Lake Naivasha or Ndabibi wells respectively.

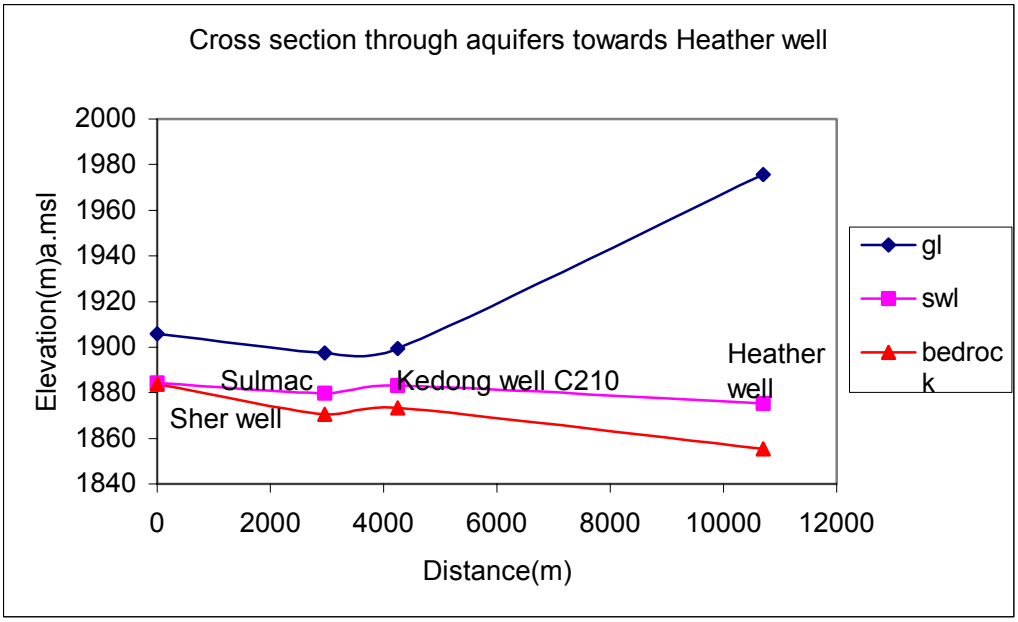

Figure 9: Hydrogeological cross section through aquifers from Sher to Heather well.

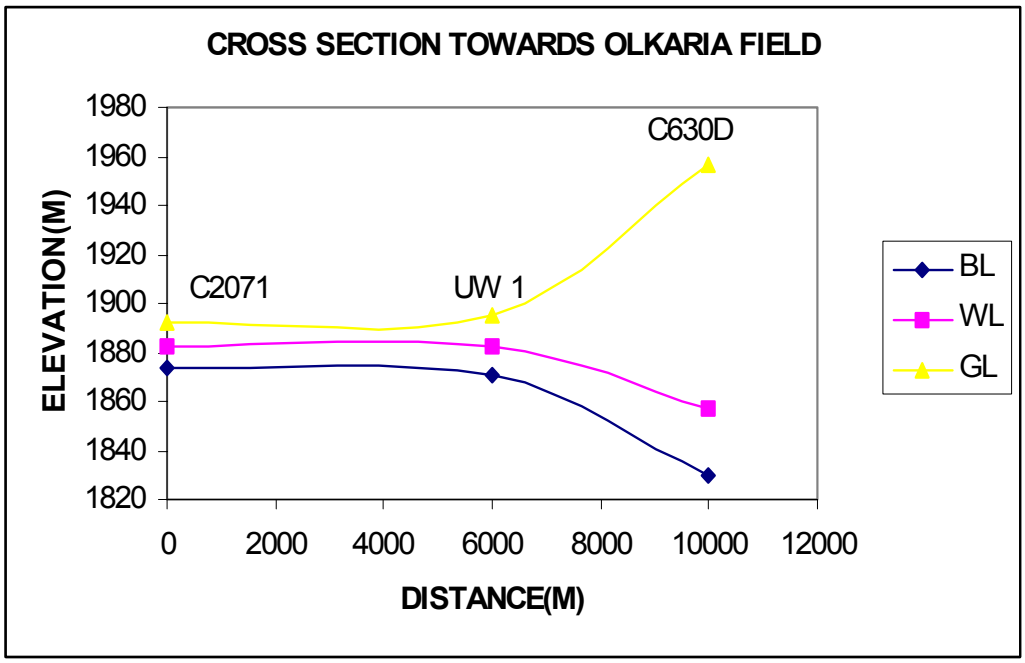

Figure 10: Hydrogeological cross section through aquifers towards Olkaria field.

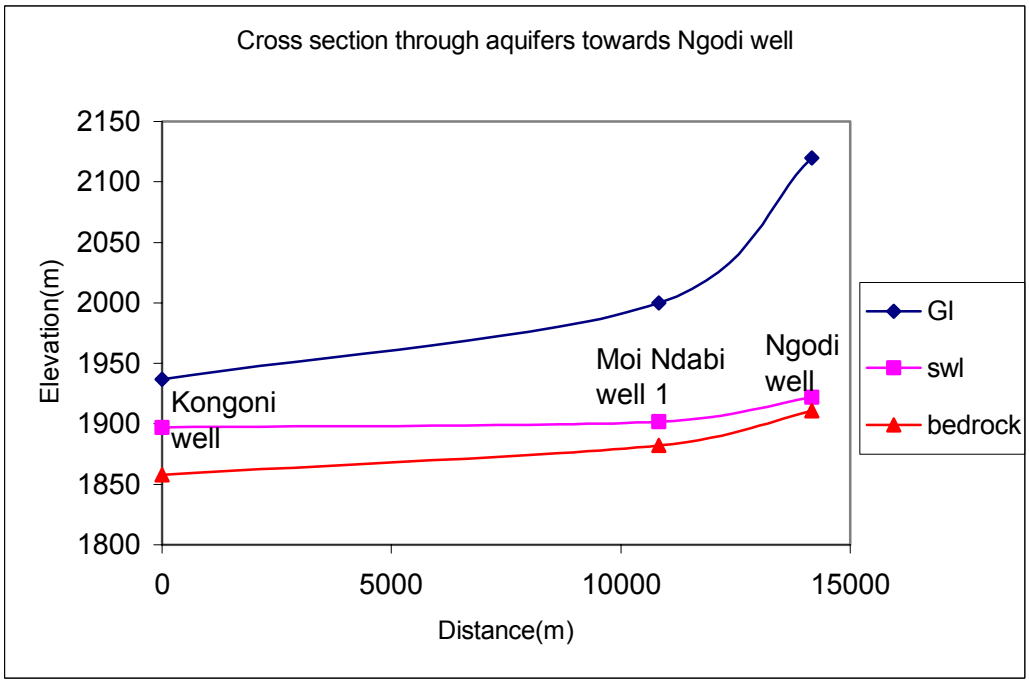

Figure 11: Hydrogeological cross section through aquifers from Kongoni well to Ngodi well.

3.5 GROUNDWATER FLOW SYSTEM FROM THERMODYNAMICS

3.5.1 GENERAL

Groundwater temperature fluctuation with depth provides clues to help delineate flow systems based the extent of mixing as it serves to redistribute terrestrial heat with depth. Temperature, electrical conductivity and depth profiles were only conducted in 2 wells located on Sulmac and Sher farms with a Diver.

The Profiles in the shallow wells were conducted on the two wells mentioned above as water column in most of the wells at the time of measurements was lower than 30meters (maximum depth) at which the 30-meter water column Diver could measure.

3.5.2 ANALYTICAL RESULTS AND DISCUSSIONS

Temperature- depth profiles in the deep geothermal wells are presented in the figure 18. The temperature increases with depth in most of the well except OW-204 and OW-703 where different pattern is encountered.

However, from the thermal profiles, the temperature of groundwater is seen to be increasing from the shallowest well OW-M2 towards the deeper aquifers in the wells OW-501, OW-703, OW-710, OW-204 and OW-R2. In well OW-M2, the temperature at depths between 400-450 meters appears to be constant. This range might be the depth of mixing of shallow groundwater and hot water from volcanic activities in the geothermal field. The interface between the shallow water and hot geothermal water could therefore be located at a depth of 400-450 meters (figure 18).

There is also an evidence of mixing in well OW-703, where the temperature decreases from the depth of about 1200 to 1400 meters. However, no evidence of mixing in the other deeper geothermal wells as no clear pattern depicting mixing are recognisable since the temperatures change significantly with depth. The interface might be beyond depth of 1500 meters r and suggests that if there is really outflow into the deeper geothermal wells, it might be occurring at a depth of about 2000 meters below ground level. The only exception is in well OW-703 and OW-204 where an appreciable interface was recognised at a depth of about 1000 and 1200 meters respectively.

3.5.3 CONCLUSION

The groundwater flow is delineated to be from well OW-M2 into the deeper wells OW-703, OW-204 and other remaining wells. There is therefore flow southwards, supported by the piezometric map (figure 7), which depicts groundwater flow further south into the deeper geothermal wells.

3.6 PUMPING TEST ANALYSIS AND EVALUATION

3.6.1 INTRODUCTION

The sustainability of groundwater resources greatly depends on the response of the underlying aquifer to pumping. The property of the material such as the transmissivity and storativity of the aquifer influence the response and help to compute the decline in water level or drawdown. These properties are evaluated by performing test pumping on a well pumped at a constant rate and the change in drawdown measured over time (Fetter, 1998).

3.6.2 GOVERNING EQUATIONS

The governing equations used to evaluate the properties of aquifers are defined by the method below:

1. Jacob's straight- line methods for confined leaky aquifer for pumping test.

2. Theis's method for recovery test.

3. Hantush's method for leaky aquifer.

The transmissivity of the aquifer computed from the formula,

$$T = 2.3Q \,/\, 4\pi\Delta Sw \qquad 3.1$$

Where T=Transmissivity, Q= Discharge and ΔSw= Drawdown per log cycle for pumping test or residual drawdown for recovery from semi-log plots.

The storage coefficient is defined by the equation,

$$S = 2.25\,Tt \circ / r^2 , \qquad 3.2$$

where r is the distance defined by the intercept of the zero drawdown and the straight line through the data points

The two equations are the governing equation incorporated into pumping test evaluation computer program AQUITEST.

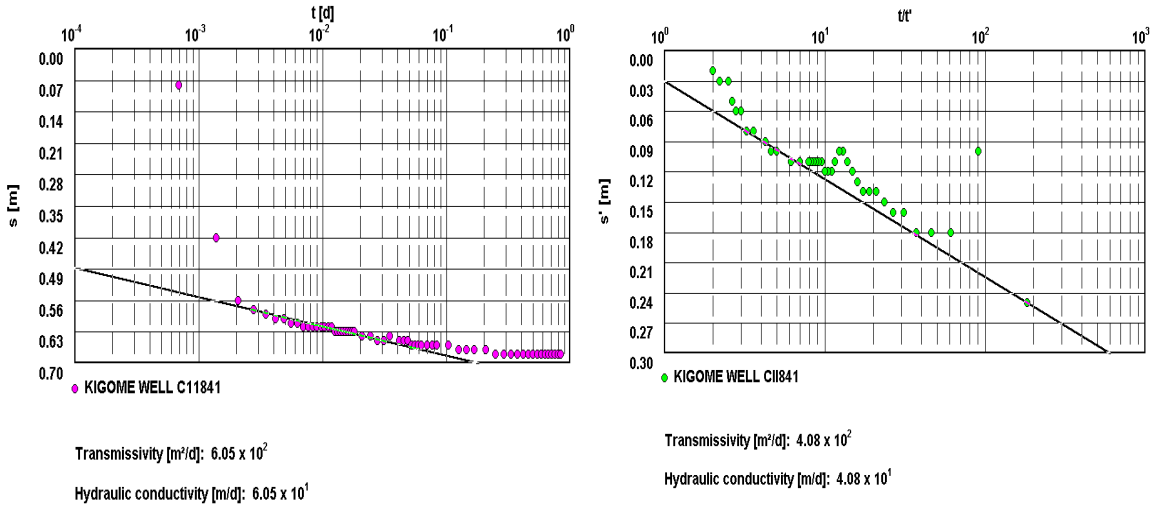

Figure 12: Plots of Jacob's straight line and Theis's methods of Pumping and Recovery of Kigome well C11841.

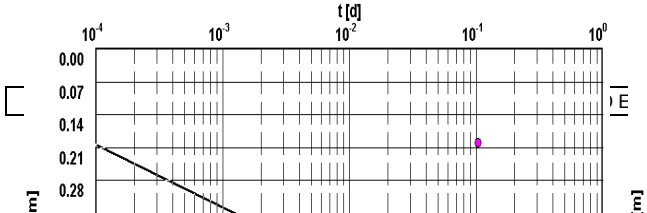

Figure 13: Plots of Jacob straight-line and Theis methods of Pumping and Recovery of well C579.

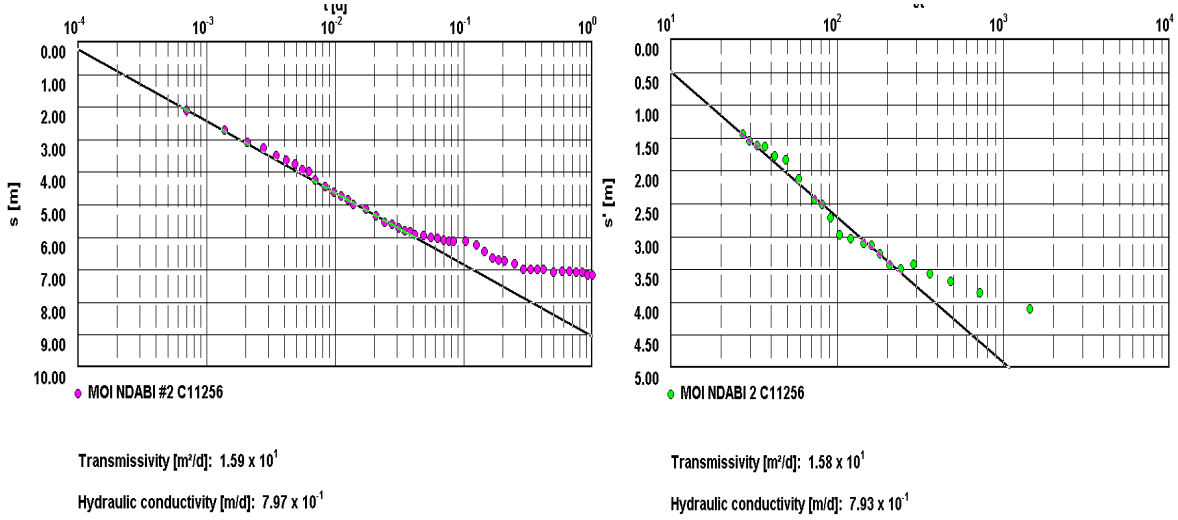

Figure 14: Plots of Jacob straight-line and Theis methods of Pumping and Recovery of Moi Ndabi well C11256.

Well	Pumping rate (m^3/d)	Hydraulic Conductivity (m/d)	Transmissivity m^2/d
Moi Ndabi 2 C11256	192	0.8	15.9
Longonot farms C4986	817.65	594	28800
Kigome farms C11841	216	60.5	605
Well C579	648	17.7	889

Table 5: Transmissivity and hydraulic conductivity values from Jacob straight-line method of confined aquifers.

Well	Pumping rate (m^3/d)	Hydraulic Conductivity (m/d)	Transmissivity m^2/d
Moi Ndabi 2 C11256	192	0.78	15.8
Longonot farms C4986	817.65	3.81	185
Kigome farms C11841	216	0.54	1.72

Table 6: Transmissivity and hydraulic conductivity values from Hantush for leaky confined aquifers.

Well	Measurement	Hydraulic Conductivity (m/d)	Transmissivity m^2/d
Moi Ndabi 2 C11256	Recovery	0.79	15.8
Longonot farms C4986	Recovery	190	9220
Kigome farms C11841	Recovery	40.8	408
Well C579	Recovery	167	2500

Table 7: Transmissivity and hydraulic conductivity values from Theis Recovery method.

3.6.3 ANALYTICAL RESULTS

Three wells from Kigome farms C11841, Moi Ndabi C11256 and Longonot farms C4986 were selected for test pumping analysis and evaluation. These are the standard field aquifer-pumping test from the drillers after well completion and involved a single well with no observation wells, which could not give a clue to the responses of neighbouring wells to pumping.

The pumping test on Kigome well C11841 was conducted for 20 hours at a discharge rate of 9 m3/h and the drawdown range from 0.08 to 0.68 meters with an average drawdown of 0.64 meters. The transmissivity value of 605 m^2/d and hydraulic conductivity of 60.5 m^2/d were obtained from Time-Drawdown straight-line method (confined aquifer) of Jacob while 1.72 m^2/d and 0.54 m/d respectively were obtained from Hantush's method of leaky aquifer. Theis and Jacob methods of recovery yielded transmissivity and hydraulic conductivity values of 408m^2/d and 40.8 m/d respectively and the average residual drawdown of 0.1meter obtained from the analysis.

In Moi Ndabi 2 well C11256, the drawdown ranges from 2.1 to 7.18 meters. Transmissivity of 15.9 m $^2/d$ and hydraulic conductivity values 0.8 m/d were obtained from the Jacob straight-line method of confined aquifer while 13.6 m $^2/d$ and 0.68 m/d were obtained from Hantush's method of leaky aquifer.

The recovery test yielded transmissivity value of 15.8 m^2/d and hydraulic conductivity of 0.79 m /d with a residual drawdown varying between 1.44 and 4.1 meters.

In Longonot farm well C4986, the drawdown remained constant at 0.08 meter after 1 minute during pumping and recovered to the static water level at 5.45m four minutes after the end of pumping. The transmissivity and hydraulic conductivity of 185m^2/d and 3.8m/d respectively were obtained while the corresponding transmissivity and hydraulic conductivity values of 28800m^2/d and 594m/d respectively were observed in C4986.

Ojiambo (1992, 1996) estimated transmissivity values of the shallow wells to vary from about 1 to 800m^2/d, with an average value of 400m^2/d for wells in lacustrine sediment aquifers near the Lake Naivasha and from 3 to over 12000m^2/d in the study area. The storage coefficient value calculated was 0.0044. The results from current pumping test analysis are shown in the Tables 6-8.

3.6.4 DISCUSSIONS ON AQUIFER PROPERTIES

The data used for the analysis is not the standard hydrogeological test pumping data to determine the properties of the aquifers, as there were not observation wells when the wells were being test-pumped. It was therefore assumed there are observation wells located at an infinitesimal distance of 0.001m from the pumping well.

The transmissivity values obtained differ significantly within the same well from the different methods used for pumping or recovery analysis (Tables 6-8). This is due to the fact that the methods used to perform the analysis have varying assumptions for confined and unconfined aquifers incorporated in the program set up.

The values obtained for Kigome well C 11841 differs very much between the Jacob and Hantush as 298 and 380m^2/d respectively with an average value of 339m^2/d from pumping. The corresponding hydraulic conductivities are 0.54 and 38 m/d respectively. From analysis in table 1, the transmissivity of aquifer decreases further away from the Lake. The Moi Ndabi well C11256 has low transmissivity value compared to the Longonot well C4986, which is closer to the lake than that of Moi Ndabi. This might be due to the type of underlying material of the aquifers and the hydraulic gradients that exist at the two places.

The well C11256 are made up of lacustrine lake sediments and the Moi Ndabi well composed of volcanic. These well near the lake shore yield water from these lacustrine aquifers and have higher yields and transmissivities than wells further away from the Lake Naivasha (Tables 6 and 7; Ojiambo, 1992). The later have lower yields and might have aquifers along weathered planes between different lithological units or fractured volcanic as seen in values from well C11256.

Hernandez (1999) computed transmissivity value of between 48-1020 m^2/d and indicated that it is quite common to find areas where transmissivities are very high as 5000m^2/d and others in the order of 0.01 m^2/d.

The lower drawdown value of 0.8m couple with high transmissivity observed in well C11256 demonstrate how replenishable the groundwater systems are in the areas around Longonot. Furthermore, the relatively high transmissivity values from the pumping test on other wells suggest that the wells in the southern part of the lake will be sustainable for irrigated agriculture when all conditions such as recharge to the groundwater system are fulfilled.

3.7 QUANTIFICATION OF GROUNDWATER FLUX INTO SHALLOW AQUIFERS

The contribution of groundwater to the flow system is quantified based on Darcy's law defined by the equation:

$$Q = \frac{-KA(h_A - h_B)}{L} \qquad 3.3a$$

where Q is the discharge into aquifer measured in m^3/day, K is the hydraulic conductivity in m/day,

A =Product of thickness and width of aquifer as the cross sectional area of saturated aquifer in the direction of flow (in sq. meters). h_A and h_B are heads of two points that define the line of flow of groundwater and h_A-h_B is the head difference between the two points and L is the length or distance of travel or flow length (in meters).

Generally, the Darcy's law from equation 1.3 is often expressed as;

$$Q = -KA\left(\frac{dh}{dl}\right) \qquad 3.3b$$

where dh/dl is the hydraulic gradient.

The above mentioned formula is used based on the assumption that there is slow moving groundwater which is the upper limit of Darcy's law and that the aquifer is confined.

The hydraulic conductivity is taken as between 0.79m/d and 60.5m/d (Tables 6-8). The flux is quantified into the shallow aquifers as a lower and upper limit as a result of varying hydraulic conductivity in the area. The average saturated aquifer thickness is taken as 25 meters estimated from the level of water struck and the depth of the wells defined by lacustrine sediment formation.

The cross sectional width of the aquifer perpendicular to the flow direction is taken at a static water level of 1880m above mean sea level from piezometric map. This area serves as the converging point of groundwater flow from the left, right flanks of the rift and the lake into the area of interest.

The distance of travel is taken to be approximately 22km from piezometric highs at the left and right flanks of the rift, which contribute groundwater inflow into the aquifer.

The hydraulic gradient was taken between piezometric surface lines 1880 and 1980m (figure 8).

Higher flux is therefore expected to be from the west than the east over equal hydraulic conductivity (K) and flow area based on the Darcy's equation. The hydraulic gradient from piezometric map is calculated to be equal to 0.0045.

The hydraulic conductivity of 17.7m/d determined from pumping test, gives groundwater flux of

$$Q_{17.7} = KiA \qquad 3.3c$$

$Q_{17.7}$ =17.7*22000*25*0.0045m^3/d

=43807.5m^3/d

=16*$10^6$$m^3$/y

The hydraulic conductivity value of 60.5m/d gives a flux ($Q_{60.5}$) of 54.7*$10^6$$m^3$/y.

The groundwater fluxes to the southern wells therefore range from 16*$10^6$$m^3$/y to 54.7*$10^6$$m^3$/y. The calculated values are similar to other the values calculated by Ase et.al. (1986). They are also approximate to the average values of lake outflow estimated as 43*$10^6$$m^3$/y by Sikes (1953) and other researchers.

Groundwater flux from the Lake Naivasha at static water level 1886 over a distance of 10km into southern well at static water level 1842 is given as:

Qout (max)=60*10000*25* 0.0044m^3/d

=24*$10^6$$m^3$/yr.

Qout (min)=17.7*10000*25*0.0044m^3/d

$=7.1*10^6 m^3/yr.$

The Darcian velocity, $V = \frac{Q}{nA}$ 3.4

where n is the effective porosity, A is the cross section area and Q is the groundwater flux.

The Darcian velocity (maximum) is calculated as:

$Vmax=24*10^6/0.2*25*10^4 m/yr.$

$Vmax=480 m/yr.$

The minimum Darcian velocity is given as, $Vmin=7.1*10^6/0.2*25*10^4 m/yr.$

$Vmin=142 m/yr.$

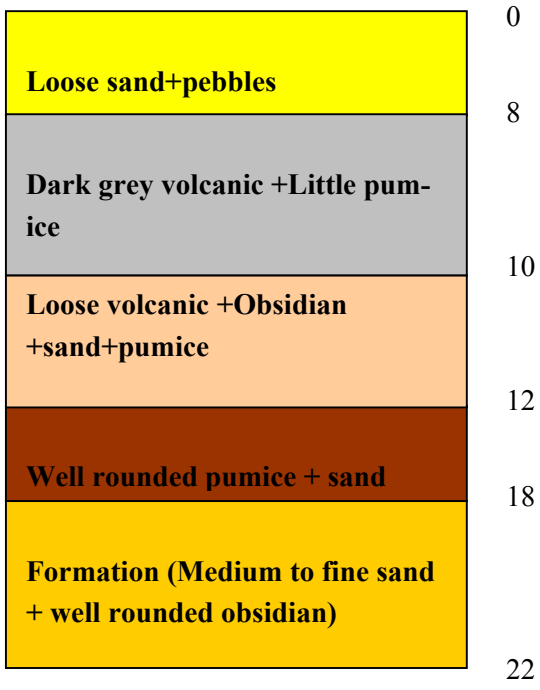

Figure 15: Stratigraphic column of new borehole (Sher Farms Limited).

3.8 LONG-TERM AREAL RECHARGE (BASED ON RESIDENCE TIME)

The long-term areal recharge, R (mm/y) is defined by the equation (Beekman, 1995):

$$R_T = \frac{(V_U A_R H_U) + (pA_T H_S)}{A_R T_T} \quad 3.5$$

where V_u is the average volumetric content within the recharge area, A (m^2) is the surface area. H (m) is the average thickness, p is the average effective porosity of the aquifer and T (yr.) is the total average residence time in the unsaturated zone, unconfined and confined part of the aquifer. The basic

assumption is that, there is steady state condition of groundwater flow and constant moisture (V_u) and surface area (A_R).

The following values were used in computing the areal recharge: V_U =0.15(Dao, 2001); A_R=60*10^{6}m^2 (taken as 3km*20km) south of the Lake Naivasha; H_U=25m (unsaturated aquifer); p=0.2; H_S=75m (saturated aquifer). Tc=5873years, Tuc=Tus=2383years which gives T_T=10,630years, the total residence times of groundwater from the modelled values for confined and unconfined aquifers and in unsaturated assumed to be the same as in unconfined aquifer.

The minimum long-term areal recharge rate, R_T from equation 3.5 is 1.76mm/yr. Ojiambo (1996) using helium and tritium age ratio and distance between static water level and calculated measurement point, calculated mean recharge rates into wells C562, C210 and C630-D as 0.27±0.10m/yr using effective porosity of 0.3.

The average recharge at the south of the Lake Naivasha is computed as 65mm/yr from the areal direct recharge zonation map depicted in figure 16.

From the long-term areal recharge, it presupposes that about 3.5% of direct recharge infiltrates to recharge the groundwater if all conditions are fulfilled.

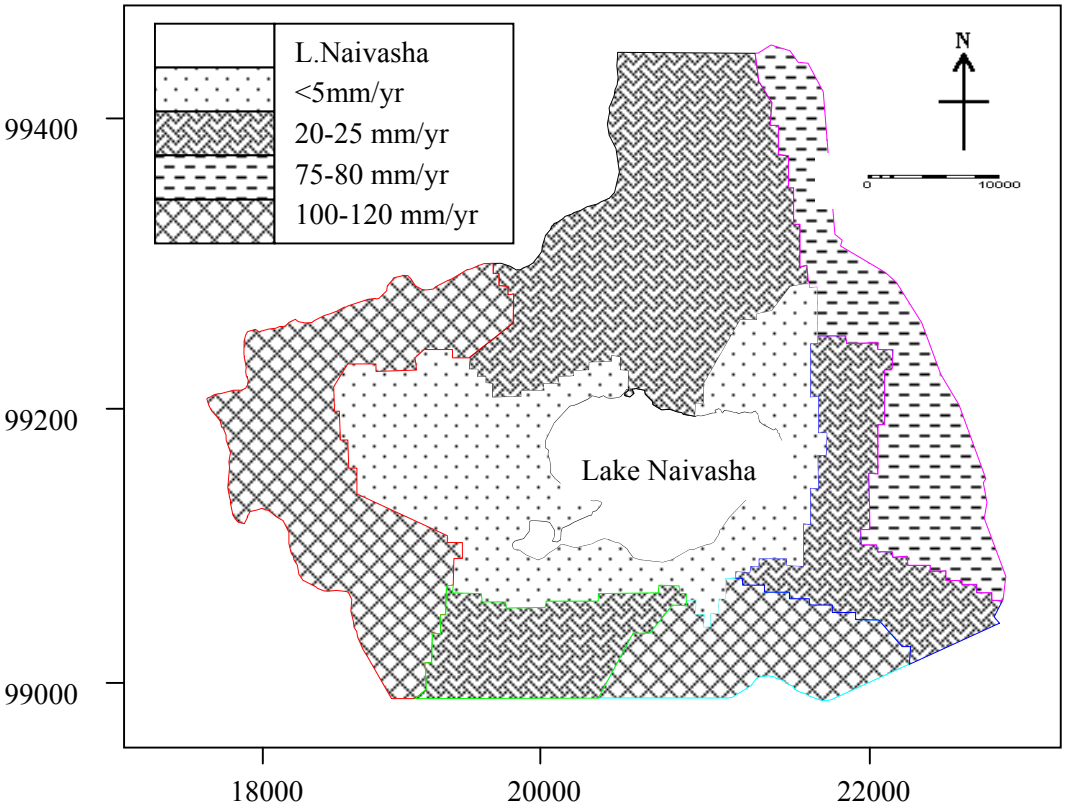

Figure 16: The spatial distribution of direct recharge in the study area in mm/yr. Source: Owor, 2000.

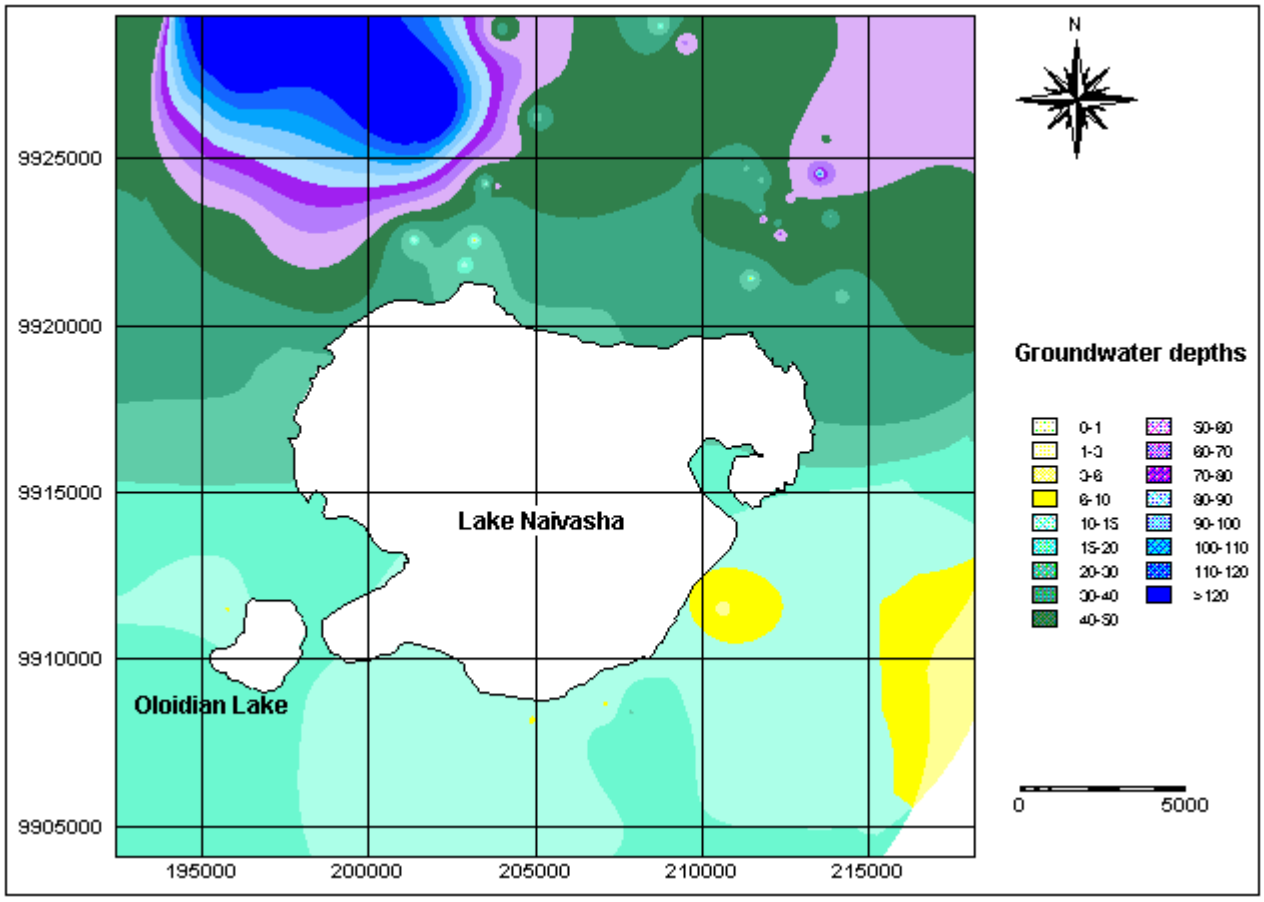

Figure 17: Groundwater depth map in the study area.

3.9 GEOPHYSICAL TECHNIQUES

3.9.1 INTRODUCTION

This technique was adopted to determine the depth to bedrock of underlying aquifer using VES resistivity profiles. This could help to evaluate how sustainable the rapid increase in groundwater usage will influence agricultural development in the study area. VES measurements are used to assess the depth to bedrock aquifer.

The data was collected during fieldwork and processed by Pastoor (2001). The geophysical data are given in Appendix E-1. The resistivity profiles at four locations south of the Lake Naivasha are depicted in figure 18.

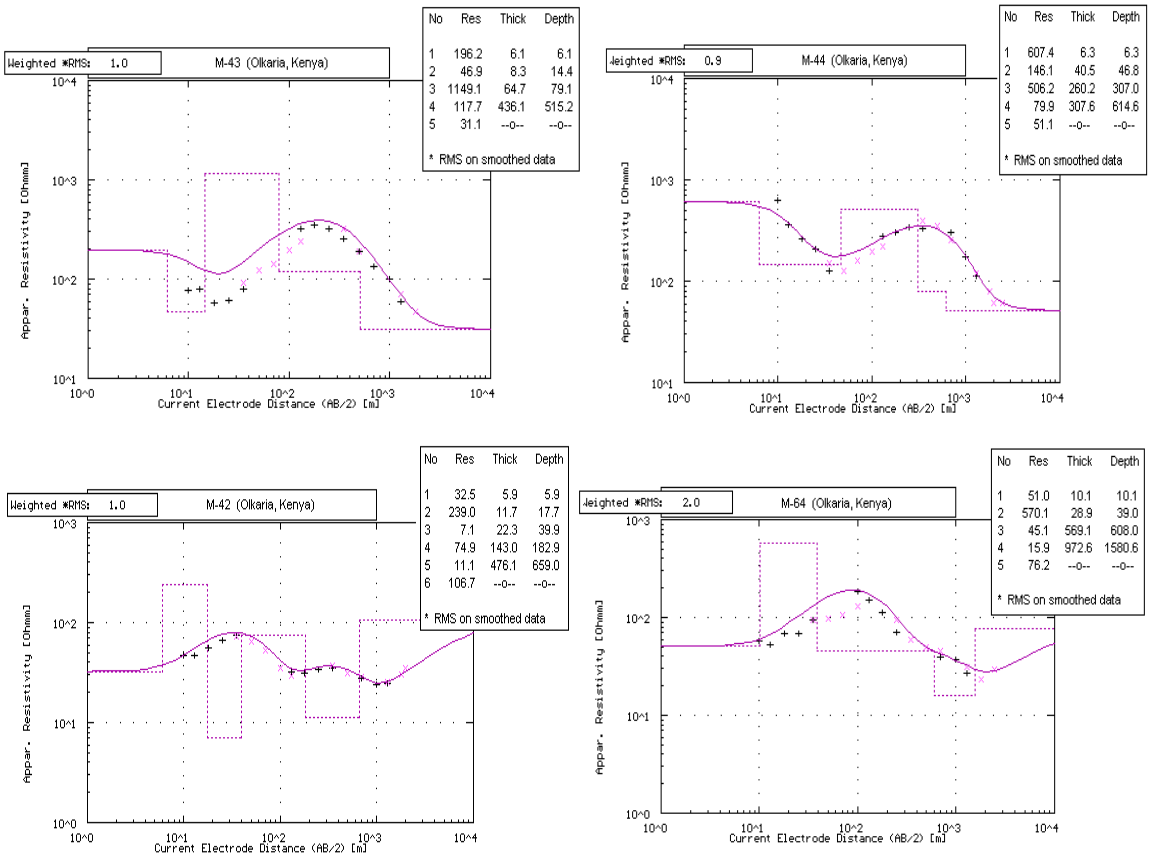

Figure 18: VES Profiles at M-42, M-43, M-44 and M-64, South of Lake Naivasha.

Source: Pastoor, 2001.

3.9.2 INTERPRETATION OF VES PROFILES

The VES profiles are depicted in figure 3.6 and indicate that there are five different layers in the vicinity. At M-43 and M-44, the first layer has an average thickness of 6.2m and the Resistively values of 196 and 607 Ω-m respectively was measured. The resistivity decreases subsequently at the second layer, increases in the third and decreases further in the fourth to the fifth layers. M-44 located close to the Lake has two first layers highly resistive compared to the measured values at M-43.

Further south towards the Olkaria field at M-42 and M-64 are highly resistive materials at the second layer at depths of 17 and 39m respectively than the top layers.

The relatively low resistivity at the bottom layers can be attributed to clayey-rich Lithology and the high values being indicative of the presence of perhaps sandy or lacustrine sediment materials. Gressando (1999) stated that the high resistivity of the third layer further south of the lake indicates a dry layer and the groundwater table is below a depth of 30-40meters.

Figure 19: Location map of VES soundings in the south of Lake Naivasha.

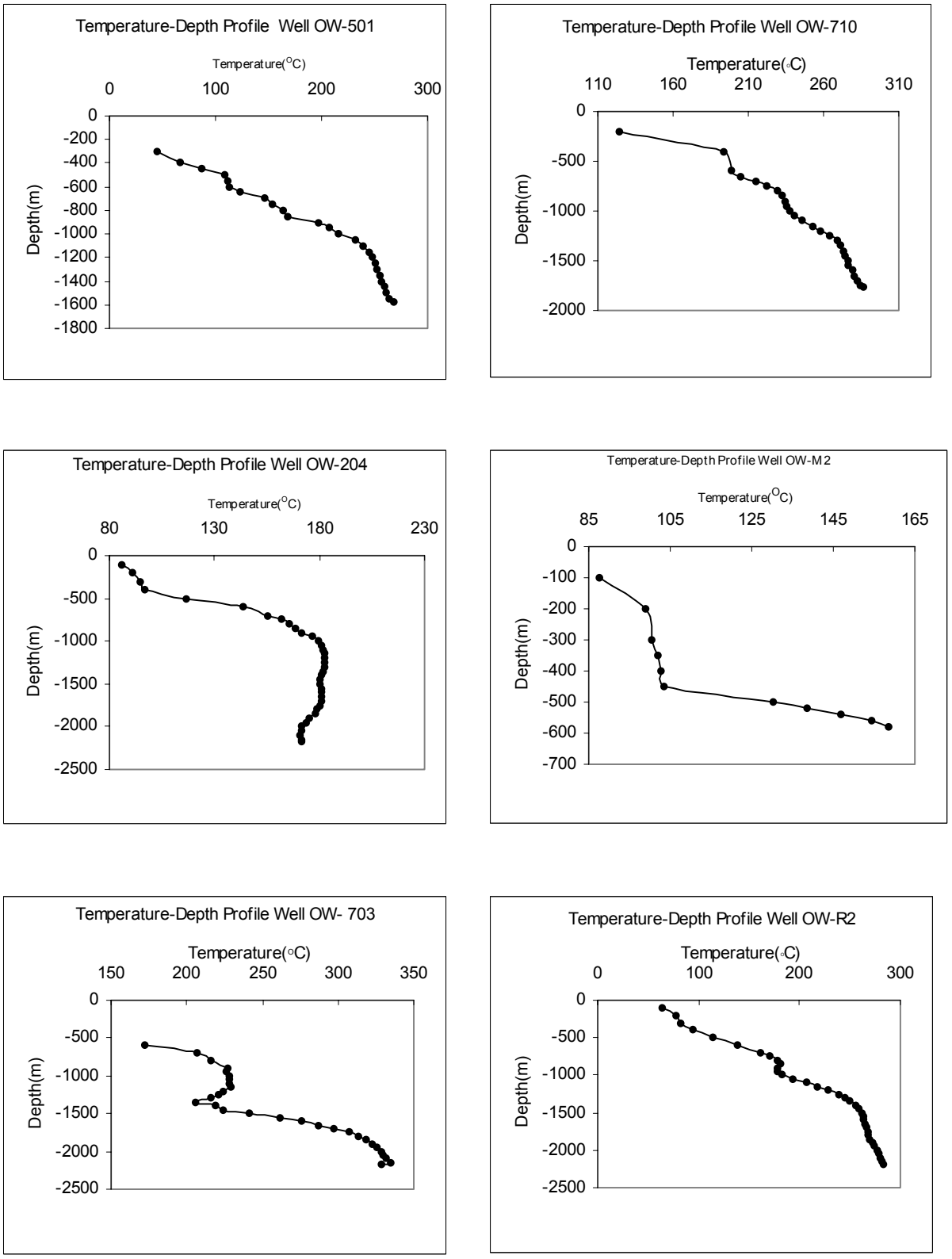

Figure 20: Temperature-Depth Profiles in geothermal wells.

CHAPTER 4

4 HYDROGEOCHEMICAL ASSESSMENT

4.1.1 INTRODUCTION

The purpose of this chapter is to characterise the quality of groundwater for Irrigation in accordance with the USDA classification standards for Irrigation water. Groundwater geochemistry is an essential component in the evaluation and assessment of groundwater resources as it gives in-depth analysis onto the origin and history of water (Appelo and Postma, 1993).

The quality of groundwater is defined by the physical, chemical and biological characteristics and affected by the characteristics of the media through which the water passes on its way to the groundwater zone of saturation. These are the result of possible interactions of the groundwater with mineral composition as it flows through rock types, weathered materials and meteoric precipitation forcing it to acquire a prevalent chemical character.

Irrigation waters are therefore influenced greatly by the sodium absorption ratio (SAR) and the exchangeable sodium ratio (ESR) and the electrical conductivity, Ec that define the sodicity and salinity levels in water respectively.

4.1.2 DATASETS FOR MAJOR ION CHEMISTRY

- Dataset 1: Geochemical Data Analysis of 49 Boreholes and Wells around Longonot (south of the lake), 2000 from The Kenya Power Generation Company (KenGen).
- Dataset 2: Geochemical Data Analysis of 44 Boreholes and Wells from the University of Nevada at the University of Alabama, USA-1996.
- Dataset 3: New Data Analysis, 1998-Natalie Morgan, M.Sc.
- Dataset 4: Geochemical data of Physical parameters for Isotope studies from fieldwork, 2000.

4.2 SAMPLES LOCATIONS AND FIELD MEASUREMENTS

4.2.1 SAMPLING LOCATIONS

Twenty-seven (27) representative boreholes in the vicinity of suspected outflows from the Lake and perpendicular to the direction of groundwater flow into the Eburru, Oserian and Sulmac and Longonot areas were selected for sampling.

These wells in the areas of interest were selected from point map and Tm image of June 2000. The wells were located for sampling in the field by mapping with Global Positioning System (GPS), Topographic map, Tm image 2000 and point map of boreholes created with ILWIS software package in GIS environment. The sampling points are depicted in figure 19.

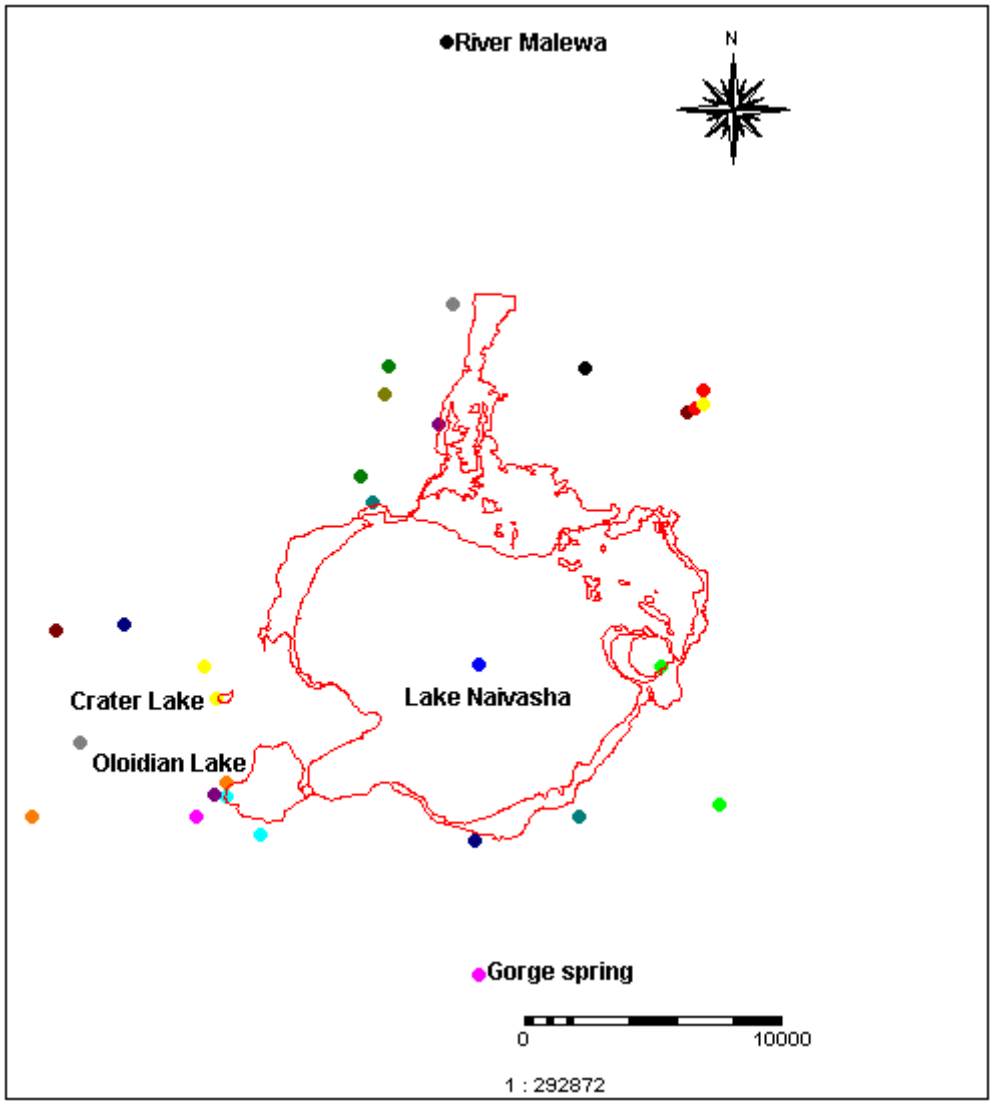

Figure 21: Spatial distribution of water sampling points in study area (fieldwork 2000).

4.2.2 WATER SAMPLING AND FIELD MEASUREMENTS

Twenty-seven (27) representative water samples were collected for chemical analysis from boreholes in along the outflow from the lake in the four areas of interest, namely: Sulmac, Oserian, Longonot and Eburru. The bulk of the samples were taken from boreholes from static water level of 17-198.15 meters in the south of the lake and the remaining from the north to spatially correlate the chemical variables.

The depths to water level were measured where possible with Electric Dipper with battery operated deeper and light. The static water level was obtained as the difference between the elevation of the wells (surveyed contour values) and depths to water level (surface water levels in the wells).

To really come out with acceptable and excellent quality groundwater for irrigation, other samples from surface water bodies were also collected. The water samples were collected from the Crater Lake, Oloidian bay, Lake Naivasha, River Malewa and the Gorge spring.

Physical parameters such as electrical conductivity, pH and Temperature were measured at the time of sampling in the field since their values in the water samples might change with time and exposure to the atmosphere.

4.2.3 RESULTS OF FIELD MEASUREMENTS

The depth to water level of sampling points range from approximately 25 to 198 meters below ground level, representing shallow groundwater. The pH values of groundwater range from 6.5 to 8.6 and the field temperature varies between 21°C and 30°C. The measured electrical conductivity range from 0.43 to 1.77mS/cm.

The pH values of surface water samples range between 7.0 to 10 whiles the Electrical conductivity range between 0.19 to 12.2mS/cm with the later measured in Oloidian bay water. The temperature varies from 21°C to 27°C.

4.3 CHEMICAL ANALYSIS AND CHECKS

4.3.1 CHEMICAL ANALYSIS

In the set-up Laboratory, the water samples were thoroughly filtered with through 0.45µm in-line filters fitted with peristaltic pump. The major ion samples were kept in 250ml polyethylene bottles and acidified with concentrated HCl solution to pH less than 2 to stabilise cations and others unacidified to preserve original chloride and bicarbonate. They were well labelled and preserved in an Ice chamber.

The water samples were analysed to measure some chemical parameters such as Total hardness (Calcium, $Ca^{2+}$and Magnesium, Mg^{2+}) and Alkalinity (Carbonates, CO_3^{2-} and Bicarbonates HCO_3^-) and Chloride were measured by titration to the methyl orange endpoint. They were measured to use in the analysis of water samples for isotopic study (discussed in details) in Chapter 6.

The results of the analysis are expressed in mg/l.

4.3.2 ACCURACY AND RELIABILITY OF ANALYSIS

The three Hydrochemical data were analysed for consistency and ionic balance using the WATEVAL program developed by Hounslow of University of Oklahoma, 1995. The WATEVAL program expresses the concentration of chemical constituents into the units of milli-equivalent per litre to cater for the ionic charges of individual elements, in order to balance the sum of positive and negative charges in water sample for the Law of electroneutrality.

The program also provides in-depth information into the possible origin of water samples. The bulk of the samples had EN <5% in accordance with the Law of electroneutrality (equation 4.1), indicating reliable chemical analysis while other samples had EN>5% for example in the Dataset 2 with no analysis for fluoride. All the three datasets were accepted for Hydrochemical analysis.

The summation was taken over Na^+, K^+, Mg^{2+}, Ca^{2+}, Cl^-, HCO_3^-, and SO_4^{2-}

$$EN\ (\%) = \frac{\sum Cations - \sum anions}{\sum cations + \sum anions} * 100 \qquad 4.1$$

where cations and anions are expressed as meq/l.

The chemical analyses were carried at entirely different periods and incorporating conjunctive use of all the three analysis in hydrogeochemical assessment gave a better idea or overview about the temporal variations in the composition of the chemical variables.

4.4 SOURCE–ROCK DEDUCTION

4.4.1 INTRODUCTION

This technique provides an insight into the possible origin of a water analysis and useful as an analytical check based on mass balance approach to water quality data. Although, the most significant effect on the groundwater chemistry comes from the source of the water and the medium through which it circulates, the geology also plays an important role as it imposes its chemical composition on the groundwater system.

WATEVAL program based on the simplified mass balance approach was used to evaluate the water quality based on source rock and reactions that might have occurred to water quality during rock weathering when Ca^{2+}, Mg^{2+}, SO_4^{2-}, HCO_3^- and SiO_2 are added to water (Hounslow, 1993).

4.4.2 RESULT OF SOURCE-ROCK EVALUATION

1 Sodium and Chloride (Na^+ and Cl^-)

In comparing Na^+ and Cl^-, it is assumed that the primary source of chloride in water is from sodium chloride, directly from halite dissolution or indirectly from rainfall. The concentration of sodium exceeds Chloride ($Na^+ > Cl^-$), which indicates Na^+ source other than halite or from the dissolution of albite-plagioclase and ion exchange.

In cases where $Na^+ < Cl^-$, then there is an analytical error or composition of the water is derived from brines through reverse ion exchange or natural softening has occurred. The ionic concentrations of Na^+ and Cl^- are low in the shallow wells but increase towards the deep geothermal wells. The highest end member is the Crater Lake in the west of Lake Naivasha. The concentrations are depleted in groundwater close to the Lake Naivasha but enriched in Oloidian bay and Olkaria waters.

The high chloride content might be from chloride- rich lake sediments beneath the volcanic, which are released into solution or probably from upconing of geothermal waters. This suggests that waters from Olkaria wells might be derived from a different source or a mixture of shallow groundwater and Oloidian bay or Lake Naivasha.

2 Calcium and Sulphate (Ca^{2+} and SO_4^{2-})

In comparing sulphate and calcium contents, the primary assumption made is that sulphate is the result of direct dissolution of gypsum or neutralisation of acid waters by limestone or dolomite. The compositions of calcium and sulphate contents in shallow groundwater are such that, $Ca^{2+} > SO_4^{2-}$, which indicates Ca^{2+} source other than gypsum such as calcite/dolomite or silicates.

The geothermal waters have $Ca^{2+} < SO_4^{2-}$, which indicates the removal of Ca^{2+} from solution which might be due to precipitation of calcite or ion exchange reactions.

3 Bicarbonate and Silica (HCO_3^- and SiO_2)

This comparison distinguishes carbonate weathering from silicate weathering. In the shallow groundwater, $HCO_3^- >> SiO_2$ which indicates carbonate rather than silicate weathering while the deep geothermal waters have $HCO_3^- << SiO_2$, indicating silicate weathering of rocks in the geothermal fields.

4 Lithium

This is a trace element with normal concentration less than 0.1mg/l (Hounslow, 1995). The Hydrochemical dataset 3, which contains this element, was used to determine the distribution of tritium concentration in waters in the study area. The concentrations of tritium are very high in Kongoni wells but depleted in the wells north of Lake Naivasha. The concentration increases with increasing temperature. In the north of the study area where temperatures are low, the concentrations are low as compared to the values in the southern wells.

Hounslow (1995) indicated that in subsurface waters, the tritium content may increase with increasing temperature, but magnesium under the same tends to decrease and Lithium is absorbed by illite and other clays and seawater contains 0.17mg/l of lithium.

Kongoni and Labelle wells have Lithium concentration of about 0.12mg/l that resembles that of seawater with 0.17mg/l Li (Hydrochemical dataset 3).

4.4.3 CONCLUSION FROM SOURCE-ROCK DEDUCTIONS

The WATEVAL program used to infer the source-rock of the waters in the study area indicated granitic type of weathering in most water samples whiles others suggested silicate and carbonic weathering of underlying bedrock material.

The chemical analysis of water samples show that most of the groundwater might have acquired their chemistry from weathered rocks and other underlying materials in the aquifer. The mineralogy in the study area has significant effect in composition of water. The study area is composed primarily of volcanic minerals and the weathering of these rocks produces waters rich in Na^+ and HCO_3^-.

(Morgan, 1998) indicated that the composition and abundance of plagioclase as well as sodic amphiboles is the primary influence on Na^+ and Ca^{2+} in the study area. As the water moves into the shallow groundwater, sodium increases more rapidly indicating continued weathering (Ojiambo, 1996).

The groundwater is composed of mainly sodium bicarbonate in the shallow wells and sodium chloride in the geothermal wells. The different groundwater types probably reflect the diversity and subsequently the products of weathering of the types of bedrock in the study area. The main source of the groundwater might be from chemical weathering of silicate and carbonate as envisaged in the deduction.

The high concentration of chloride suggests that the chemistry of the water is greatly influence by weathering or dissolution of chloride- bearing rocks such as halite, which releases enormous amount of chloride ions from the underlying rocks.

(Gaudet and Melack) indicated chemical weathering of the rocks as the source of major ions in the study area. (Gibbs, 1970) this fulfils the assertion that during return of water to the ocean, its composition is altered by rock weathering and evaporation (Appelo and Postma, 1993). The rock type and their weathered products have contributed immensely to the chemistry of the groundwater in the area.

4.4.4 PRESENTATION OF WATER QUALITY DATA

1 Trilinear Piper Diagrams

The Piper diagrams were generated from PLOTCHEM computer program. The diagrams were used to determine the water types and divides water into four basic types according to the placement near the corners of the diamond part of the diagrams.

From the two plots, the cations are mainly composed of Sodium, Potassium and Calcium while the anions are Bicarbonate and Chloride types. The bulk of the water plot toward the lower corner of the diamond indicating that the waters are primarily composed of alkaline carbonates (Na^{+}+K^{+}) and (HCO_3^{-}+CO_3) (figure 20).

Other waters plot on a straight line within the diamond whiles some extend towards the cation and anion triangle indicating precipitation of calcite or dissolution of calcium and bicarbonate.

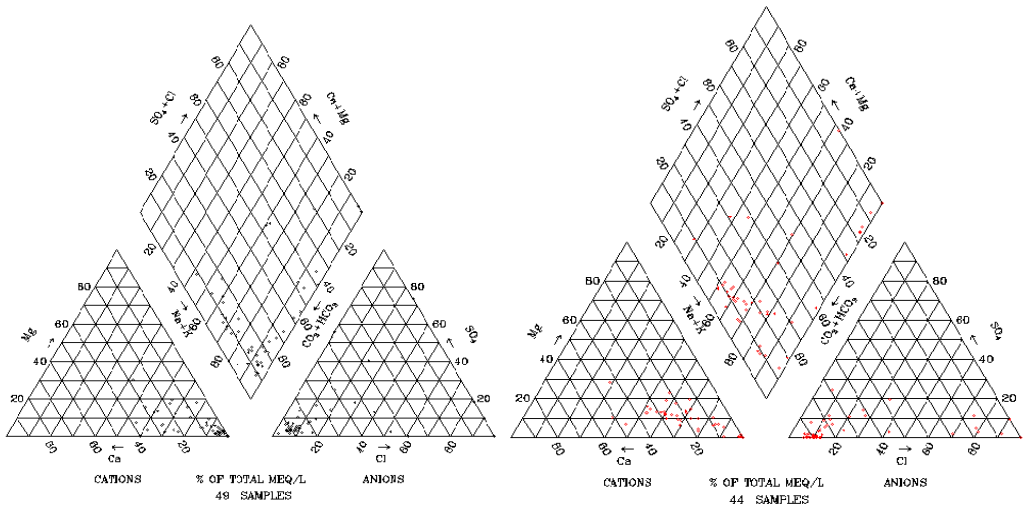

Figure 22: Trilinear Piper Diagrams of Hydrochemical Datasets 1 and 2.

2 TDS-Ionic ratio Plots (Gibbs, 1970)

This approach was used to obtain an overview of controlling processes on solute compositions in water by Gibbs (1970). The relative fractions defined by Na/(Na+Ca) and Cl/(Cl+HCO_3) of the cations and anions were plotted against the total dissolved solid and are shown of figures 21 and 22.

The water compositions are displayed as a function of the dominance of end-member components Na^{+} and Cl^{-} at one end and Ca^{2+} and HCO_3^{-} at the other end in the plots (Hounslow, 1995).

The groundwater from the shallow wells has very low total dissolved solids and their compositions are found at the lower end of the TDS axis, indicating short residence time of the shallow groundwater in the area. The relative content of Ca^{2+} and HCO_3^{-} increases in shallow groundwater and the water composition moves upward to the centre of the plot, which could be due to weathering of rocks which releases enormous amount Ca^{2+} and HCO_3^{-} into solution.

This indicates that the shallow groundwater may have acquired their chemistry from the weathered materials from the underlying or parent rocks.

In the geothermal, Lakes Oloidian and Crater waters, there is dominance of Na^{+} and Cl^{-} coupled with high TDS. In the geothermal waters, Ca^{2+} and HCO_3 contents are low and might have been lost by

precipitation of $CaCO_3$ and evaporation. The three waters plot at the terminal part of the upper branch and resemble seawater composition dominated by Na^+ and Cl^- (figures 21 and 22).

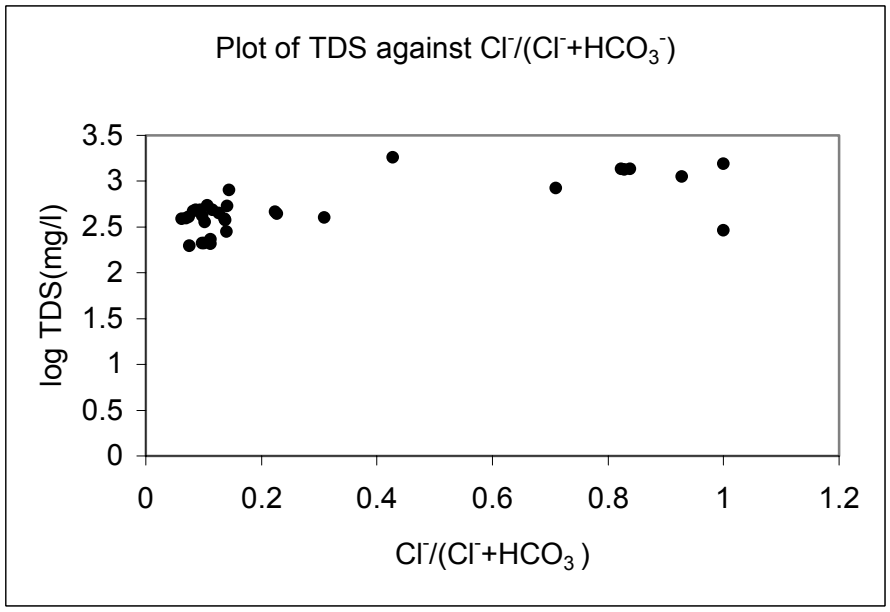

Figure 23: Plot of TDS Vs Cl/(Cl+HCO_3) ratio.

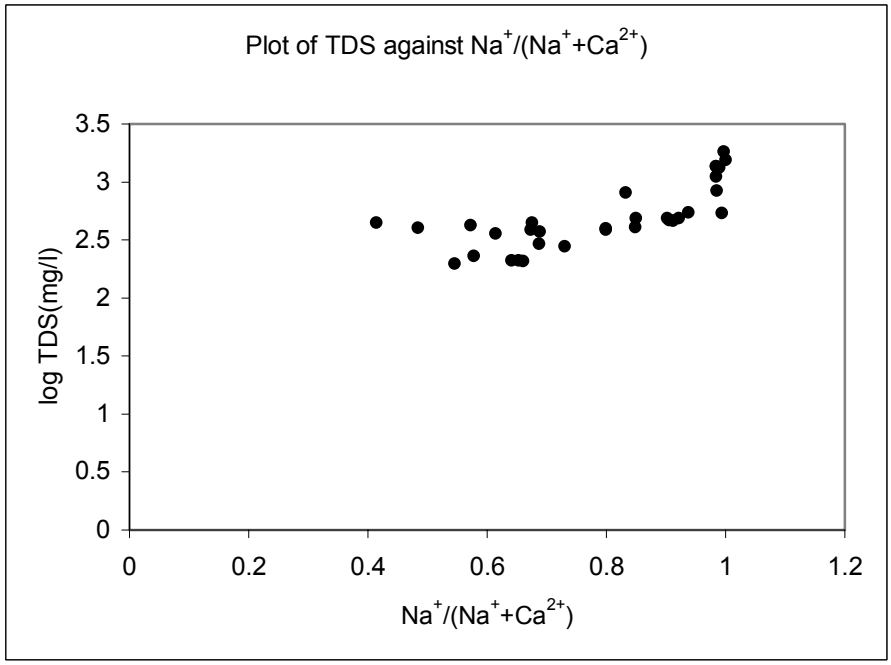

Figure 24: Plot of TDS Vs Na/(Na^++Ca^{2+}) ratio.

3 Stiff and Radial Diagrams

The stiff diagrams were generated with PLOTCHEM program, which plot anions and cations in meq/l on the three axes of the diagrams.

The stiff and radial diagrams show the different water types (figures 23 and 24). They were used to represent the samples graphically in order to ascertain the dominant cations and anions and the chemical trend. The chemical constituents are recognised from the shape and width of the Trilinear and stiff diagrams (Appelo, 1993).

The most dominant cation and anion are Na^+, HCO_3^- respectively and less dominant anion, Cl^-(figures 23 and 24). The Na^+ and HCO_3^- components are found in the shallow groundwater while Na^+ and Cl^- components are predominant in closed basins (Oloidian and Crated Lakes) and geothermal waters. The waters in the study area are therefore sodium bicarbonate and sodium chloride types.

This might be attributed to ionic exchange and dissolution of rock, which have contributed immensely to the type of groundwater in the study area. The dominant water types are confirmed by the Trilinear Piper diagrams (figure 20) and also from the source–rock deduction.

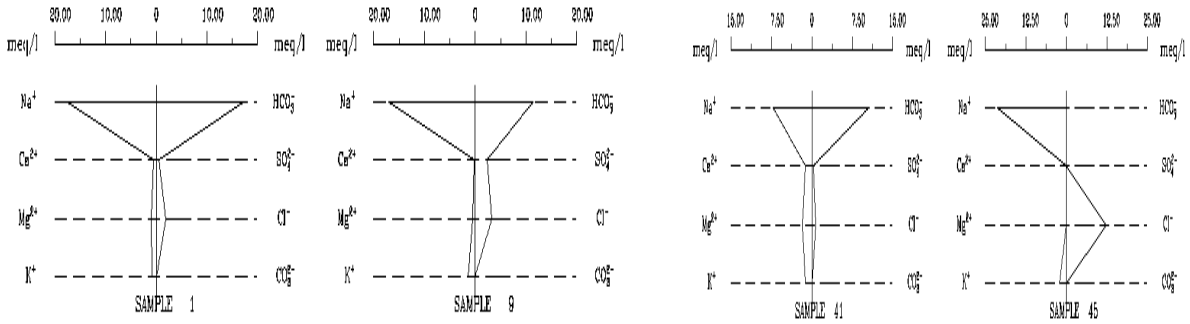

Figure 25: Stiff diagrams of groundwater in the study area from Hydrochemical Dataset 1.

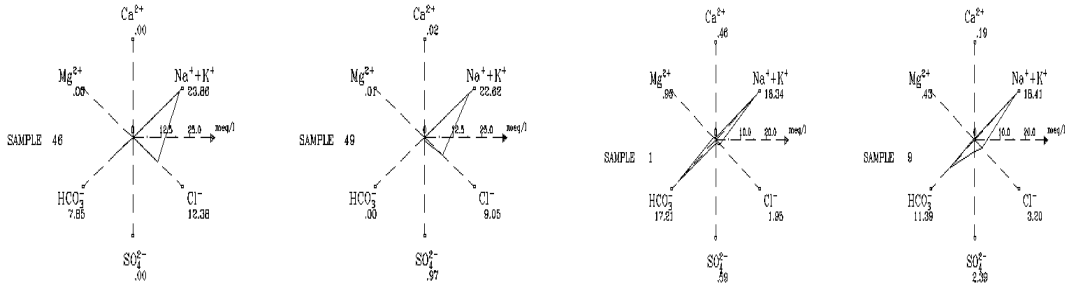

Figure 26: Radial diagrams of groundwater in the study area from Hydrochemical Dataset 1.

4 Ionic concentrations of chemical variables from Binary plots

The chemical variables are represented graphically in the form of binary plots in figures 29 and 30 from datasets 1 and 2. The mean concentration of the cations is in the order of Na>K>Ca>Mg while for anion it is HCO_3>Cl>SO_4>F in the three Hydrochemical datasets.

The rainwater lie at the lower dilute side of the plots, which suggests is depleted in major concentrations compared to other waters. The shallow groundwater plots as intermediary water and form clusters on most of the plots. They are enriched in sodium, bicarbonate and other variables and form high concentration end-members (figure 29).

A plot of Na Vs HCO3 shows an increase in sodium with bicarbonate and increases in sodium with chloride. They are the Na-HCO3 waters and are recognisable on the binary plot, where they lie at highest ionic concentration portion of the Na^+ Vs HCO_3^- plot (figure 29).

The deep geothermal waters made up of high concentration of sodium and chloride fall at the upper portion of the Na^+ Vs Cl^- plot and form the predominant Na-Cl waters (figure 29). However, they are depleted in Ca and Mg compared to other waters.

Ojiambo 1992 indicated that the geothermal waters are extremely depleted in Ca and Mg compared to the shallow groundwater by about two orders of magnitude and attributed this to removal of these ions from solution during water-rock reactions and deposition of calcite and hydrothermal alteration of minerals such as chloride.

4.5 CHARACTERISATION OF GROUNDWATER

The water types in the study area are characterised based on their chemical composition. They are determined from the Piper diagrams generated with PLOTCHEM program (figure 4.2). The diamond part of the diagram was used to characterised different water types, according to the placement at the corners of the diagram (Hounslow, 1995).

The waters from the shallow aquifers in the south of area are characterised by the dominance of calcium, magnesium and bicarbonate but have relatively low concentration of chloride, sodium and sulphate. They are therefore composed of chemical constituents of HCO_3^- (weak acid) over constituents such as Cl^- and SO_4^{2-} (strong acids).

Further south towards the deep aquifers are waters dominated by sodium, potassium, and chloride but low composition of calcium, magnesium, and bicarbonate except in well OW-101, where an extremely higher values were observed. The degree of concentration of the cation Na^+, Ca^{2+}, K^+ and Mg^{2+} correlates directly with the proportion of these elements in the underlying rocks.

From the placement of the water on the Trilinear Piper diagram (1994) and HYDROWIN program, water in the study area are grouped predominantly into three types;

1.$Na\text{-}HCO_3$

2.Na-Cl

3.$Ca\text{-}Na\text{-}HCO_3$

1 $Na\text{-}HCO_3$ Waters

These water types are found in the shallow groundwater wells. They constitute 75% of the total number of water samples, having an appreciable amount and dominant end members of $Na\text{-}HCO_3$. This is usually an indication of cation-exchange processes as proven by the ionic ratios from the source rock evaluation. Darling (1996) indicated that all waters in the rift valley are of the $Na\text{-}HCO_3$ type, in certain cases reaching very high concentrations.

These are often referred to as exchange waters as there is more HCO_3^- than the available alkali -earth metals ions such as $Ca^{2+}$and Mg^{2+} in equivalent concentration. These excess bicarbonates are released to cause an enormous amount of alkali ions in the form of Na^+ into the solution by exchange reaction with cation exchanges such as in clay and other minerals, which are part of the aquifer materials. This enriches the shallow groundwater with $NaHCO_3^-$.

2 Na-Cl Waters

These are mainly sodium chloride waters from the geothermal, Crater Lake and Oloidian bay waters. The Oloidian and Crater Lake waters are interpreted to made up Na-Cl sediment deposition, which have undergone significant evaporation and evapotranspiration from vegetation. The Na-Cl geothermal waters are interpreted as a mixture of recharge waters from the rift escarpments and evaporated water from the Oloidian bay-Lake Naivasha waters (Ojiambo, 1996). This is evident in increase in TDS values southwards from the lake towards the geothermal wells.

The water from the rift flank percolates deep into the hot geothermal field through faults and the hot water mixes with the shallow groundwater to form the Na-Cl rich geothermal waters (Ojiambo, 1992). In this area, groundwater tends to acquire chemical composition similar to that of seawater, thus having more dissolved solids and Chloride ions. This is evident in the Hydrochemical dataset 2, where higher concentrations of $Na^+$and Cl^- are recognisable in the geothermal waters from wells OW-2, OW-725, OW-728, OW-708 and OW-903. Omenda, 1998 indicated that the fluid chemistry at Olkaria broadly falls into two types: predominantly neutral pH-chloride and exclusively bicarbonate rich waters at the east and west of Olkaria hill respectively.

The high chloride content might be from chloride- rich lake sediments beneath the volcanic, which are released into solution or probably from upconing of geothermal waters. This suggests that waters from Olkaria wells might be derived from a different source or a mixture of shallow groundwater and Oloidian bay or Lake Naivasha.

This change in water chemistry compared to the shallow groundwater might be attributed to long residence time for reaction with underlying aquifer material through confinement of the waters within clay-rich aquifers and probably evaporation of concentration of chemical constituents in the process of recharge.

3 Na-Ca-HCO_3

This type of water is found in wells such as C7829, C4397, C4420, C579 and C2660 close to the Lake Naivasha as well as river samples. This water type constitutes about 50% of total number of samples (Hydrochemical dataset 2) and has an appreciable amount of Na-HCO_3.

The presence of calcium clearly distinguishes them from other water types in the area. The chemistry of this water type might be from calcite precipitation and high rate of evaporation in the Lake Naivasha study area.

Plate 4: Crater Lake (highly saline water body) in the west of Lake Naivasha, Kenya.

4.6 EVALUATION OF GROUNDWATER AS POTENTIAL IRRIGATION WATER

4.6.1 GENERAL

The chemical character of groundwater determines its quality and utilisation. The quality of the groundwater for irrigation is evaluated based on various agricultural water criteria. The criteria for classification of suitability of water for irrigation are often evaluated by Total dissolved solids (TDS) and sodium absorption ratio (SAR) if all other factors such as amount of Irrigation water and climatic conditions have been fulfilled or satisfied. These represent anions and cations of elements in water sample determine the usability of the water for irrigation.

In irrigation waters, USDA classification is often adapted to ensure that the concentrations of water samples are within the maximum permissible level.

4.6.2 GOVERNING PRINCIPLES OF IRRIGATION WATER QUALITY

4.6.2.1 SODIUM ABSORPTION RATIO (SAR)

The sodium absorption ratio, SAR is defined by the formula,

$$SAR = \frac{m_{Na^+}}{\sqrt{\frac{(m_{Ca^+} + m_{Mg^+})}{2}}} \qquad 4.2$$

It is a measure of the sodicity/alkalinity hazards of irrigation water (Richards, 1969).

The SAR measures the degree to which sodium in irrigation water replaces the absorbed (Ca^{2+}+Mg^{2+}) in the soil clays and damages the soil structure.

The quality of groundwater is not only determined by SAR in water at the time of application, since the ratio of Na/Ca+Mg concentration in water may change as a result of reaction in the soil, leading to precipitation of calcite and the effect of evapo-transpiration. These phenomena often result in SAR values being above the measured (Appelo and Postma, 1993).

The initial SAR values were computed using Hydrochemical datasets 1 and 2. They range between 0.2-350 and 0.14-1039 and adjusted SAR values range from 0-102 and 0.2-49 in water samples respectively. Adjusted SAR values were determined to take into account calcite precipitation, since the study area lies within semi -arid environment where evapotranspiration values are very high and precipitation of calcite very prevalent.

Ayers and Westcot (1985) postulated a formula for adj. SAR given by:

$$Adj.SAR = SAR\,(1 + 8.4 - pH) \qquad 4.3$$

The SAR -Conductivity plot on the US salinity laboratory diagram was generated in WATEVAL using Hydrochemical dataset 2 (from the University of Nevada). This contains in-situ electrical conductivity of the water samples and was used to determine the suitability of water for irrigation according to the SAR and salinity hazards on the US Salinity Laboratory diagram (figure 25).

The shallow groundwater falls into four classes, C1-S2, C2-S1, C3-S1, C3-S2 and geothermal waters into C3-S4 and C4-S4. The waters are thus classified into low to very high salinity water and low to very high sodicity waters (figure 25).

These were not verified in accordance with any recent soil information, as the soil analysis was not available to assess the validity of the calculated results.

Figure 27: SAR-Conductivity Plot of Hydrochemical Dataset 2.

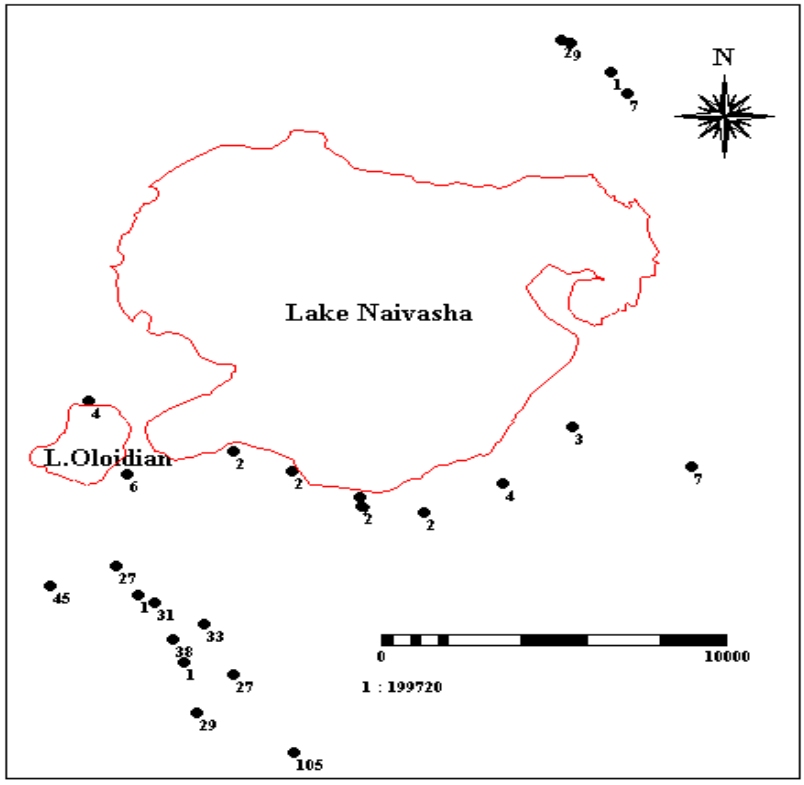

Figure 28: Spatial distribution of SAR in the study area.

4.6.2.2 EXCHANGEABLE SODIUM RATIO (ESR) ON SOIL PROPERTIES

The main source of the formation and occurrence of salt affected soils is the presence of dissolved sodium salts in the soil and/or exchangeable Na^+ ions in the soil adsorption complex. The two

phenomena, directly or indirectly lead to bad physical structure of the soil as the permeability is reduced due to high degree of swelling of particles that make up the units of soil and when sodium (Na^+) makes up about 15% of the exchangeable cations (Appelo and Postma, 1993).

The exchangeable sodium ratio (ESR) is thus given by the formula

$$\frac{\beta}{1-\beta} = K^{G}_{Na\backslash Ca} * \frac{Na}{\sqrt{Ca+Mg}} \qquad 4.4$$

Where the quotient $\frac{\beta}{1-\beta}$ is termed ESR, which is related to the activity of Na^+ over the square root of the sum of Mg^{2+} and Ca^{2+} activities and $K^{G}_{Na\backslash Ca}$ is the Gapon constant equal to 0.5.

In simplified form (Appelo 1993), ESR=0.0158*SAR 4.5

The criteria value 1.58 is attained in waters with SAR equal to 10 (Appelo and Postma, 1993).

The suitability of groundwater for irrigation is based on the effects on the mineral constituents of water on both the plant and the soil. The salt may retard the growth of plants and high sodium water reacts with the soil to reduce its permeability.

The bulk of the shallow groundwater has low SAR values (less than 10) and the ESR values are below the critical value. The shallow groundwater has very minimal exchangeable sodium on the soil. This will minimise the sodium saturation of soil when irrigating and boast infiltration rate in the soil. Further south of the Lake Naivasha, the SAR in groundwater exceeds the critical value and infiltration rate will be reduced as soil properties will deteriorates to sustain irrigation.

Class of water	Ec(mS/cm)	SAR	SO_4^{2-}	Cl^-	Na^+ (%)
Excellent	0.25	1	4	4	20
Good	0.25-0.75	1-10	4-7	4-7	20-40
Permissible	0.75-2.0	10-18	7-12	7-12	40-60
Doubtful	2.0-3.0	18-26	12-20	12-20	60-80
Unsuitable	>3.0	>26	20	20	80

Table 8: Permissible limits for Class of water for irrigation (Adapted from James et al, 1982.)

Well	SAR	Ec µS/cm	Salinity hazards	Sodium (alkali hazards)	Symbol of water Class
C10887	9.23	800	high	low	C3-S1

C3366	1.25	920	high	low	C3-S1
C3677	1.48	796	high	low	C3-S1
C3675	6.87	1620	high	low	C3-S1
C210	3.17	774	high	low	C3-S1
C562	3.0	779	high	low	C3-S1
C567	6.35	976	high	low	C3-S1
C1707	4.52	963	high	low	C3-S1
C2071	1.74	772	medium	low	C3-S1
C7829	2.02	781	high	low	C3-S1
C4397	1.74	715	medium	low	C3-S1
C4420	1.70	867	high	low	C3-S1
C2660	3.42	812	high	low	C3-S1
C579	2.09	560	medium	low	C3-S1
UW-1	1.35	832	high	low	C3-S1
C4366	4.77	888	high	low	C3-S1
C630-D	24.24	1071	high	high	C3-S3
OW 101	34.40	3650	Very high	Very high	C4-S4
OW 2	26.82	2250	high	high	C4-S3
OW 26	24.68	1676	high	high	C3-S3
OW 725	30.92	2740	Very high	Very high	C4-S4
OW 728	35.02	2740	Very high	Very high	C4-S4
OW 708	29.81	2740	Very high	Very high	C4-S4
OW 903		2310	high	Very high	C3-S4

Table 9: Water class according to SAR and salinity hazards (US Salinity Laboratory diagrams).

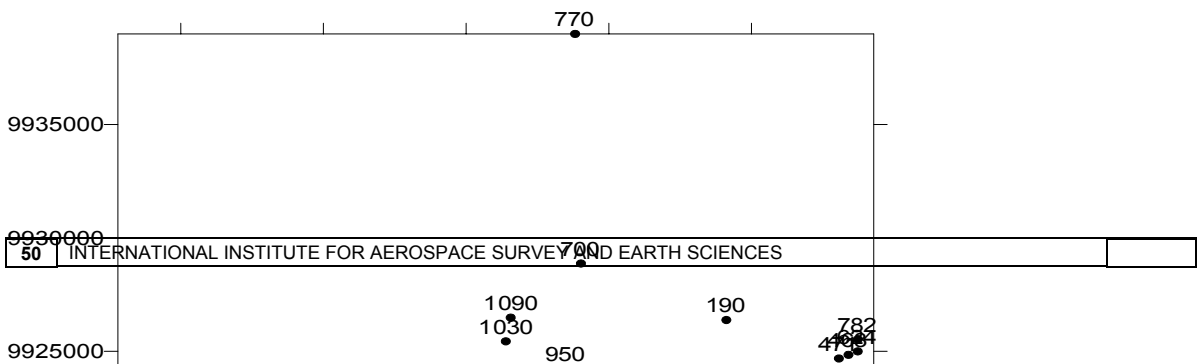

Figure 29: Spatial distribution of Ec in the study area (Hydrochemical dataset 2).

4.7 ANALYTICAL RESULTS AND DISCUSSION ON SAR AND SALINITY HAZARDS IN WATER SAMPLES

The SAR distribution is depicted in the figure 4.8. The value range between 1.1-24.2 in the water samples from shallow wells whiles those from deep geothermal well ranges from 34.4-1039 (Appendix A-4). The water samples from wells close to the lake in the southern part have SAR less than 10 indicating low to medium sodicity hazards except water from well C630-D, which exhibits very high sodicity hazards quite similar to the geothermal waters. The shallow groundwater ranges from medium to high in salinity and low to high sodicity hazards.

The geothermal and Oloidian bay waters have prevalent high TDS and SAR values, hence they are they are more saline and sodic compared to those from the shallow wells close to the Lake Naivasha. They plot in sections C3-S1, C3-S2, C3-S3, C3-S4 and C4-S4 on the US Salinity Laboratory diagram (figure 4.7) and have poor water quality for irrigation. The high TDS might be due to the decrease in the concentration of calcium further south through precipitation of calcite and high rate of evaporation.

This high value of SAR affects the long-term use of water as it reduces the permeability of the soil and occurs when irrigation water contains relatively more sodium ions than calcium and magnesium ions.

The accumulation of sodium ions will break down the soil aggregates required for good soil structure for free movement of water and air through the soil.

4.8 CONCLUSION ON WATER QUALITY AND USABILITY FOR IRRIGATION

The suitability of groundwater for irrigation is determined by the effect of mineral constituent of the water on both the plant and soil. The groundwater types have been identified to be of predominantly

Na-HCO3 and Na-Cl in the study area. Most of the shallow well waters have low to high salinity hazards and low to moderate Sodicity hazards.

They are the contributing factors of the Irrigation water criteria, which are dependent on water conductivity and the sodium absorption ratio in water applied to irrigate. The low SAR values and medium to high salinity hazards in the waters from shallow wells make the waters good to moderate for irrigation based on the US Salinity Laboratory diagram (figure 4.7) and water quality standards for irrigation (Table 4.4).

The shallow well C630-D water has high salinity and very high sodicity hazards as it behaves as the transit point between the shallow wells and deep geothermal wells. The presence of salt will limits the uptake of water through modification of osmotic pressure and chemically by metabolic reactions. Beyond well C630-D, there is sudden increase in Total dissolved solids (TDS) and SAR values, higher than the maximum permissible levels. The groundwater therefore deteriorates in quality for irrigation.

The groundwater in these vicinities are unsuitable and could hardly be used for irrigation unless otherwise treated to reduce the salinity and sodicity hazards by mixing with fresh water form the lake Naivasha.

In conclusion, groundwater from the shallow wells in the Sulmac, Longonot and Oserian areas are therefore of good quality for irrigation, except C630-D waters and further south close to the Olkaria fields.

CHAPTER 5

5 STATISTICAL AND GEOSTATISTICAL ANALYSIS

5.1 INTRODUCTION

This chapter deals with Statistical and Geostatistical analysis on the chemical variables to determine the relationship between water samples made up of different chemical components in the study area.

There exist more than one explanatory and independent variables in water in which a slight change in one variable affects the other. The determination of trends in a collection of water analysis is accomplished using X-Y plot (Hounslow, 1995).

The Hydrochemical datasets 1 and 2 were used to make the X-Y plots to obtain the coefficient of correlation between pairs of chemical variables. Statistical analysis using product-moment coefficient of correlation was adopted to determine correlation between the pairs of parameters such as Na^+, K^+, Ca^{2+}, Mg^{2+}, Cl^-, $SO_4^{2-}$and HCO_3^- based on X and Y plots.

5.2. LINEAR AND BINARY PLOTS OF CHEMICAL VARIABLES

The correlation between the chemical variables was obtained from X-Y plot on a linear scale. However, the graphical representations were done on a logarithmic scale (binary plot) to have a clearer pattern of distribution of different waters and reduce the variability of the distribution, as they will have on a linear scale. A log-transformation is thus most frequently used for data transformation when working with geochemical data. The distributions are depicted on the binary plots in figures 28 and 30.

5.2.1 CORRELATION IN HYDROCHEMICAL DATASET 1

In dataset 1, the correlation between TDS and Ec could not be established, as the electrical conductivity data was not included in the dataset. There is weak correlation between some of the variables: Na and K, have the correlation coefficient of 0.26; Ca and Mg (r=0.5); Ca and HCO_3 (r=0.1); pH and HCO_3 (r=0.2); Na and Cl (r=0.56). However, a seemingly high correlation was ascertained between Na and HCO3 (r=0.78).

5.2.2 CORRELATION IN HYDROCHEMICAL DATASET 2

From Hydrochemical dataset 2, the correlation between the Hydrochemical parameters were obtained from X-Y plots of Ec and TDS, pH and HCo_3^-, $Ca^{2+}$and Mg^{2+}, Na and HCO_3^-, Na^+ and K^+, HCO_3^- and Cl^-, Na^{2+} and Cl^-, pH and Cl^- as well as Na^{2+} and HCO_3^-.

The relationship between TDS and Ec is near perfect, with the correlation coefficient being very high at 0.98. There are also strong correlation between Na^+ and HCO_3^- with r=0.79 and also between Na^+ and Cl^- with r=0.75. Weaker correlation was obtained between pH and Cl^- (r=0.56), pH and HCO_3^- (r=0.12), HCO_3^- and Cl^-(r=0.32). However, a very weak inverse correlation was obtained between (Mg^{2+} and Cl^-) and Ca^{2+} and HCO_3^- with r=-0.09 and -0.11 respectively.

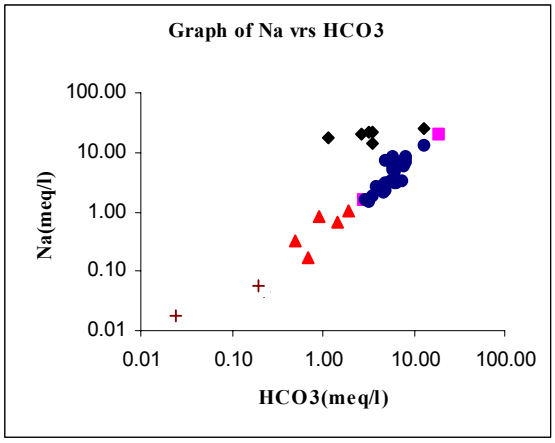
Graph of Na vrs HCO3
Na(meq/l)
100.00
10.00
1.00
0.10
0.01
0.01
0.10
1.00
10.00
100.00
HCO3(meq/l)

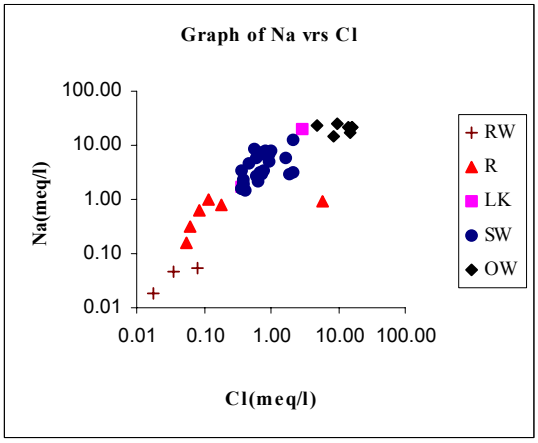
Graph of Na vrs Cl
Na(meq/l)
100.00
10.00
1.00
0.10
0.01
0.01
0.10
1.00
10.00
100.00
Cl(meq/l)
RW
R
LK
SW
OW

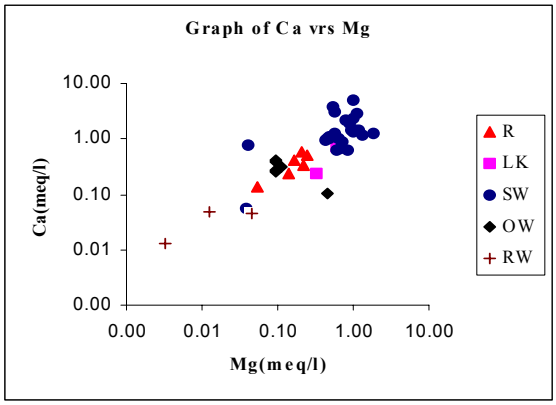
Graph of Ca vrs Mg
Ca(meq/l)
10.00
1.00
0.10
0.01
0.00
0.00
0.01
0.10
1.00
10.00
Mg(meq/l)
R
LK
SW
OW
RW

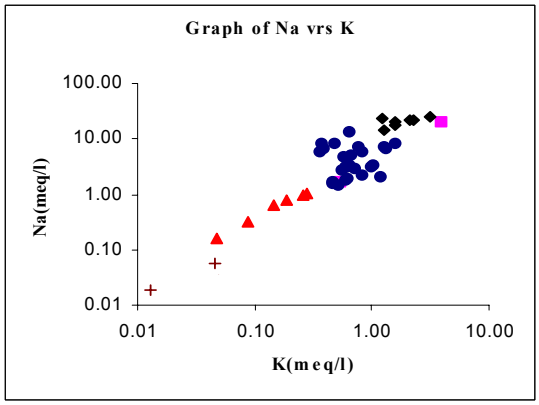
Graph of Na vrs K
Na(meq/l)
100.00
10.00
1.00
0.10
0.01
0.01
0.10
1.00
10.00
K(meq/l)

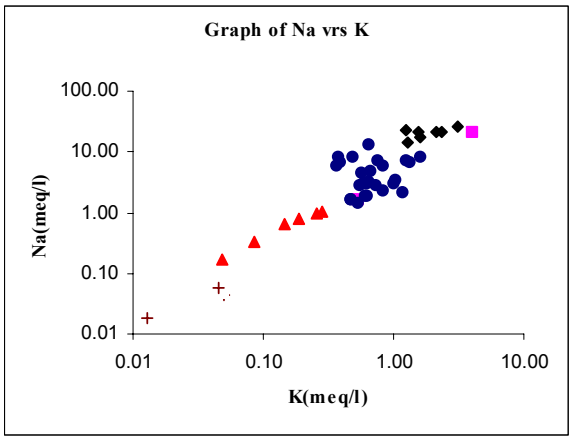
Graph of Na vrs K
Na(meq/l)
100.00
10.00
1.00
0.10
0.01
0.01
0.10
1.00
10.00
K(meq/l)

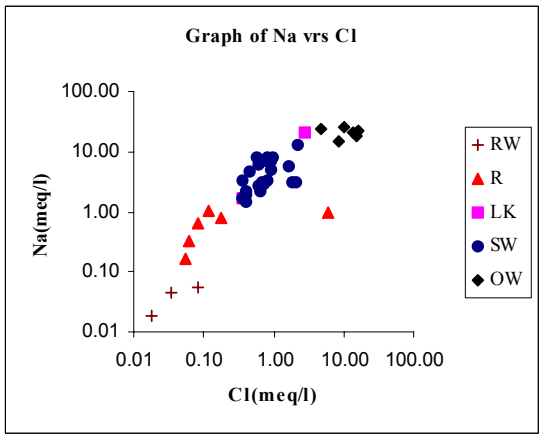
Graph of Na vrs Cl
Na(meq/l)
100.00
10.00
1.00
0.10
0.01
0.01
0.10
1.00
10.00
100.00
Cl(meq/l)
RW
R
LK
SW
OW

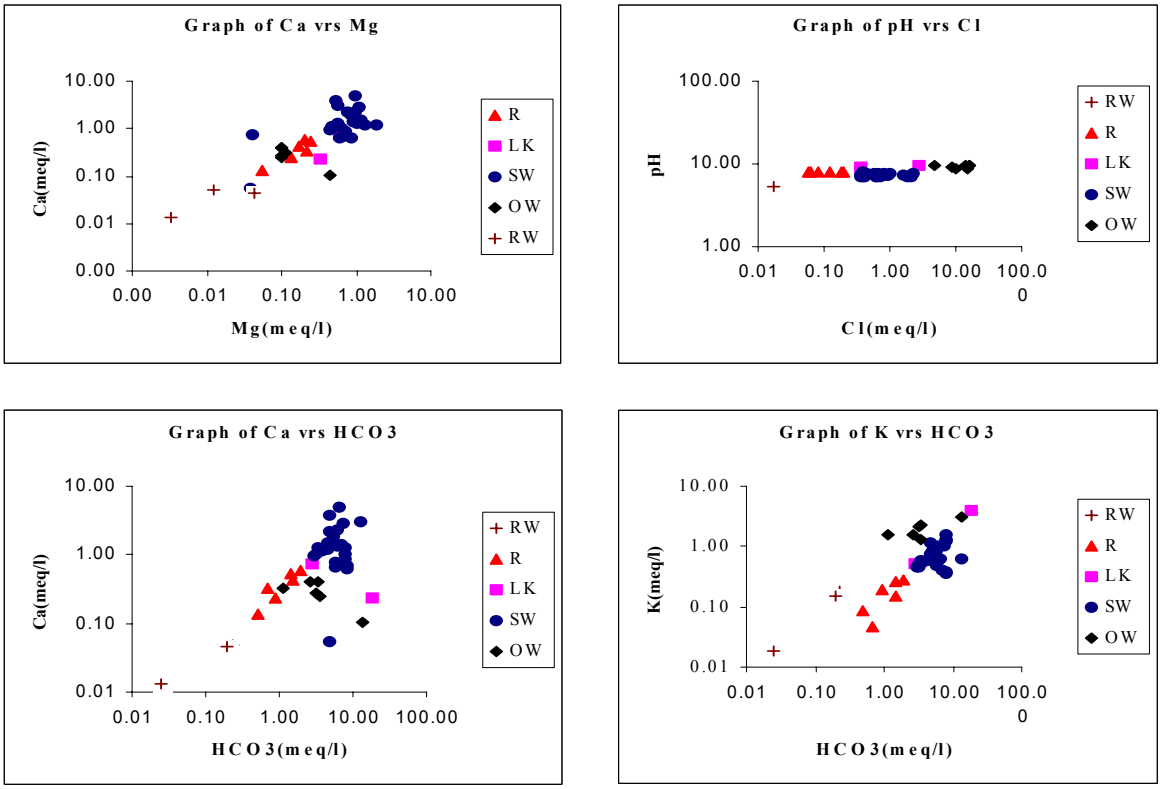

Figure 30: Binary plots of chemical variables (Hydrochemical dataset 2).

Hydrochemical variables	Correlation coefficient(r)
Na and HCO_3	0.78
Na and K	0.26
Ca and Mg	0.50
Ca and HCO_3	0.10
Na and Cl	0.56
pH and HCO_3	0.20

Table 10: Correlation between some of the chemical variables (Dataset 1).

Hydrochemical variables	Correlation coefficient (r)

TDS and Conductivity	0.98
Na and HCO_3	0.79
Na and Cl	0.75
pH and Cl	0.56
pH and HCO_3	0.12
HCO_3 and Cl	0.32
Ca and HCO_3	-0.11
Mg and Cl	-0.09

Table 11: Correlation between some of the chemical variables (Dataset 2).

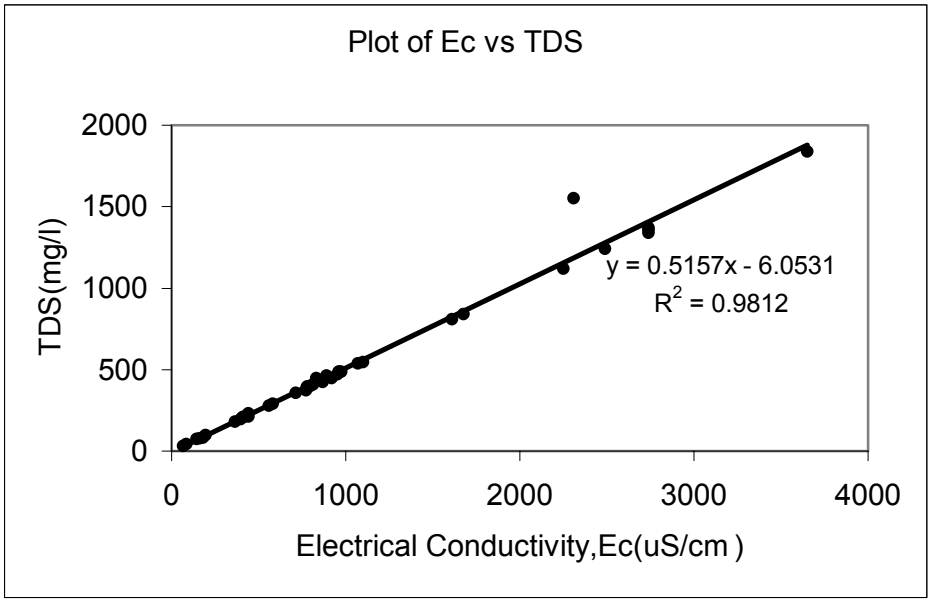

Figure 31: Linear Plot of Ec Vs TDS for Hydrochemical dataset 2.

5.3 DISCUSSION ON STATISTICAL ANALYSIS

From the results of the bivariate statistics, there is strong positive correlation between some pairs of chemical variables from the scatter plots whiles other show very weak linear correlation/ relationships.

The correlation coefficients between Na and HCO3 from both Hydrochemical datasets 1 and 2 was similar with (r=0.78 and r=0.79) respectively. The values from Na and Cl was (r= 0.56 and r=0.75) which are statistically different. They were significant at $p<0.05$ from t-test analysis.

Though, good correlation was obtained between Na and HCO3, sodium increases with increasing bicarbonate in the shallow groundwater but the opposite was envisaged in the geothermal waters, where sodium decreases with decreasing bicarbonate. However, the close correlation coefficients in the two cases support that assertion that the waters in the study area are predominantly NaHCO3 and NaCl water types. The good correlation of Na Vs Cl, Na Vs HCO_3 and pH Vs Cl may be the results of a number of possible processes such as addition of ions via water-rock interactions and mixing of two different water bodies with different end member compositions. Reimann and Filmoser (1999) indicated that the strong skew in datasets from geochemistry and environmental sciences is often that

the samples represent more than one population/process. This is evident in the three hydrochemical datasets of samples taken from different rock units that make up the aquifers.

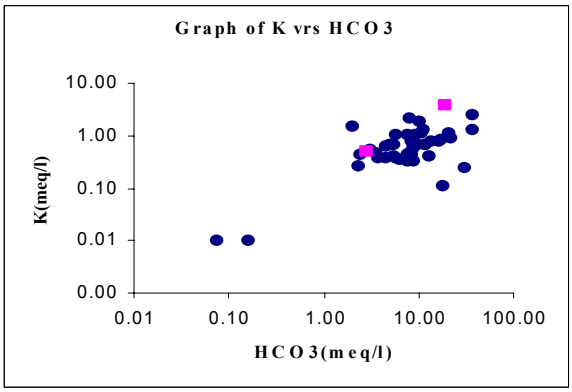

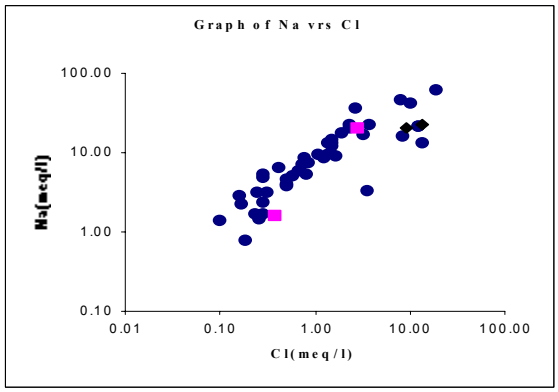

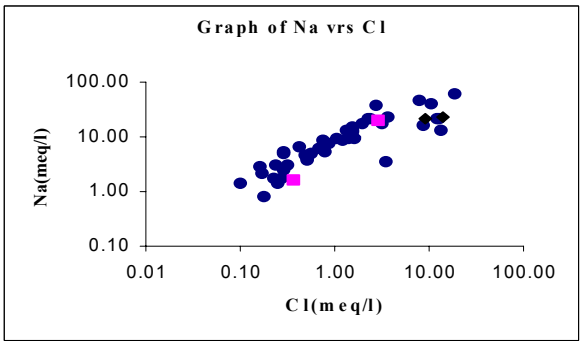

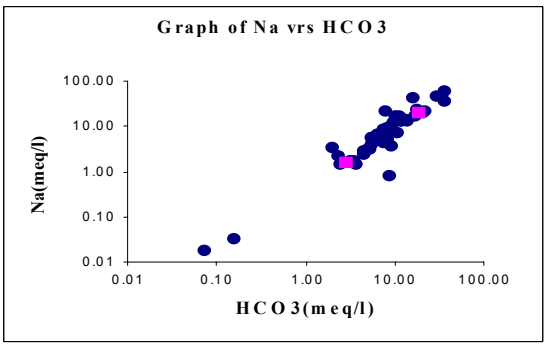

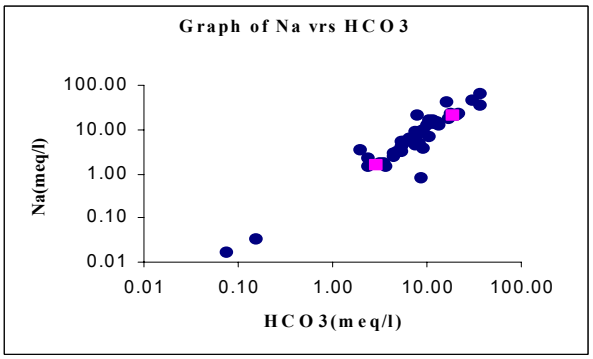

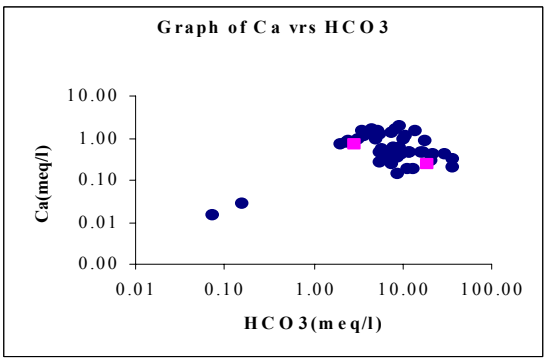

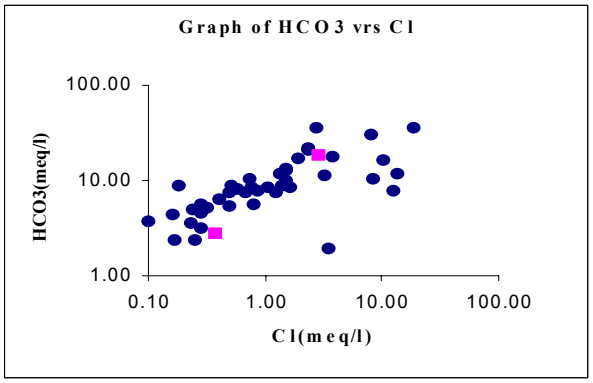

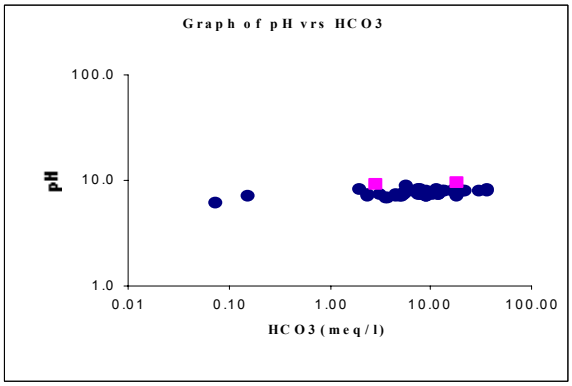

5.4 GEOSTATISTICAL ANALYSIS

5.4.1 INTRODUCTION

Compositions of Hydrochemical elements are functions of space and are often highly variable (De Marsily, 1986). However, the spatial variability is not purely random in general (Gieske, 1999). If measurements are made at two different locations, the closer the measurements are to each other, the closer the measured values.

Variogram analysis provides evidence into the extent of correlation amongst chemical variables and the components are made up the Sill, Nugget and Range. These components are used for kriging in GIS environment to estimate values for points or locations that were not sampled. The Variogram tends towards an asymptotic value equal to the variance called the sill of the Variogram and the distance at which the Variogram reaches its asymptotic value is called the range. Variograms often show a jump at the origin, which is the result of nugget effect.

5.4.2 RESULTS OF INDICATOR VARIOGRAMS AND STRUCTURAL ANALYSIS

5.4.2.1 VARIOGRAMS

The Semi-Variograms generated for all the seven chemical constituents are depicted in figure 33. They show pure nugget effect and could be associated to the fact that the samples have not been collected within sufficient small interval (scale) to show continuous behaviour of the phenomenon. This is due to the fact that at large distances, points play vital role in Variograms analysis and may introduce errors into the estimation.

Gieske, (1999) indicated that the Variograms become more and more complex as the distance increases and express pure random phenomenon without spatial structure This effect is often minimised or corrected by adding the nugget value to the Variogram to make the model behave as if it starts from the origin.

5.4.2.2 STRUCTURAL ANALYSIS

Structural analysis was performed to fit semi-variogram model to the indicator Variograms. However, no definite models were found to fit into the Semi-Variograms. There was no clear-cut spatial correlation as the Variograms reflected pure nugget effect. This is proven in analysis and discussions in subsection 5.3.

In Ilwis, Omni-directional and bi-directional options for anisotropy were incorporated at various lag spacing of 1.5km, 2km and 5 km to minimise the spatial variability in the chemical variables. The scale was further reduced 500m and 1km but could not reveal any spatial correlation data points were limited at these lag spacing. The output Variograms could still not be fitted with semi-variogram models indicating that there is absence of spatial dependence at the scale where samples were taken.

5.5 CONCLUSION

The non-spatial correlation of chemical variables discussed above is plausible in the study area. The wells in the area are not close to each other to show continuous behaviour in the water chemistry. Consequently, chemical variables depend greatly on the type of underlying material that makes up the aquifer, which in the strict sense vary from one location to the other in Naivasha study area.

It must be emphasised that (C.Reimann and P.Filzmoser, 1999) unprecise measurements are often associated in sampling, sample preparation and analysis of water samples.

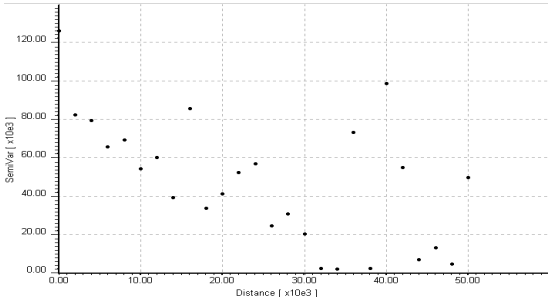

Semi-Variogram for Sodium (Na)

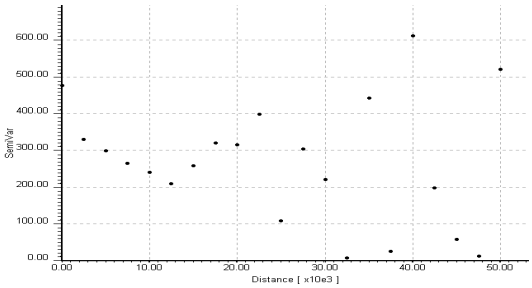

Semi-Variogram for Potassium (K)

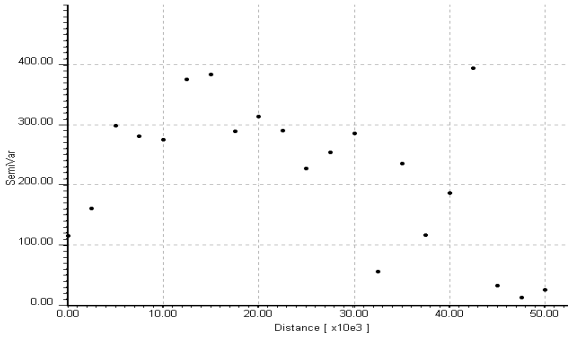

Semi-Variogram for Calcium (Ca)

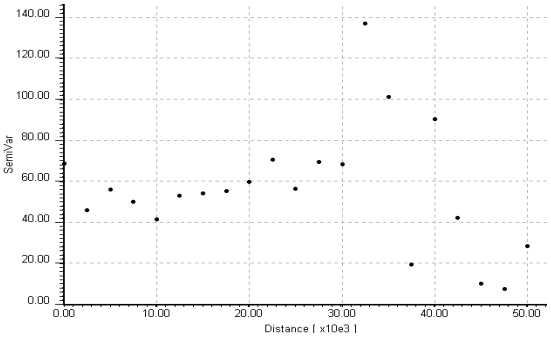

Semi-Variogram for Magnesium (Mg)

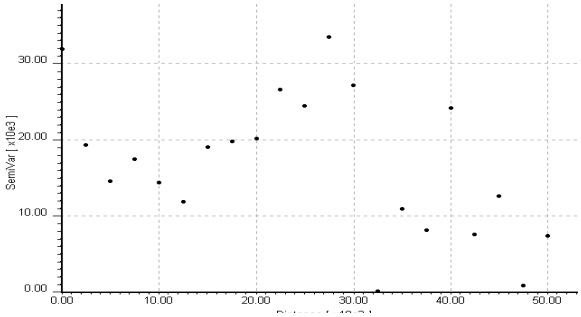

Semi-Variogram for Chloride (Cl)

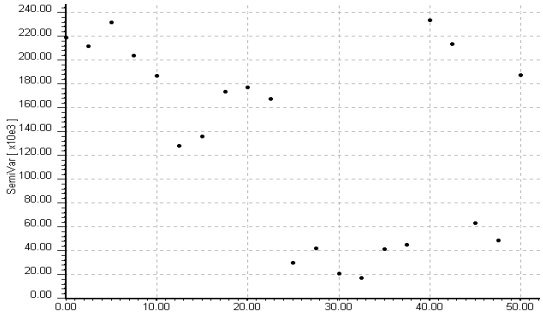

Semi-Variogram for Bicarbonate (HCO3)

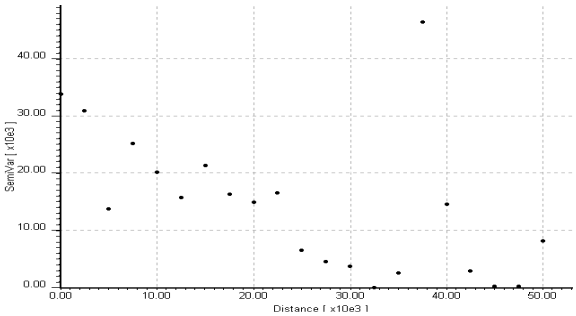

Semi-Variogram for Sulphate (SO_4^{2-})

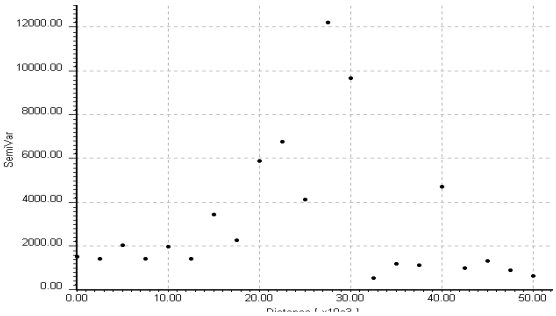

Semi-Variogram for Silica ($Si0_2$)

Figure 33: Semi-Variograms of chemical variables.

CHAPTER 6

6 ISOTOPIC EVIDENCE OF THE ORIGIN OF GROUNDWATER FLOW SYSTEM

6.1 INTRODUCTION

The purpose of this chapter is to ascertain how effectively environmental isotopes content could help to improve the understanding of the shallow and deep groundwater flow system in the study area in terms of the recharge sources and flow pattern.

The development and management of groundwater resources require to greater extent an investigation into the recharge source and the flow direction of the groundwater system. This could help in the management the underlying aquifers to meet the increasing demand and address environmental issues for a viable long -term development of groundwater resources.

Stable isotopes ratios of oxygen and hydrogen are routinely used to study the origin of water in aquifers and the dynamics between surface water and groundwater. They are used together in order to characterise the present and past processes in which water is a dynamic component (Ghomshei and Allen, 2000).

Craig (1961) used $\delta^{18}O$ and δD isotope values of unevaporated precipitation from locations around the globe (US Geological Survey report) to define the Global Meteoric Water Line (GMWL) given by the general equation:

$\delta D=8\delta^{18}O+10$, and have $r^2>0.95$

The different types of meteoric waters and their seasonal variations deviate and/or fall on the global meteoric line and GMWL is redefine for the area of investigation represented by Local Meteoric Water Lines (LMWL) from local precipitation. This is characterised by slope, which differs from that of the general equation (slope of 8).

Mook (2000) gave the general relation of GMWL as:

$\delta D= s*\delta^{18}O+d$, where the slope s=8 and the deuterium excess, d refers to the intercept on the δD axis.

The isotopic ratios $^2H/\ ^1H$ and $^{18}O/^{16}O$ of V-SMOW are (Mook, 2000) as follows:

$^2H/^1H=(155.75 \pm 0.08)*10\text{-}6$ (De Wit et. al.1980)

$^{18}O/^{16}O=(89.12\pm 0.07)*10\text{-}6$ (De Wit et. al.1980)

6.2 ISOTOPIC DATASETS

Four datasets were used to determine the possible source of groundwater and the extent of mixing of the different waters in the study area.

- Isotope Dataset 1: Consists of stable Isotopes of Oxygen, Deuterium, Tritium and Radiocarbon Isotopes of water samples collected during fieldwork, 2000.
- Isotope Dataset 2: Consists of stable Isotopes of Deuterium and Oxygen and Radiocarbon Isotopes of Lake Naivasha, shallow wells and geothermal wells. They were analysed at the British Geological Survey for studies on the lake-groundwater relationship and fluid-rock interaction in the East African rift valley.

  Source: Darling, 1996.

- Isotope Dataset 3: Consists of stable Isotopes of Deuterium and Oxygen from (local and National rainfall), River, Lakes (Naivasha, Oloidian bay and Crater), Shallow wells and deep geothermal wells analysed at the University of Rochester, USA.

  Source: The University of Nevada, 1992.

- Isotope Dataset 4: Consists of stable Isotopes of Deuterium and Oxygen and Carbon-14 radiocarbon of rainfall, rivers, lakes (Naivasha and Oloidian bay), shallow and deep geothermal wells.

  Source: The University of Nevada, 1996.

- Isotope Dataset 5: Consists of stable Isotopes of Deuterium and Oxygen of precipitation, used for estimating effect of climate and altitude on isotopic composition.

  Source: The British Geological Survey, 1990.

6.3 METHODOLOGY AND ANALYSIS

Sixteen- (16) water samples for isotopic analysis were collected during fieldwork in September 2000 (Dataset 1). The unfiltered samples from surface and groundwater were collected in 30ml bottles with polysealed caps for stable isotopic analysis and those for tritium analysis were collected in 300ml bottles. The samples for ^{14}C analysis collected in 300ml bottles with polysealed caps and poisoned with Ammonium chloride to prevent growth of carbonate minerals in the water samples.

The samples were analysed at the Centrum voor IsotopenOnderzoek, Royal University of Groningen, in The Netherlands for oxygen-18, deuterium, tritium, ^{13}C and ^{14}C stable and radioactive isotopes.

The Oxygen–18 was measured by degassing in water samples a vacuum system and brought into isotopic equilibrium with CO_2 at 25°C and a fraction of $^{18}O/^{16}O$ of CO_2 measured with Isotope ration mass spectrometer. The Deuterium was measured by directing a vapour of the water samples over hot uranium and then measured with mass spectrometer. Tritium was measured by directing water sample over hot Mg and changed into ethene or ethane gas by adding hydrogen. Carbon-14 was measured by treating water sample in vacuum with 85% of H_3PO_4. The CO_2 released was graphitised after drying with hydrogen at 600°C and measured on AMS mass spectrometer.

The stable isotope compositions are reported in the standard δ notation:

$$\delta=[(R_{sample}-R_{standard}]/R_{standard}]*1000$$

where R_{sample} and $R_{standard}$ are the isotope ratio of ($^{2}H/^{1}H$ or $^{18}O/^{16}O$) the samples and standard respectively.

The internationally accepted standard of measurement of deuterium and oxygen isotopic (ratios) composition of natural water samples is the Vienna Standard Mean Ocean Water, VSMOW (Mook, 2000). The values of δD and $\delta^{18}O$ are reported in per mil in reference to V-SMOW with tolerance measurement accuracy of ± 1‰ and 2‰ units respectively. Positive values show that the sample is enriched in the heavy isotope species and negative show depletion in the heavy isotope species compared to the standard.

6.4 ANALYTICAL RESULTS AND DISCUSSIONS

6.4.1 DEUTERIUM AND OXYGEN-18 ISOTOPES

Deuterium and Oxygen 18 isotopic composition in water are defined in a two-dimensional space vector by plotting the isotopic signatures of δD vs. $\delta^{18}O$ diagrams and compared with the different local signatures of rainfall, lake, river and groundwater.

Stable isotope data of Deuterium and Oxygen-18 of the datasets are plotted with the global meteoric water line (GMWL) defined by (Craig, 1961) and the regression line for the Lake water samples in the study area (figures 6.1, 6.2 and 6.3).

The dataset 1 being the most recent isotopic data (2000) have isotopic compositions of surface and groundwater similar to those in other datasets. The most enriched waters are those from Lakes Naivasha, Crater and Oloidian bay with isotopic compositions of ($\delta^{18}O$ =+6.56‰ and δD=+36‰), ($\delta^{18}O$ =+12.43‰ and δD=+59.3‰) and ($\delta^{18}O$ =+10.24‰ and δD=+56.7‰) respectively. The Gorge spring have isotopic composition ($\delta^{18}O$ =+4.47‰ and δD=+25.5‰) similar to that of Lake Naivasha. The most depleted water samples are groundwater from Moi Ndabi BH2, Ngodi BH, Marula BH2, 3-Point farm BHM. They have isotopic compositions similar to that of River Malewa. The other groundwater from Sulmac, Olsuswa, Kongoni and Kedong wells south of the Lake Naivasha have isotopic signatures similar to that of Lake Naivasha.

The $\delta^{18}O$ value of groundwater ranges from +2.9‰ to +4.19‰ and δD from +19.1‰ to +29.2‰ in Sulmac and Heather wells respectively. The isotopic composition of the Gorge spring ($\delta^{18}O$ = +4.47‰ and δD= +25.5‰) is identical to that of Heather well with $\delta^{18}O$ =+4.19‰ and δD= +29.2‰. The Olsuswa wells have isotopic compositions similar to Kongoni M13. The compositions are $\delta^{18}O$ =+3.53‰ and δD= +23.9‰ for Olsuswa well and $\delta^{18}O$ =+3.25‰ and δD= +23‰ The most enriched water is that from Crater Lake with isotopic composition of $\delta^{18}O$=12.43‰ and δD=59.3‰.

The groundwater is defined by the regression line, $\delta D=5.66\delta^{18}O+4.20$ (r^2=0.99) and line of regression through the surface waters defined by:$\delta D=4.52\delta^{18}O+6.29$ (r^2=0.99).

The Dataset 2 was used to infer the mixing line of Lake Naivasha and groundwater. The correlation between the different water bodies in the study area is r^2=0.90, indicating a very strong correlation. The Lake water sample has the highest isotopic composition of Oxygen and Deuterium ($\delta^{18}O$ =+6.6‰ and δD=+36‰). The $\delta^{18}O$ in the groundwater ranges from –4.4‰o to +4.5 ‰o and δD from -24‰ to +34‰. The most depleted groundwater samples are those from the shallow wells C4178, C5002 and EW-1. They are more depleted than the seawater (δD=0‰ and $\delta^{18}O$=0‰) and suggest a meteoric origin for the groundwater. The values in the deep OW wells in the Olkaria areas are more enriched in δD and $\delta^{18}O$ and suggest a source other than meteoric. The mixing line between the rift side recharge of boreholes from the east and west and the Lake water has line of regression defined by the equation $\delta D=5.37\delta^{18}O-0.62$ (r^2=0.90).

In Dataset 3, the values of $\delta^{18}O$ and δD in groundwater samples vary from –4.6‰o to 6.4‰o and –28‰o to 32.9‰o respectively. The most depleted groundwater sample ($\delta^{18}O$ =-4.6‰o, δD= -28‰o; $\delta^{18}O$ =-+0.7‰o, δD= -8‰o) are from shallow wells C1404 and C729 respectively. The most enriched groundwater samples were those from the deep geothermal wells such as OW-703, OW-17, OW-4. The groundwater samples plot on a line of regression defined by the equation δD=5.98δ18O-4.63 (r^2=0.87). The evaporation line for the lake samples lie on the regression line of equation $\delta D=2.23\delta^{18}O$ +15.98 (r^2=0.69). The $\delta^{18}O$ values of rainfall from regional and local locations were –5.1‰o and –6.4‰o respectively whiles that of δD were -32.8‰o and –39‰o respectively.

The most depleted rainwater samples were from the local rain whiles that from the regional were quite enriched. This might be due to the fact that the local rain samples were collected from heavy rainfall and the regional from light rainfall (Dansgaard, 1964), thus the local site experienced heavier

downpour compared with the regional. The river sample is also depleted with $\delta^{18}O$ =-2.7‰, δD= -13‰ whiles that of the Lakes Naivasha, Oloidian bay and Crater are heaviest in Oxygen-18 and Deuterium isotopes composition.

In Dataset 4, isotopic composition of $\delta^{18}O$ and δD in groundwater are similar to those obtained in the datasets 2and 3. The groundwater isotopic compositions of $\delta^{18}O$ range from –4.2‰ to 4.3 ‰ and δD from –22‰ to 29‰. The most depleted values were found in samples from shallow groundwater wells C3366, C3677 and C3675, located in the north-eastern part of lake Naivasha. They exhibit isotopic compositions similar to that of rainfall and rivers but depleted than that of seawater and suggest that the groundwater might be derived from meteoric source. They lie in the regression line of equation defined by δD=5.64δ18O+0.66 (r^2=0.94).

The surface water bodies have isotopic compositions of $\delta^{18}O$ values ranging from –3.8‰ to –1.4‰ and δD range from-19‰ to 5‰ in rivers; Lake Naivasha ($\delta^{18}O$ =6.4‰, δD=39‰) and Oloidian bay ($\delta^{18}O$ =6.4‰, δD=39‰). Mook (2000) indicated that high $\delta^{18}O$ values are often enriched in (saline) Lakes subjected to a high degree of evaporation. The isotopic composition of the rain samples shows that $\delta^{18}O$ values range between –3.75‰ and +1.45‰ with mean value of –1.6‰ while δD values range between –14.5‰ and +19‰ with a mean of value of +3.1.

The line of regression describing the relation is defined by the equation: $\delta D=7.02\delta^{18}O+14.44$ (r^2=0.83). The slope of 7.02 is less than that of Global Meteoric Water Line (GMWL) and the deuterium excess value, ($d=\delta D-8\delta^{18}O$) of 15 was obtained, which is more than that of GMWL (about 10). The increase in deuterium excess could be attributed to significant addition of re-evaporated moisture from continental basins to the water vapour travelling inland, which produces lighter $\delta^{18}O$ values of the isotopic composition of the water vapour.

In summary, the most enriched samples in the study area are Lake Naivasha and Oloidian bay waters, with $\delta^{18}O$ and δD compositions (Lake Naivasha, $\delta^{18}O$=+6.4‰ and δD=+39‰) and (Oloidian bay, $\delta^{18}O$=+10.6‰ and δD=+60‰). The typical composition of Lake Naivasha is $\delta^{18}O$=6.6‰ and δD=36‰ (Ojiambo, 1996). This is due to high rate of evaporation of these lakes, which is responsible for the high Ec values in surface water bodies except Lake Naivasha which is recharge by river Malewa (low Ec water) in the study area.

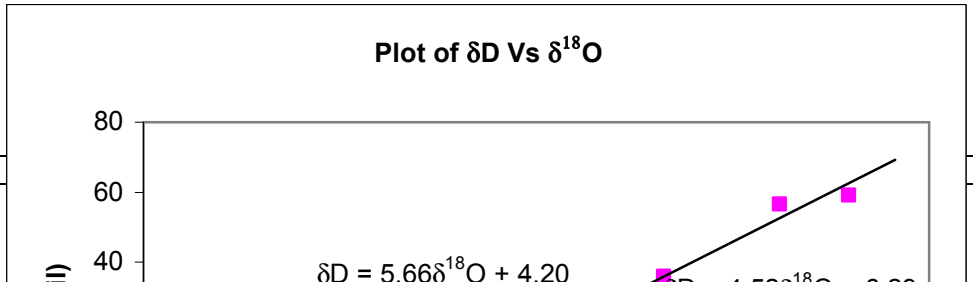

Figure 34: Plot of δD against $\delta^{18}O$ showing the regression lines of surface and groundwater waters (Dataset 1).

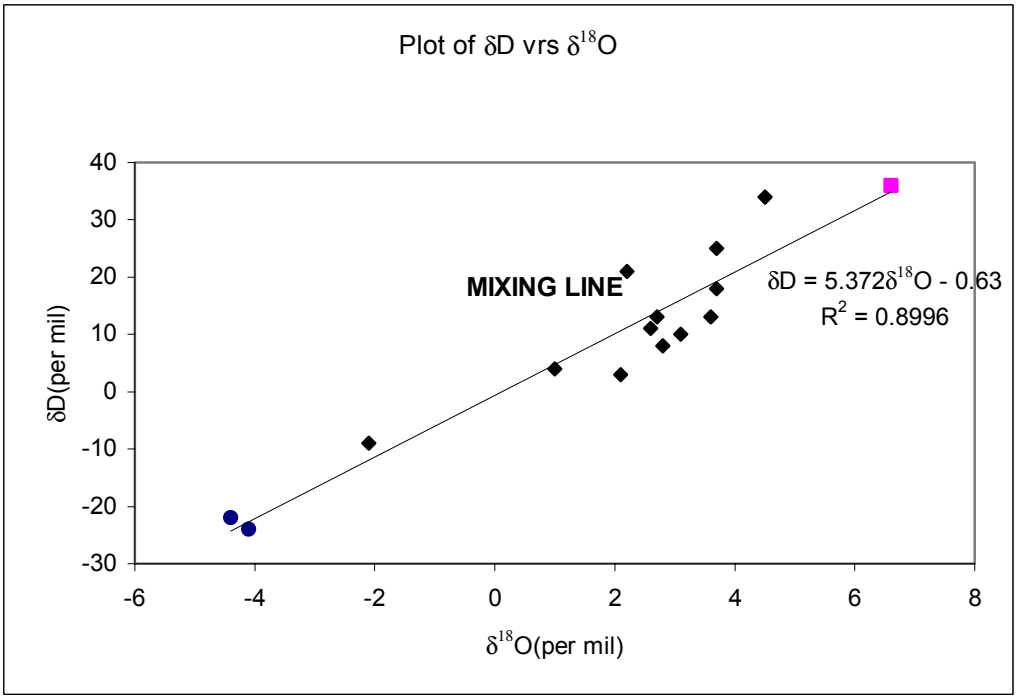

Figure 35: Plot of δD-$\delta^{18}O$ showing the mixing line of Lake Naivasha and groundwater (Dataset 2).

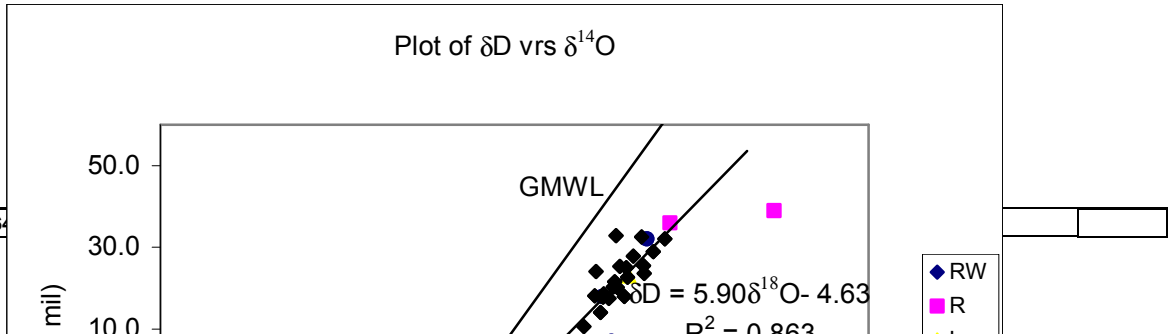

Figure 36: Plot of δD-δ^{18}O showing GMWL and Line through groundwater (Dataset 3).

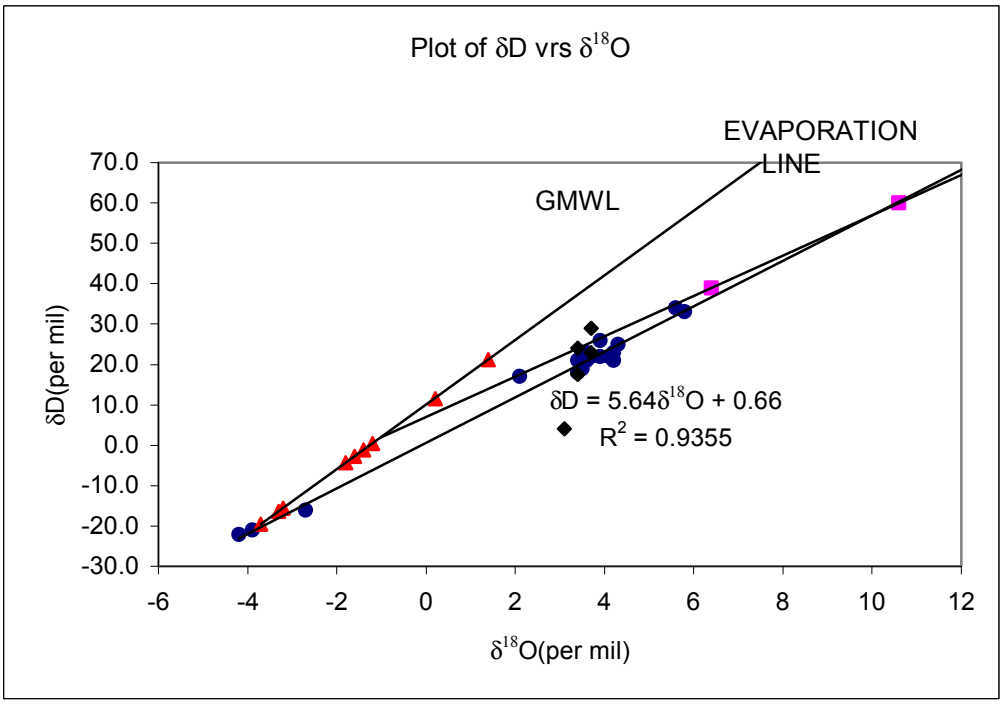

Figure 37: Plot of δD against δ^{18}O showing the GMWL and Evaporation lines (Dataset 4).

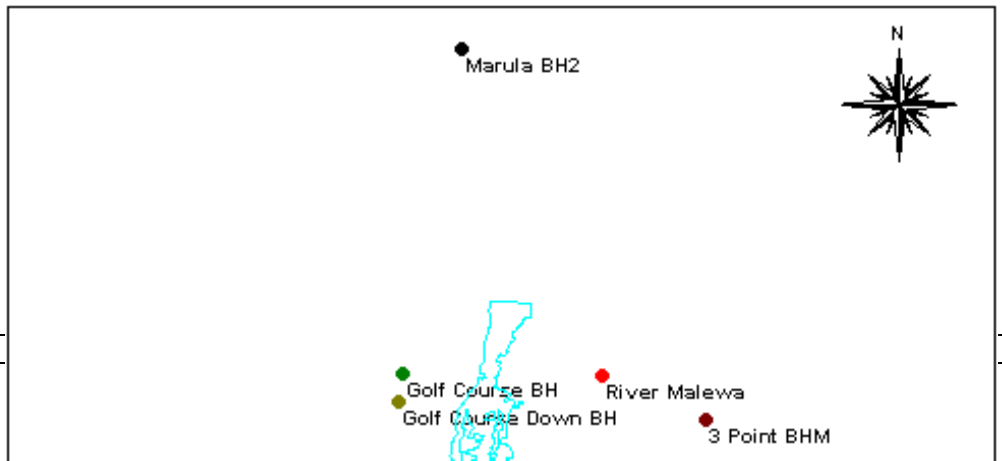

Figure 38: Sampling points of water for Isotopes during fieldwork, 2000.

6.4.2 CARBON-13 (^{13}C), CARBON-14(^{14}C) AND TRITIUM (^{3}H) ISOTOPES

From Dataset 1(recent measurements), the C-13 values in groundwater range from –31.9‰ to –3.12‰. The Sulmac well has the least depleted C-13 composition of –3.12‰ and Ngodi well most depleted with composition of –31.9‰. The C-13 composition in Sulmac and Kedong C210 waters are similar with –3.12‰ and –3.48‰ in the two waters respectively. The C-14 compositions of groundwater are as follows: Sulmac farm well has C-14 value of 96.2pMC, Kedong farm C210 96.5pMC and 3 point farm BHM 53.8pMC, with corresponding residence times using equation 7.3 of about 1023, 1049 and 3781years respectively.

The average tritium values in Sulmac well is 2.6 TU, 3 point farm BHM is 0.35 TU, Kedong C210 is 2.4 TU, Ngodi BH is 0.37 TU and Marula BH2 is less than 0.2 TU and being more depleted. The tritium values in Kedong C210 and Sulmac wells are identical and similar to that of Lake Naivasha measured as 2.6 TU by Ojiambo, 1996 (Dataset 4).

From Dataset 4, the tritium values observed in Lake Naivasha and Oloidian waters are 2.6 and 3.1 TU respectively. In the shallow groundwater the value ranges from 0 to 5.3 TU and in the deep geothermal wells the tritium values range from 0.1 to 0.9. The wells C3366, C3677, C3675, C210, C562, C567, C4397, C579, C3767, C2660 and the geothermal wells OW101, OW-2, OW-26, OW-725 and OW-728 have tritium concentrations below the threshold value of 3.1 T.U. The samples from wells C2071 and C7829 located south of Lake Naivasha have tritium concentrations more than the threshold value of 3.1 T.U.

6.5 TEMPERATURE, INTENSITY AND ALTITUDE EFFECTS ON $\delta^{18}O$ AND δD OF PRECIPITATION

6.5.1 TEMPERATURE EFFECT ON $\delta^{18}O$ AND δD

6.5.1.1 INTRODUCTION

The dependence of isotope fractionation on temperature, T ^{O}C results in a seasonal variation of $\delta^{18}O$ and δD values. They are more positive in summer than winter (Klaus and co, 1991). Temperature

controls the partitioning of isotopes in precipitation and provides input variable to trace the origin of groundwater recharge. Decreasing temperature therefore gives rise to increasingly depleted $\delta^{18}O$ and δD values in precipitation and the vice versa.

The linear relationship between surface air temperature, $\delta^{18}O$ and δD of mean annual precipitation is given by Dansgaard (Klaus and co, 1991) is:

$$\delta^{18}O=0.69T(°C)_{annual} - 13.6‰ \text{ SMOW} \quad 6.1$$

$$\delta D=5.6T(°C)_{annual} - 100‰ \text{ SMOW} \quad 6.2$$

The mean monthly formula (Yutsever and Gat, 1981) is:

$$\delta^{18}O=(0.338\pm0.028)T_{monthly} - 11.99‰ \text{ VSMOW} \quad 6.3$$

6.5.1.2 RESULTS AND DISCUSSIONS

The rainfall sampling was done between the months of March and July, with month of March being the end of the dry period (Darling et. al.1990). The temperature effect varies for different rainfall event as the mean monthly air temperatures in the study varies month after month. The samples collected in March are enriched in isotopic composition while those sampled in April to July the same year are quite depleted (Dataset 4).

The mean annual temperature in the study area is 18°C, which gives change of –1.2‰ in $\delta^{18}O$ with the corresponding change of +0.8‰ in δD (based on equations 6.1 and 6.2). Klaus and co, 1991, indicated similar effect of 1‰ decrease in average annual $\delta^{18}O$ from a decrease of about 1.1 to 1.7 °C in average annual temperature and indicated that in coastal areas, the gradient can rise to some +0.2‰ per degree Celsius.

The higher rate of evaporation caused by high temperature has enriched the isotopic composition of $\delta^{18}O$ and δD in some surface water bodies (Crater Lake, Oloidian bay and Gorge spring) with corresponding increase in Chloride (Isotope dataset 1 and Hydrochemical dataset 4). The temperature effect is therefore significant on surface water bodies than the groundwater in the study area.

In summary, precipitation is lighter in isotopic compositions on account of lower temperature and enriched in isotopic compositions during high temperature due to high rate of isotopic fractionation. Mook, 2000 indicated that in regions with temperate climate experience seasonal effect with more negative δ^{18} values during winter.

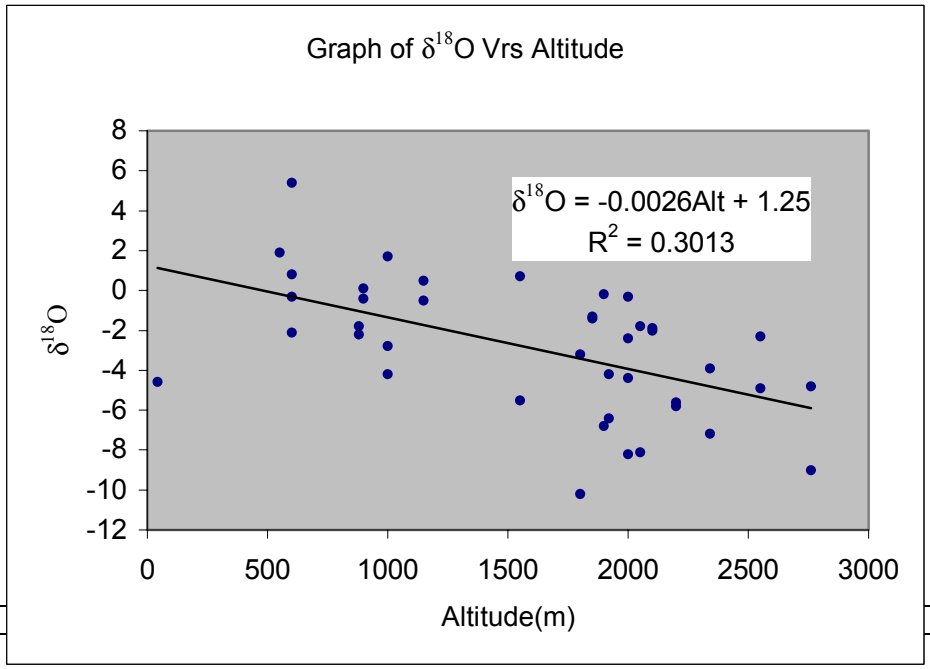

Figure 39: **Plot of $\delta^{18}O$ -Altitude Relation (Dataset 5).**

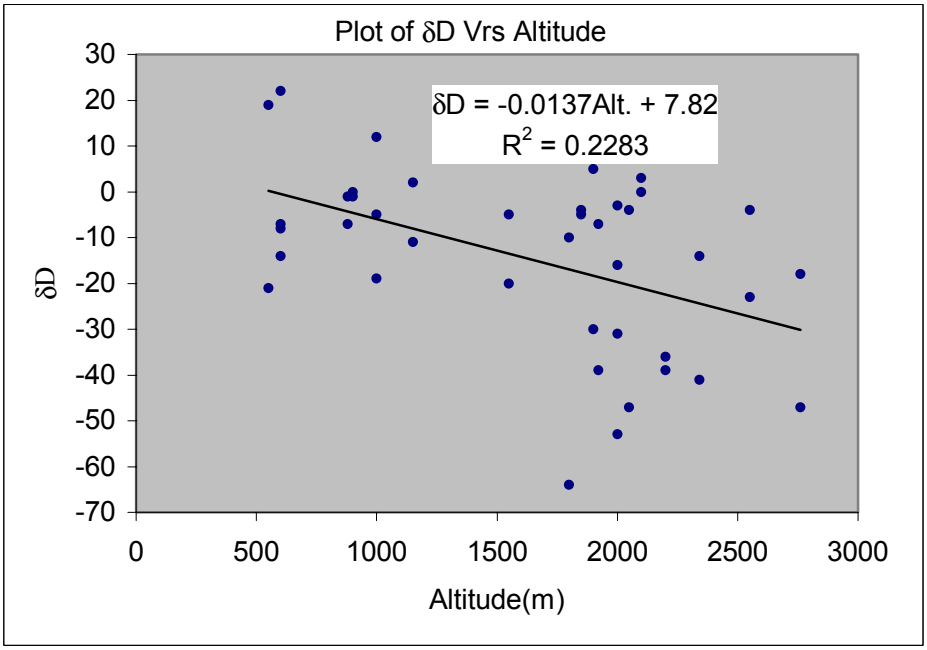

Figure 40: **Plot of $\delta^{18}D$ -Altitude Relation (Dataset 5).**

6.5.2 ALTITUDE EFFECT

6.5.2.1 INTRODUCTION

Altitude significantly affects the mean isotopic composition of rainfall as a result of high topographic relief. At higher altitude where the average temperatures are lower, it is expected that isotopic composition of precipitation will be depleted and the vice versa. The $\delta^{18}O$ depletion in general varies between about –0.15 and –0.4‰ per 100 meters rise in elevation, with the corresponding decrease of about –1 to -4‰ for δD or about a factor of 8 larger (Klaus and co, 1991). From this, groundwater produced from diffuse recharge can therefore be distinguished from groundwater derived from localised recharge areas.

6.5.2.2 RESULTS AND DISCUSSIONS FROM $\delta^{18}O$ AND δD-ALTITUDE PLOTS

The plots of $\delta^{18}O$ and δD against altitude are depicted in figures 37 and 38. They were plotted using data from the Ministry of Energy- Report on Geothermal activities in Lake Naivasha (1990).

The lines of regression of the plots are defined by the equations:

$$\delta^{18}O=-0.0026*altitude+1.25 \quad (6.4)$$

$$\delta D=-0.0137*altitude+7.82 \quad (6.5)$$

The average change in $\delta^{18}O$ composition of precipitation (based on equations 6.4 and 6.5) is estimated as-0.26‰ reduction per 100 meters rise in elevation (-0.26‰ per 100m) and δD estimated as –1.37‰ reduction per 100 meters change in elevation (figures 37 and 38).

It can be concluded that the altitude effect on the isotopic composition of rainfall was minimal within the vicinity of Lake Naivasha where the difference in elevation are less than 300 meters, thus flat areas.

The altitude effect is minimal on $\delta^{18}O$ and δD composition of rainfall and therefore no corrections to the measured values.

Clarke et al, 1990 indicated based on hypothesis of latitude dependent effect is inadequate, supported by available data and there is no evidence of systematic variation in isotopic composition from one side of the rift to the other. This is in line with the results from the two plots in figures 41 and 42.

6.5.3 RAINFALL INTENSITY EFFECT

The is the result of the phenomenon called "amount effect', a process whereby the isotopic composition of samples from light rainfall is more enriched than samples collected from heavy rainfall. This is evident in Isotope Dataset 5 where low rainfall values corresponds to higher δ values and high rainfall intensity yielded more depleted δ values. This supports the assertion that at a given location, heavy storms produce more negative values in $\delta^{18}O$ composition (Mook, 2000).

The month of March experiences the heaviest rainfall and the samples are depleted in isotopic composition compared to the samples collected in the lean period from April to July in the same year (light rain period) which are isotopically enriched. Dataset used to infer was compiled from Darling et. al. 1990 as Isotope Dataset 5.

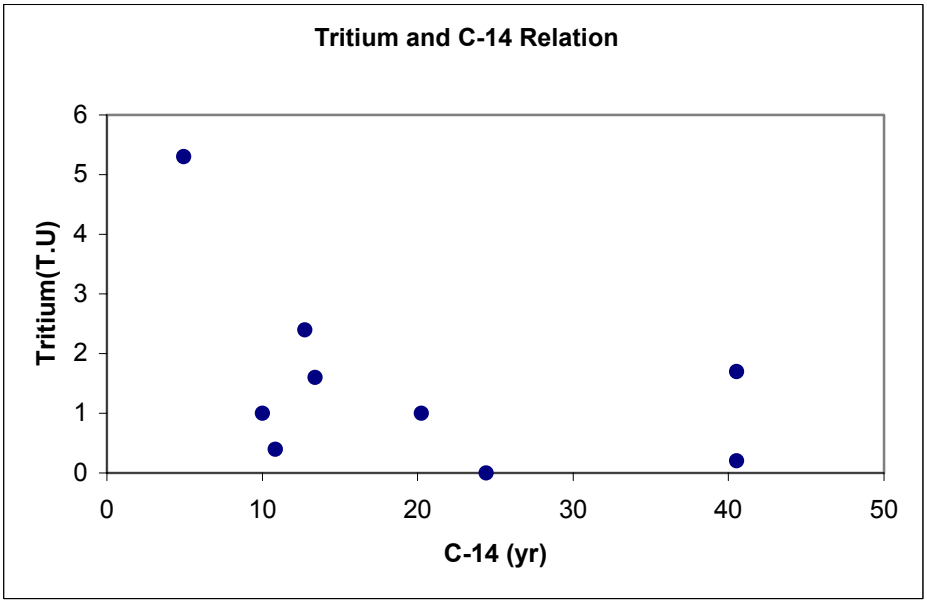

Figure 41a: Plot of Tritium-C-14 (yr.) relation of isotopes (1996).

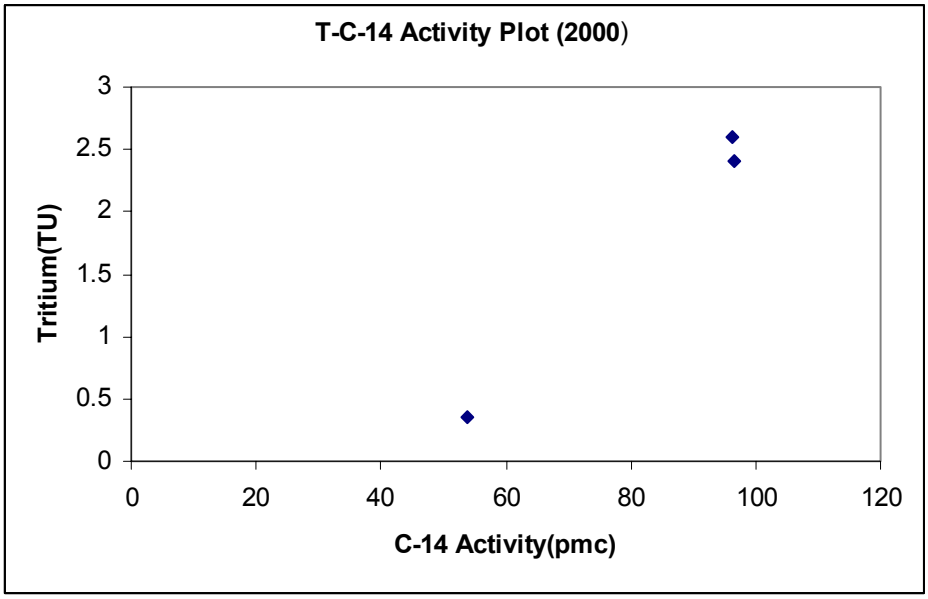

Figure 42b: Plot of Tritium-C-14 Activity relation of isotopes (2000).

6.6 SOURCES OF AQUIFER RECHARGE

6.6.1 OXYGEN-18 AND DEUTERIUM ISOTOPES

The isotopic concentrations of deuterium and ^{18}O give in-depth information into recharge conditions of groundwater and its interaction with surface groundwater. They act as conservative elements, which are unaltered with time or in the process of ionic exchange on transit through aquifer materials and are altered in the region where geothermal activities are prevalent like in the deep geothermal wells further south of the study area.

From Dataset 1, wells south of the Lake Naivasha are enriched in isotopic compositions and have isotopic signatures similar to that of Lake Naivasha. The source of water to these wells could be the Lake Naivasha or a mixture of Lake Water and less depleted rainwater. The depleted isotopic signature in the South-western wells suggests Moi Ndabi BH2 and Ngodi wells are been recharge by groundwater from greater altitudes (Ndabibi mountains) in the form of infiltrated water of runoff from precipitation.

Likewise, Marula BH2 and 3 Point farm BHM boreholes have depleted isotopic compositions similar to that of River Malewa and suggest these wells have sources from precipitation and river other than the Lake Naivasha. The Golf course BH and Golf course down BH have less enriched isotopic signature signifying a mixture of old water and quiet recent water.

The groundwater plots on or below the GMWL suggests that the groundwater have not been fractionated or subjected to evaporation (figures 34 and 35). The lines of regression show groundwater lie on lines of gradients 5.66, 5.64 and 5.90 in figures 32, 33 and 35 respectively. This is statistically similar to that obtained from the mixing line of the lake Naivasha and groundwater of gradient 5.37 (figure 33). The low isotopic composition in North-eastern and western wells EW 1, C3366, C3677 and C3675 suggests that the groundwater might be recharge from meteoric source than from the Lake Naivasha (Dataset 2).

The slope of regression line through surface water is 4.52 (figure 32) and similar to Kenya Rift Meteoric Water Line (KRML) defined by (Clarke et al., 1990) as $\delta D=5.49\delta^{18}O+0.08$, r=0.9 and gradient equal to 5.49. The slope is equivalent to those obtained for groundwater samples but less than that of GMWL (equal to 8) for unevaporated rainfall.

The similarity between the gradients indicates there is an inter-connection between the lake Naivasha and the subsurface groundwater system and most of the recharge water might have been affected by significant evaporation before entering the shallow groundwater system. The evaporation line intercepts GMWL at $\delta^{18}O$=-1.0‰ and δD=+2.0‰. This is defined as the mean composition of isotopes from rainfall into the surface water bodies. The Lake Naivasha is thus recharged with $\delta^{18}O$=-1.0‰ and δD=+2.0‰ from rainfall (figure 35).

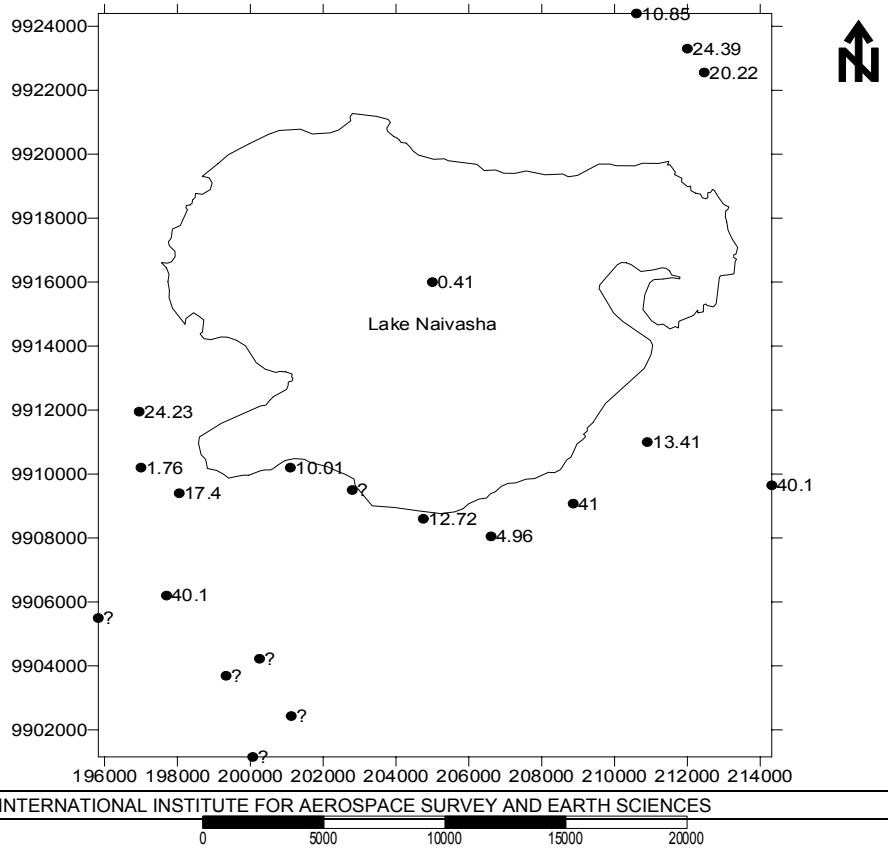

Figure 43: Spatial distribution of C-14 age (yr.) in the study area.

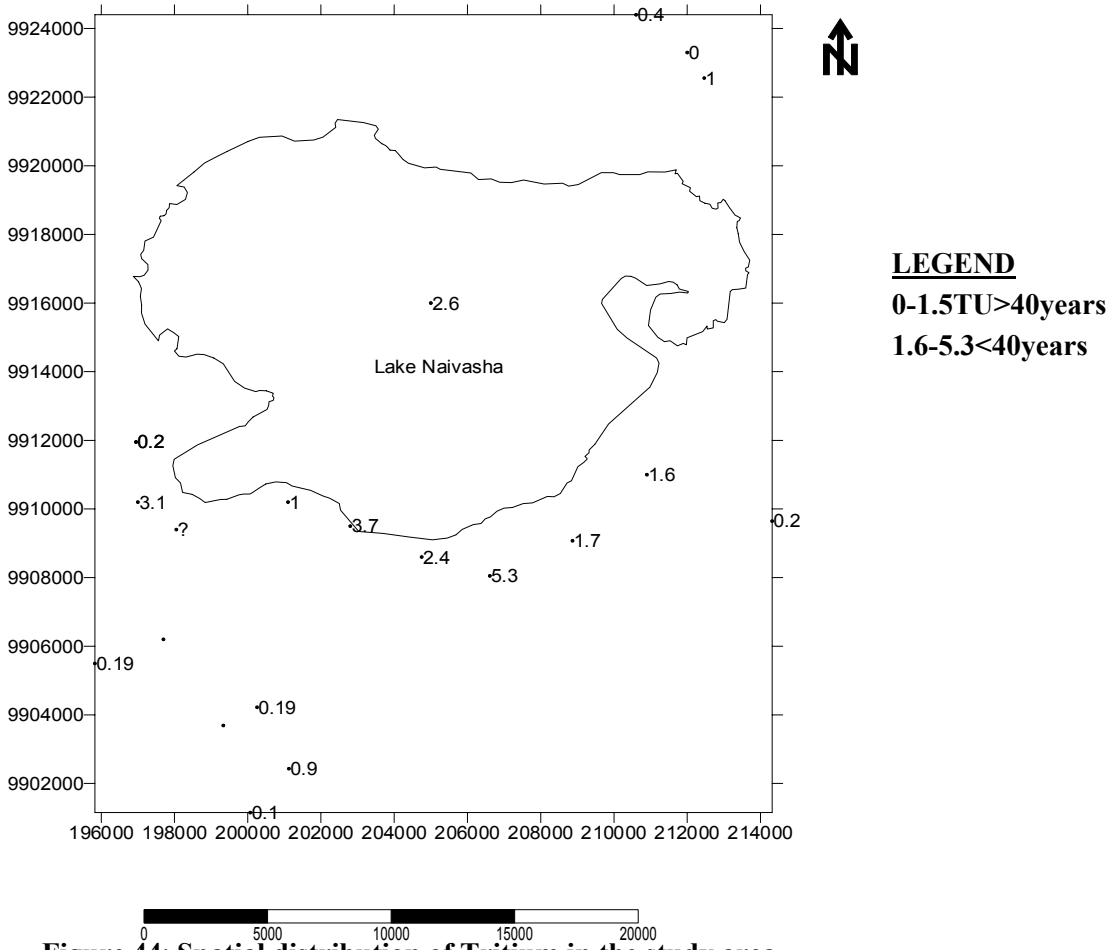

Figure 44: **Spatial distribution of Tritium in the study area.**

6.6.2 $\delta^{13}C$, CARBON-14 AND TRITIUM ISOTOPES

From recent isotopic data (isotope Dataset 1), $\delta^{13}C$ in Ngodi BH is more depleted at –31.9‰ and suggests recent groundwater with mean residence times less than 20 years, perhaps being recharge from precipitation or recent groundwater. The Sulmac and Kedong C210 are least depleted in $\delta^{13}C$ and suggest young groundwater in the two wells and their source could be linked to recharge from Lake Naivasha, which is about 0.3 year or mixture of Lake and precipitation.

The similar calculated residence time of about 1000years of groundwater in Sulmac and Kedong C210 suggest the same period of time elapsed since the infiltration or recharge of water whiles 3 Point farm BHM has residence time of about 3000years, presumably from mixture of old groundwater and modern direct recharge.

From the current tritium isotopes measured (Dataset 1), the high and identical tritium values of 2.6 and 2.4 measured in Sulmac and Kedong well C210 respectively suggest the waters are quiet recent. They have composition close the threshold value of 3.1TU and similar to that of the Lake Naivasha, which presupposes that these waters are inter-linked and are being recharge from the identical source of water, preferably from the Lake Naivasha. Likewise, the low tritium values measured in 3 Point farm, Marula BH2 and Ngodi suggests the waters are very young and might be recharge from direct rainfall in the form of infiltrating from runoff other than Lake Naivasha.

Concurrently, from dataset 3 the tritium values in waters from wells C3366, C3677, C567, C3767 and C2660 and the geothermal waters from OW101, OW2, OW26, OW725 and OW728 and C7829 are below 1 T.U, indicating that the waters are at least 25 years old. The distribution of Tritium is depicted

in figure 43. The relatively higher tritium values above the detection limit of 1.5-3.1 T.U found in waters from wells C210, C562, C4397, C2071 and C7829 suggests the waters to be sub-recent and might have been recharge from modern rainfall or a mixture of young and old water (Mook, 2000). The age of groundwater range from about 2 years up to more than 40 years in the south-east wells C3366, C3677 and C3675 and southern wells C630-D, C210 C2660 suggest they are older then the Lake Naivasha.

The C-14 (age) distribution map shows that the age increases from the Lake towards the south-western part of the study area (figure 42). The relation of C-14 (age) -Tritium shows no consistent pattern between the two variables (figure 41a), suggesting Tritium and C-14 age are independent. The recent data shows consistent pattern in Tritium-C-14 activity plot (figure 41b) where lower Tritium values corresponds to lower C-14 activity and the vice versa. This suggests that the two variables are spatially dependent on each other.

The old age of deep groundwater might be due to long residence time of water through the medium of transport. The relatively high ^{14}C activities observed for the waters from the southern wells C630-D, C567 and C210 and the low ^{14}C activity of the lake water suggests local young recharge source of water to the shallow groundwater system. The modern recharge is the result of groundwater in equilibrium with the atmosphere contaminated with high level of tritium up to four order of magnitude between the early 50's and 1963/64 from nuclear tests (Klaus and co; 1991).

In summary, the tritium composition in water decreases significantly towards south-western wells and appreciably towards south–eastern wells. The waters could be said to be recent or might have been recharged from Lake Naivasha, which is young. Mook 2000 indicated that water with $^{3}H<5TU$ must have a mean residence time of more than 40years and having $^{3}H>20TU$ must date from after 1961(less than 40years). The low tritium content of 0.3TU and low ^{14}C activity of 53pmc in 3point farm suggest probably mixing of old groundwater and modern rainfall. Likewise, the high ^{3}H (>1.5TU) and high ^{14}C activities (>96pmc) in Sulmac and Kedong C210 waters suggests they are subrecent (less than 50 years old) or mixture of young and old water or certain percentage of recent water.

In spite of the enrichment in stable isotope content of the Lake Naivasha sample, the Ec is low suggesting that stable isotopes are vulnerable or sensitive to evaporation compared to the Ec (low Ec input from River Malewa).

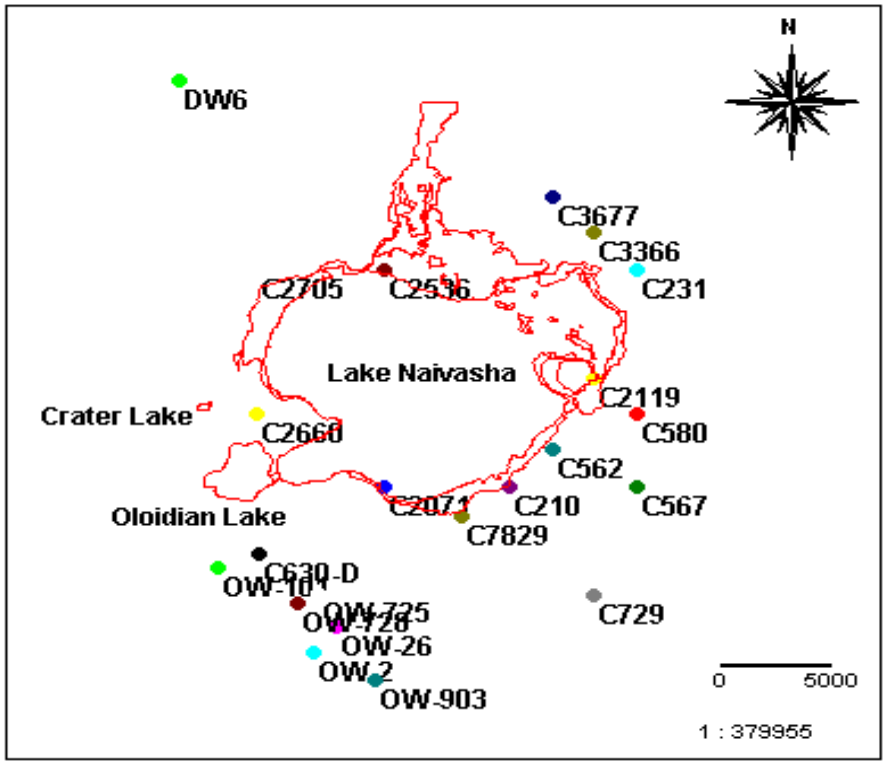

Figure 45: **Sampling points of water for Isotopes in the study area (1996).**

6.7 CONCLUSIONS ON GROUNDWATER ORIGIN FROM ISOTOPE GEOCHEMISTRY

The Deuterium, Oxygen-18, tritium and carbon-14 isotopic signatures of the surface and groundwater have provided evidence into the source of recharge into the groundwater flow system in the study area.

The high values of Deuterium and Oxygen 18 in the Lake waters suggest that these water have undergone significant evaporation. The groundwater from the shallow wells in the south of the Lake Naivasha are more recent than that from the deep geothermal wells based on their tritium and carbon-14 isotopic compositions. The high ^{14}C activity observed in Sulmac and Kedong C210 samples suggest a local young recharge source of water for the area, probably from the Lake Naivasha. The low^{14}C activity in 3point farm BHM suggests the groundwater is quite old and might be deriving its source from old groundwater system.

The groundwater samples exhibit variation in stable isotopic composition and slightly distributed along the Global Meteoric Water Line, GMWL (figures 36 and 37). These moderate variations might have resulted during the process of recharge when different storms at sampling sites with variable isotopic composition infiltrate to recharge the Lake Naivasha and groundwater in the study area. Also it might have been that the water is at times subjected to physical process before entering the groundwater flow system, as there is consistent pattern of isotopic enrichment in the southern groundwater. These lower values (depleted) in some groundwater suggest that they might have been derived from mixture of Lake Naivasha and infiltrating water in form of runoff from precipitation.

The low tritium values observed in some of the wells are below the detection limit of 1 T.U indicating that recharge might have occurred in those wells over fifty years ago or that there is mixing of younger and older water which might have caused the low tritium content. This is supported by the groundwater flow direction deduced from the piezometric map and agrees with the assertion that there is outflow from the Lake Naivasha into the shallow and deep groundwater flow system in the study area. This has been postulated by various researchers and tested with NETPATH modelling in chapter 7.

In conclusion, the shallow receives bulk of its recharge from Lake Naivasha and mixed with direct recharge while deep geothermal wells receive appreciable amount of recharge. This supports the assertion that there is subsurface outflow from the Lake traced to a distance of about 30km beyond the geothermal field (Darling et. al; Clark et. al; Ojiambo, 1996). The groundwater flow system will not be affected significantly by irrigation from the shallow wells or boreholes in the southern part of Lake Naivasha. Though, the Lake Naivasha sample is enriched in stable isotope, the Ec is very low and shows that the stable isotopes are vulnerable to evaporation than the Ec, which is low from the input source of River Malewa.

Isotopic modelling (chapter 7) into the source of groundwater has demonstrated that the southern aquifers are recharge significantly from the Lake Naivasha and direct recharge as infiltrating water from the piezometric highs in the study area. The flow directions proposed are therefore plausible, indicating that the shallow and deep groundwater aquifers are replenishable. The development of Irrigation schemes in the south of the Lake Naivasha will therefore be sustainable if comprehensive management schemes are incorporated into the use of groundwater in the study area.

CHAPTER 7

7 NETPATH MIXING AND HYDRODYNAMIC MODELLING

7.1 INTRODUCTION

The purpose of this chapter is to test the groundwater flow direction using NETPATH (Plummer and others 1991) hydrodynamic model developed by the US Geological Survey from some selected wells.

The NETPATH computer program has used to interpret net Geochemical mass balance reactions between initial and final water along a hydrogeologic flow path and determining the age of groundwater (dating). Thus, to find out the time elapsed since the water became groundwater as it infiltrated into the soil from precipitation or surface water bodies.

NETPATH program (Plummer et al., 1991) computes the mixing ratios of two to five end members as well as reactions for observed water compositions and the net Geochemical reactions that account for the observed composition of the final water. (Appelo and Postma, 1993) indicated that mixing of different water types could induce reactions, which lead to a water composition that is different from the conservative mixture.

The basic concept in constructing net Geochemical mass balance reactions is the selection of truly evolutionary initial and final waters sampled along the selected groundwater flow path in a confined regional groundwater system. The evolutionary waters were selected based on hydrologic and hydrogeologic intuitions. The model defines the masses (per kilogram H_2O) of a set of plausible minerals and gases that must enter or leave the initial solution in order to define a set of chosen elements and isotopic constraints observed in the final (evolutionary) water.

7.2 GOVERNING EQUATIONS

7.2.1 ISOTOPIC AND CHEMICAL MASS BALANCE CALCULATIONS

NETPATH (Plummer et al., 1991) considers two types of isotopic calculations: (1) Isotopic mass balance and (2) Rayleigh distillation calculations. Wigley and others (1978, 1979) gave analytical solutions to the general differential problem of chemical and isotopic mass balances and are given as (Plummer et. al., 1991):

Carbon mass balance: $$d(m_c) = \sum_{i=1}^{N} dI_i - \sum_{i=1}^{M} dO_i \qquad 7.1$$

Isotopic mass balance: $$d(Rm_c) = \sum_{i=1}^{N} R_i^{*} dI_i - \sum_{i=1}^{M} R_i \alpha_{is} dO_i \qquad 7.2$$

O and I refer to the incoming and outgoing masses of the element such as through dissolution and precipitation, Superscript * refers to the incoming phases and α_{is} is the fractionation factor between the I^{th} phase and the solution. M and N are the total numbers of incoming and outgoing phases.

Assumption: The analytical solution to the isotopic evolution problems assumes constant relative rate of reaction along the flow path. Thus, the ratio of incoming to outgoing mass of an element is assumed constant along flow path.

7.3 CONSTRAINTS AND PHASES AS INPUT PARAMETERS

NETPATH groundwater modelling requires various constraints as input parameters to determine the potential movement and evolution of groundwater in the study area of which physical parameters such as Temperature, Conductivity and pH were stated in the model set up.

The constraints are included in the model to constrain the masses of selected phases (minerals and gases) that can enter or leave the aqueous solution. The chemical constituents such as Calcium, Sodium, Potassium, Silica and Magnesium were used in the modelling.

In case of dating of groundwater for true isotope mass balance, isotopic constraints consisting of Deuterium, oxygen-18 and carbon-13 were incorporated into the model to determine the mixing of two/three water masses and mineral sources along flow paths respectively. In addition to the constraints, various phases were selected to provide a source or sink for each element in the initial and final solutions.

Although, the calculated mass transfer for one or more phases might be zero, indicating the phase(s) did not participate in the reaction, it is often included to perform the calculations (Hounslow, 1995).

7.4 METHODOLOGY

7.4.1 WATEQF from Initial Solutions

The Lake Naivasha sample, wells C562, C567, C630-D and OW-26 representing the shallow and deep groundwater in the south of the Lake Naivasha were selected for modelling. The WATEQF of initial solutions used as input for NETPATH phases of the modelling were generated for all the selected water samples. The oxidation-reduction, partial pressures, Saturation indices and phases from WATEQF phase for NETPATH were generated and are attached as appendix D-1.

7.4.2 NETPATH modelling

This step involved the use of WATEQF output file as input file to run the NETPATH. Various phases were stated for chosen constraints in some cases for dissolution only, precipitation only or both for the Hydrochemical mass balance calculations.

The constraints were taken into account in modelling potential groundwater movement and evolution in the study area. Amongst the chemical constituents used to model are calcium, magnesium, sodium and potassium.

For the rock-water interaction, phases such as albite, dolomite, hornblende and calcite were used to model to determine the extent of reaction of water with respect to the geological characteristics of the underlying aquifer.

The model is governed by the equation,

Initial water + 'Reactant Phase' = Final water + 'Product Phase'

7.5 ANALYTICAL RESULTS AND DISCUSSIONS FROM WATEQF

7.5.1 PARTIAL PRESSURES (Pco_2) and SATURATION INDICES

The carbon dioxide partial pressures (Pco_2) were generated from WATEQF phase of the program based on Alkalinity and pH. There is an increase in PCO_2 values in magnitude from the recharge area (Lake Naivasha) to topographically low areas at wells C567 and OW-26. The saturation indices and speciation computation of the samples from various phases are given in Table 13 and Appendix D1.

The PCO_2 value of $7.87*10^{-5}$atm was obtained in LK001 (Lake Naivasha), $1.67*10^{-2}$atm in C630-D and $1.67*10^{-4}$atm in OW-26 at the geothermal field along flow path 1. Along flow path 2, PCO_2 of $2.38*10^{-2}$ and $2.82*10^{-3}$atm were obtained in wells C562 and C567 respectively. The Pco_2 values from WATEQF are given in Table 12. The Pco_2 along flow path 1 decreases from $1.67*10^{-2}$atm in C630-D to $1.67*10^{-4}$atm in OW-26. Likewise, along flow path 2, the Pco_2 decreases from PCO_2 of $2.38*10^{-2}$ in well C562 to $2.82*10^{-3}$atm in well C567. The trend in Pco_2 from initial to the final wells suggests CO_2 is being used up during weathering or chemical reaction and is replenished in areas with abundance of vegetation and high Pco_2 associated with respiration of plants.

The Pco_2 in groundwater is high compared to that of Lake Naivasha along the two proposed flow paths taken from Lake Naivasha to wells C567 and OW-26 in the South. Lake Naivasha experiences dissolution of calcite and CO_2 is being used up when calcite dissolves and might not be replenished, hence the lower Pco_2 value. Appelo and Postma (1993) indicated that when further down a flow path calcite is encountered and dissolved, Pco_2 would rapidly decrease and given an initial Pco_2 the amount of bicarbonate in solution will be higher in the case of open system dissolution than closed system dissolution.

The calculated Pco_2 values in wells C567 and OW-26 are higher than the value of present day atmosphere ($0.3*10^{-3}$atm) and vary along the proposed flow paths. There is therefore enough $CO_{2\ in}$ the soil zone, which reacts to produce Na-HCO_3 type of water in wells C567 and C562. The CO_2 results from mineralisation or decomposition of organic matter and plant root respiration, which builds up the high partial pressures in wells C630-D, C562 and C567.

There is also increase in Total dissolved solids (TDS) along the two flow paths, which suggests CO_2 are being converted into Ca^{2+} and HCO_3^- during mineral weathering process as proven in the Hydrochemical analysis (Appendix A-2). (Appelo and Postma, 1993) indicated that for a given initial

Pco_2, the amount of HCO_3 in solution would be higher in the case of open system dissolution than in closed system dissolution.

The Lake Naivasha (LK001) is supersaturated with respect to Calcite, Dolomite, Talc and Aragonite but subsaturated with Chalcedony, Quartz, Gypsum and Anhydrite. The final well C567 is subsaturated in all the minerals and OW-26 water is supersaturated with all minerals except Anhydrite and Gypsum.

Ojiambo (1992) indicated that the geothermal waters are oversaturated with respect to quartz, chalcedony and cristobolite based on saturation indices from WATEQ4F. The loss of calcium in the shallow wells C567 and C562 near the geothermal field might be due to the precipitation of calcite ($CaCO_3$), which reduces the calcium concentration in these waters.

In summary, shallow well C567 might be undergoing open system dissolution whiles deep geothermal well OW-26 might be undergoing closed system dissolution.

Chemical reactions

- Considering the evolution of a Na-Ca-HCO_3 water at LK001 to Na-Cl water at OW-26 along flow path 1, the possible chemical reaction that accounts for the change in chemistry is given as:

Na-Ca-HCO_3 water + 14.2Albite+3.2K-Montmorrilonite-40SiO_2-0.09Exchange

=Na-Cl water

- Likewise for Na-Ca-HCO_3 water at LKOO1 to Na-HCO_3 water at C567 along flow path 2 (figure 45), chemical reaction that accounts for the change in chemistry is given as:

Na-Ca-HCO_3 water +7.3Albite-0.03Exchange-0.29Illite-5.84Na-Montmorrilonite

=Na-HCO_3 water

where the numbers are mass transfer in mmol/kg water.

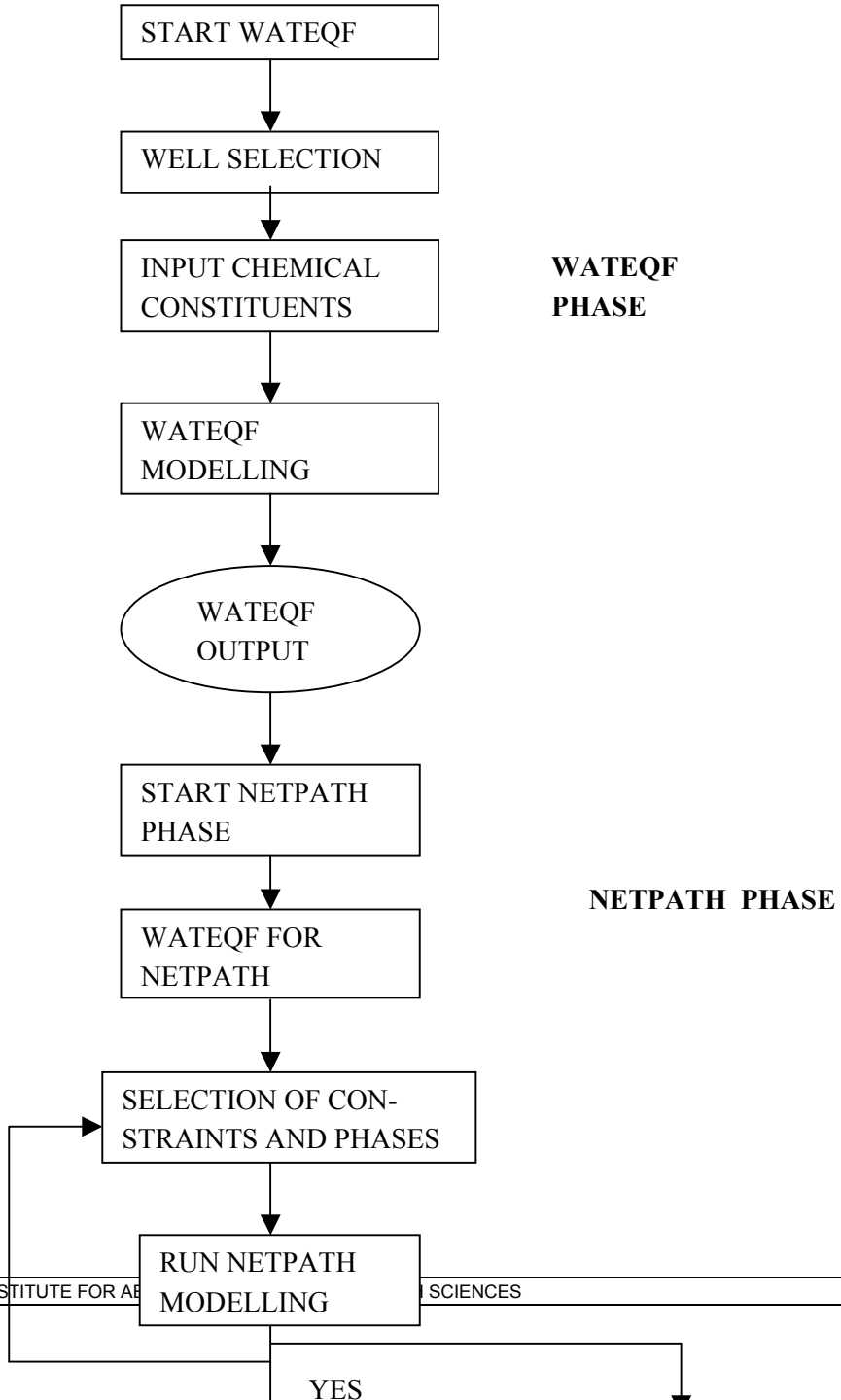
START WATEQF
WELL SELECTION
INPUT CHEMICAL CONSTITUENTS
WATEQF MODELLING
WATEQF OUTPUT
START NETPATH PHASE
WATEQF FOR NETPATH
SELECTION OF CON-STRAINTS AND PHASES
RUN NETPATH MODELLING
YES
WATEQF PHASE
NETPATH PHASE

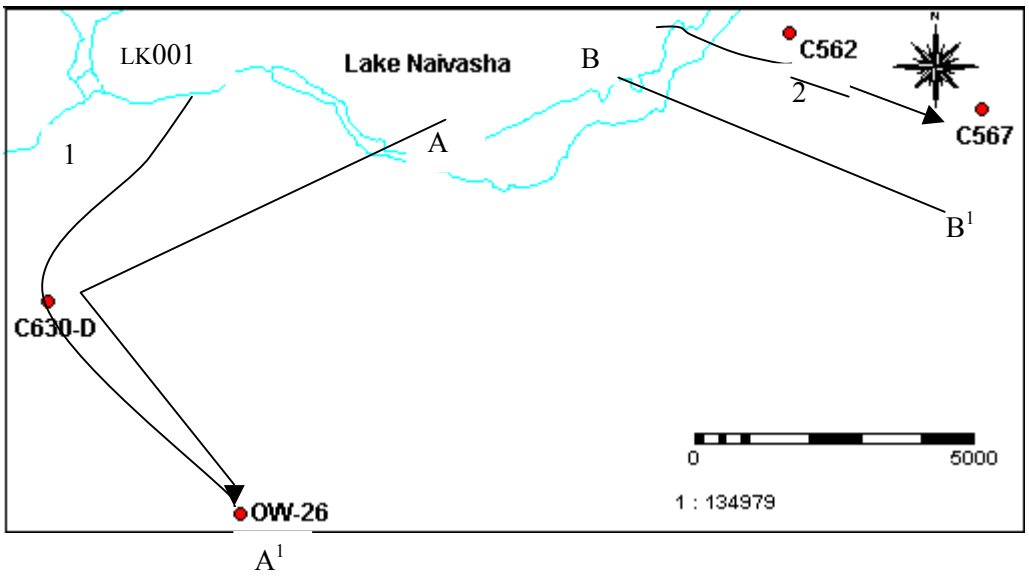

Figure 46: Map showing the proposed flow directions (mixing waters) in wells C562, C567, C630-D, OW-26 and Lake Naivasha.

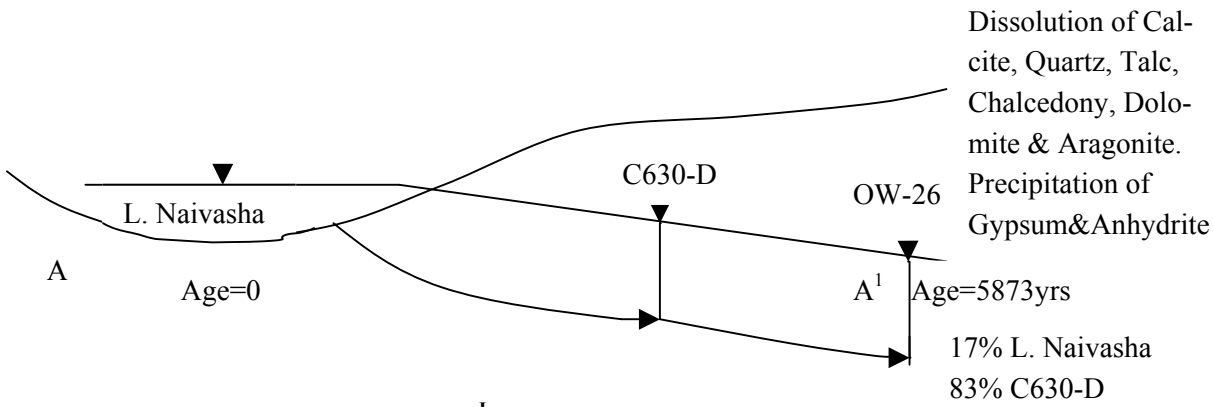

Figure 47: Sketch of Cross section (A-A^{I}) along proposed flow path 1.

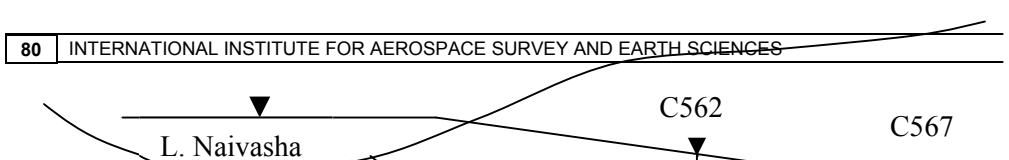

Figure 48: Sketch of cross section (B-B^{I}) along proposed flow path 2.

Sample ID.	Location	P_{CO2} atm.	Log P_{CO2}	^{14}C age 1 (yr.)	$^{14}C_2$ age 2 (yr.)
LK 001	Lake Naivasha	$7.87*10^{-5}$	-4.1	modern	modern
C562	Lake-shore	$2.38*10^{-2}$	-1.62	modern	modern
C567	Kedong ranch	$2.82*10^{-3}$	-2.5	>27	>2383
C630-D	Oserian farm	$1.67*10^{-2}$	-3.7	>40	>40
OW-26	Olkaria field	$1.67*10^{-4}$	-1.7	>8806	>5873

Table 12: P_{CO2} (atm) and Ages (yr.) of Groundwater and Lake Naivasha in the study area.

Sample	Talc	Arago-nite	Anhy-drite	Dolo-mite	Chal-cedony	Quartz	Calcite	Gypsum
LK 001	2.000	0.918	-5.061	2.231	-1.736	-1.310	1.061	-4.845
C562	-0.777	-0.500	-3.545	-0.729	0.687	1.124	-0.355	-3.315
C567		-0.314	-3.487	-0.465			-0.167	-3.251
OW-26	16.870	0.767	-3.459	1.348	0.718	0.973	0.871	-3.854
C630-D	-0.656	-1.474	-4.161	-2.581	0.671	1.044	-1.343	-4.048

Table 13: Saturation indices of various phases (From WATEQF).

7.6 RESULTS AND DISCUSSIONS OF MIXING MODEL(NO RAYLEIGH DISTILLATION)

The NETPATH program (Plummer et al., 1991) was used to model the possible evolution or mixing waters to determine whether the flow directions proposed are plausible. At this stage, it was assumed that there is no change in composition of compound during transition from one state to the other (No Rayleigh distillation). The mixing modelling was performed with waters from wells C562, C567,

C630-D and OW-26 along two possible outflows from the Lake Naivasha into the groundwater flow systems based on piezometric map (figure 3.1).

One mixing model was obtained from the mixing of Lake Naivasha and water from well C630-D to form water in well OW-26 water (Appendix D1). The model shows dissolution of albite and K Montmorillonite and precipitation of silica and exchange.

From the mixing model, final well OW-26 water can be said to be a mixture of 17% of LKOO1 (L. Naivasha) and 83% of well C630-D water and is dissolving 14.3mg/l and 3.22mg/l of albite and K-Montmorillonite respectively. Likewise, there is precipitation of 40.24mg/l and 0.09mg/l of silicate and ion exchange respectively (Appendix D1).

In the mixing of Lake Naivasha and well C562 waters to form well C567 waters, three mixing models were found at different phases (Appendix D2). The model 1 shows that water could evolve from precipitation of exchange, clay minerals Illite and Na- Montmorillonite and dissolution of Albite.

In model 2, the water could evolve from Illite precipitation and dissolution of albite, exchange and calcite. The model 3 is similar to model 2, except that there is dissolution of gypsum in addition. The three models in terms of the mixing proportion of initial waters show the final well C567 water is made up of 62% of Lake Naivasha (LKOO1) and 38% of water from well C562.

Clarke et al (1990), indicated that the general increase in TDS content across the eastern wellfield from north to south support the regional model of southerly flow from Lake Naivasha deduced from isotopic evidence. He attributed this to the long residence time for reactions with underlying bedrock materials.

Phase						
ALBITE	Na 1.0000	Al 1.0000	Si 3.0000			
K-MONT	K 0.3300	Al 2.3300	Si 3.6700			
SiO2	Si 1.0000					
EXCHANGE	Ca -1.0000	Na 2.0000	Mg 0.0000			
DOLOMITE	Ca 1.0000	Mg 1.0000	C 2.0000	RS 8.0000	I1 0.0000	I2 0.0000
ILLITE	K 0.6000	Mg 0.2500	Al 2.3000	Si 3.5000		

Table 14: **NETPATH phases of mixing model of well C630-D and Lake Naivasha to well OW-26.**

Phase						
ALBITE	Na 1.0000	Al 1.0000	Si 3.0000			
EX-CHANGE	Ca –1.0000	Na 2.0000	Mg 0.0000			
DOLOMITE	Ca 1.0000	Mg 1.0000	C 2.0000	RS 8.0000	I1 0.0000	I2 0.0000
ILLITE	K 0.6000	Mg 0.2500	Al 2.3000	Si 3.5000		
Na-MONT	Na 0.3300	Al 2.3300	Si 3.0000			

K-MICA	K 0.3300	Al 3.0000	Si 3.0000			
CALCITE	Ca 1.0000	C 1.0000	RS 4.0000	I1 0.0000	I2 0.0000	
SiO2	Si 1.0000					
GYPSUM	Ca 1.0000	S 1.0000	RS 6.0000	I3 22.0000		

Table 15: NETPATH phases of mixing model of well C562 and Lake Naivasha to well C567.

7.7 MODELLED AGES (RADIOCARBON DATING) ALONG FLOW PATHS

7.7.1 INTRODUCTION

The model is based on carbon and isotopic mass balance equations, including isotopic fractionation between the various dissolved carbon species (equations 7.1 and 7.2). The ^{14}C activity of dissolved carbonate in groundwater is a function of the age of the water, the initial activity and the effect of interaction with the aquifer matrix.

In modelling the ages of groundwater, δ^{13} value in carbonate minerals were assigned –5‰ and C-13 in soil gas CO_2 –26‰ (Darling 1990). The C-14 activity in carbonate minerals was taken as 0‰ and C-14 content of soil CO_2 was taken as 95pmC since most of samples have tritium values less than 3.1 TU and $\delta^{13}C$ in initial solution were assigned –0.4‰.

Mean Residence Time (age)

Mook (2000) gave the mean residence time in confined aquifer according to the formula:

$$T_c = 8270 \quad \ln\left(\frac{^{14}C_i}{^{14}C_0}\right) \qquad 7.4$$

Beekman (1995) used the formula for residence time (Gieske, 1995; Vogel, 1970) in an unconfined aquifer defined as:

$$T_{uc} = 8270 \ln\left(^{14}C_i \big/ {}^{14}C_o - 1\right) \qquad 7.5$$

where $^{14}C_i$ is the initial ^{14}C activity (pMC) and $^{14}C_o$ is the observed ^{14}C activity of groundwater.

7.7.2 ANALYTICAL RESULTS AND DISCUSSIONS

7.7.2.1 MODELLED ^{14}C ACTIVITY

There is significant variation in ^{14}C activity between the original values and the modelled values for well OW-26. From the initial ^{14}C activity and carbon –13 value of groundwater taken 0.4‰ and 84.6pMC,

average modelled values of carbon-13 and C-14 obtained as 4.298‰ and 143.547 pMC respectively, based Mook fractionation method incorporated in NETPATH (Plummer et al., 1991) modelling with Rayleigh distillation of isotopic parameters.

7.7.2.2 MODELLED AGES

The modelled age of the water (residence time) at OW-26 in models 1 and 2 are 8806 and 5873 years respectively. The equivalent modelled ages calculated from mass balance are 9919 years and 6985 years from models 1 and 2 respectively. The modelled age of groundwater (travel time) in the final well C567 (close to Kedong ranch) from models 1 and 2 are 27 years and 2383 years respectively.

The negative values (model 1) obtained as modelled ages of well C567 from other models (Tamers and mass balance) might be result of charge imbalance or might be due to assumptions made on the initial parameters as well as analytical errors in the chemical analysis for the dissolved species. The mass balance reaction models combine positive and negative charges in water analysis to compute masses of unchanged phases. NETPATH model also assumes that a single value of the additive fractionation factor (relative to the solution) applies over the entire length of the flow path (Plummer and Others, 1991). (Plummer and Others 1991) indicated that, Rayleigh distillation equation to mass balance results in isotopic evolution problems due to uncertainties in isotopic and compositional data of the selected phases.

The modelled ages are in conformity seem to be realistic as all the processes believed to be taken place in the aquifers have been incorporated into the modelling. The summarised modelled ages and other values from various models are given in Tables 18 and 19.

Phase						
SiO2	Si 1.0000					
EXCHANGE	Ca -1.0000	Na 2.0000	Mg 0.0000			
BIOTITE	Al 1.0000	Mg 1.5000	K 1.0000	Si 3.0000	Fe 1.5000	RS 3.0000
CALCITE	Ca 1.0000	C 1.0000	RS 4.0000	I1 0.0000	I2 0.0000	
DOLOMITE	Ca 1.0000	Mg 1.0000	C 2.0000	RS 8.0000	I1 0.0000	I2 0.0000
ILLITE	K 0.6000	Mg 0.2500	Al 2.3000	SI 3.5000		

Table 16: NETPATH phases in mixing model of well C630-D and Lake Naivasha to well OW-26.

Model (for initial A0)	**Age(final)yr.Model 1**	**Age(final) yr. Model 2**
Original Data	8806	5873
Mass Balance	9919	6985
Vogel	8806	5873
Tamers	4547	1614
User-defined	10150	7217

Table 17: Modelled ages (travel time) of groundwater to final well OW-26 (Models 1 and 2).

Model (for initial A0)	Age (final) yr. Model 1	Age (final) yr. Model 2
Original Data	27	2383
Mass Balance	476*	1880
Vogel	39	2395
Tamers	3710*	1354*
User-defined	1382	3739

Table 18: Modelled ages (travel time) of groundwater to final well C567 (Models 1 and 2).

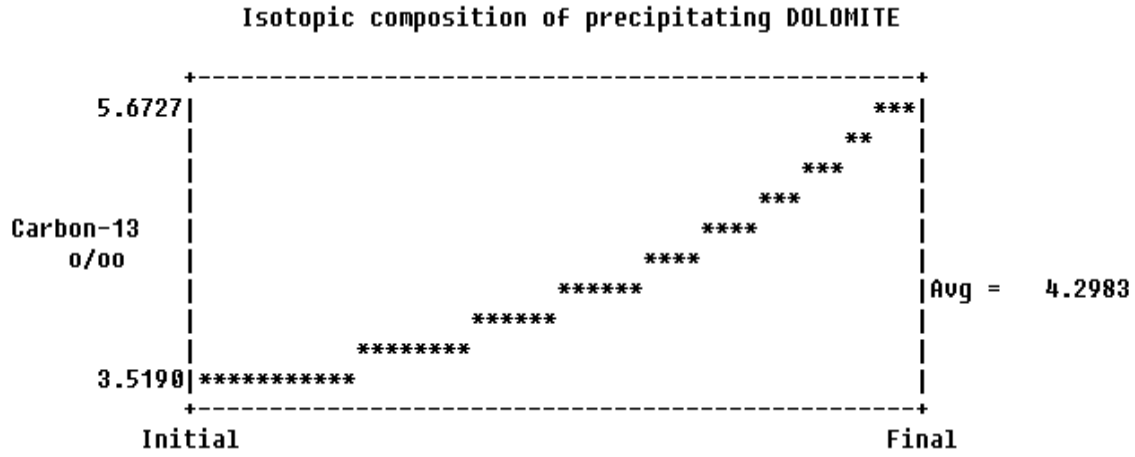

Figure 49: Isotopic composition of precipitating DOLOMITE from model 1 (C-13 data).

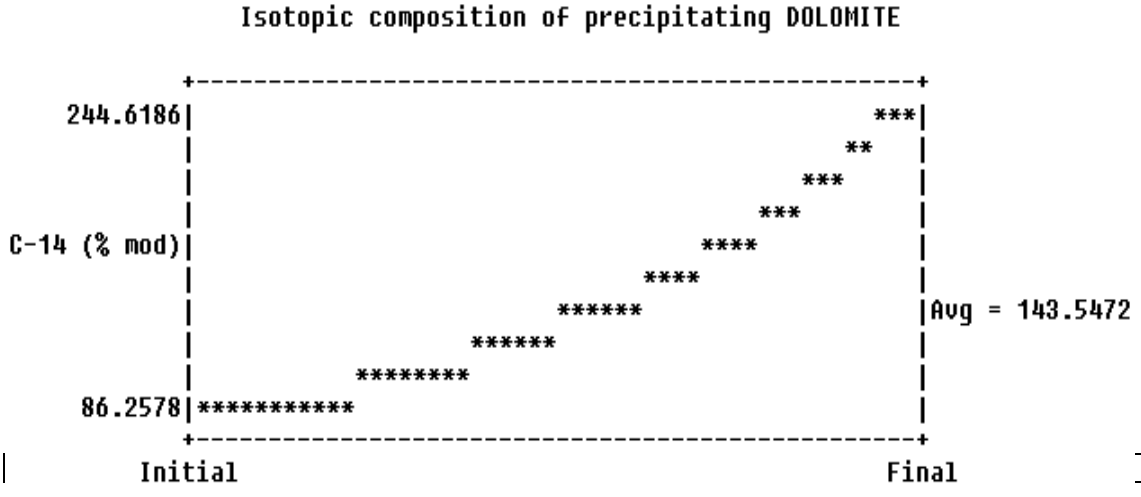

Figure 50: **Isotopic composition of precipitating DOLOMITE from model 1(C-14 data).**

7.8 CONCLUSION ON NETPATH HYDRODYNAMIC MODELLING

The speciation and saturation index computations have revealed that the Lake Naivasha and OW-26 waters are saturated with respect to calcite whiles other waters are undersaturated with respect to calcite in the study area.

NETPATH modelling have shown that water from the shallow well C567 in south-east and OW-26 in the south of the Lake Naivasha have evolved from a mixture of Lake Naivasha and recharge. The travel time (age) of 8806 years of water from Lake Naivasha and well C630-D to the final well OW-26 suggests that groundwater have over travelled a long distance or have been recharge from old water. A rough estimate of the flow velocity based on outflow rate ($24*10^6 m^3/yr$) at outflow zone of width 10km, thickness 25m and effective porosity of 20% gives flow velocity range of 142- 240m/yr.

The old age of the water in the well OW-26 suggests therefore that this water is not passing the analysed wells. Thus, either the bulk of the water is not flowing through the Olkaria area. It might also be that the water follows preferential flow path through faults and the analysed wells are situated in rather stagnant areas. The areas close to the Olkaria field are known to have numerous faults and stratigraphic seals, which at times form hydraulic barriers that reduce or inhibit zones of enhanced permeability.

The mixing model shows that water in final well OW-26 is made up of 17% Lake Naivasha and 83% of C630-D waters. The water in well OW-26 evolves from a mixture of Young Lake water and old water in well C630-D and suggests that well OW-26 might be recharged from old groundwater and the Lake Naivasha.

The mixing model shows that water in C567 is made up of 62% of Lake Naivasha water and 17% of groundwater from well C562. The value 27 –2383 years obtained along flow path 2 from Lake Naivasha and well C562 into well C567 suggest short distance of travel of groundwater into the later well C567. This suggests water in well C567 could evolve from a mixture of young lake water and quiet old groundwater in well C562. The relatively low age observed for C567 samples suggest a young local recharge source of water and the groundwater flow is not restricted much by fault or any stratigraphic seal as it is in the case of Olkaria well OW-26.

The long residence time for reaction of groundwater with underlying aquifers materials from the shallow wells to the geothermal field might be the cause of changes in groundwater chemistry from predominant Na-HCO3 and Ca-Na-HCO3 into Na-Cl water types. These Na-HCO3 and Na-Cl waters could therefore evolve from different bedrock aquifers, as the geology is diverse in the study area. They may therefore really not be evolutionary but independently formed during and after the recharge process.

The mixing models have demonstrated the shallow and deep wells further south to Olkaria fields are made up of some amount of the sub-surface outflow of the Lake Naivasha. The two proposed flow paths are plausible and support the assertion that the shallow wells in the south receive significant amount of recharge from the Lake Naivasha and the remaining probably from the flanks of the basin in the form of infiltrating direct recharge. The greater part of the Lake outflow (62%) ends up in well C567 around Longonot and Kedong farms. In the case of Olkaria fields, OW-26 receives it waters probably from the rift flanks as it contains small percentage (17%) of Lake Naivasha water.

The negative values shown by asterisks (*) of modelled ages of well C567 from Tamer and mass balance models might be due to different initial ^{14}C values used in the two models and assumptions in

each model incorporated into NETPATH program. (Plummer and Others, 1991) indicated that 'Tamers model' is similar to the 'mass balance' model except that 'mass balance' is performed only on carbonates assuming reaction of pure water with calcite, dolomite, gypsum and CO_2 gas on the initial water composition. Another possibility might be from errors in measured/input parameters, which result in ionic imbalance or the flow might also not be plausible for the proposed flow path 2 into well C567.

7.8.1 FINAL CONCLUSION ON SAFE DISTANCE OF WELL

In conclusion, the use of groundwater for irrigation from the southern well will not affect the Lake level significantly if the rate of abstraction does not exceed the subsurface outflow calculated as $55.2*10^6 m^3$/month (Mmbui, 1998). Likewise the drop in the level of Lake Naivasha might not have been caused by development activities in the south of the Lake and therefore calls for potential use of groundwater in the south of the Lake for Irrigation.

However, if a specified amount say 5 m^3/sec south of the Lake is pumped, it does not necessarily mean that the natural outflow is 5 m^3/sec but might be less before exploration.

Considering, rough calculation of say a distance 500meters from the Lake Naivasha, using the minimum and maximum Darcian velocities of flow of 142 and 240m/yr gives possible time frame of about 5 years and 1year respectively at which abstraction effect is manifested on the Lake level. Thus, on average 3 years after abstraction of groundwater from the shallow wells.

This presupposes that at an adequately far distance from the Lakeshore, the effect of groundwater abstraction on the Lake level will be negligible if the outflow is tapped for agricultural activities.

Therefore, the 'safe distance' from the Lake Naivasha is needed to capture the natural outflow. How far this distance, needs to be calculated using MODFLOW.

CHAPTER 8

8 CONCLUSION AND RECOMMENDATIONS

8.1 CONCLUSION

The development and management of groundwater require the understanding and identification of the quality of groundwater and sources of recharge of the groundwater flow system.

The hydrogeological investigations have demonstrated that areas south of the Lake Naivasha are in the subsurface outflow from the Lake. The hydrogeological profiles through the underlying aquifers show the static water levels in the southern wells Sulmac, Kedong C210 and geothermal wells are below the Lake level. The cross sections have shown that an outflow from the Lake Naivasha spans into Sher, Kedong C210 and Sulmac farms. The section into geothermal well C630-D supports the assertion that there is a subsurface flow into the shallow wells and deep geothermal well with a flux of $4.6*10^6 m^3$/month (Mmbui, 1998).

The hydrogeological cross-sections into Ndabibi area shown that the Moi Ndabi 1 and Ngodi wells are recharging the Lake Naivasha. The areal recharge based on residence time of travel of groundwater was computed to be about 1.76mm/yr, representing 3.5% of direct recharge in the form of infiltration water into the aquifers.

The assessment of geohydrology indicates a strong influence of underlying bedrock materials and their weathered products as well as infiltration from precipitation on the chemistry of water in the area. Hydrochemical characterisation shows that the shallow groundwater is made up of predominantly NaHCO3 and the deep geothermal NaCl type of water, which reflects the diversity of bedrock types and products of weathering.

The salinity and sodicity hazards are moderated to high in most of the shallow groundwater and the water ranges from good to moderate for irrigation. This deteriorates towards the geothermal well with higher salinity and sodicity hazards above the maximum permissible limit, which might be associated from precipitation of calcite ($CaCO_3$). This renders the groundwater in these wells unsuitable for irrigation. This phenomenon is observed well C630-D and perhaps wells beyond. These waters will demand treatment and improvement of the stature of soil and these have to be evaluated for the high economic percussion.

Stable and radioactive isotopes have been used to investigate the extent of mixing of waters and the flow direction of the groundwater system in the study area. The tritium concentrations in groundwater south of the Lake are below the detection limit of 1.5TU, which indicates the waters in the area quite old. The stable isotopes of Oxygen-18 and Deuterium of water samples indicate similar isotopic signatures between the Lake Naivasha and the groundwater. The $\delta^{18}O$-δD plots have shown that the southern groundwater is made up a mixture of recharge waters from the flanks and Lake Naivasha.

The Sulmac and Kedong C210 have similar isotopic signatures as the Lake Naivasha. They are quite young waters (about 1000years) indicating they might be recharged from the Lake or mixture with quite old groundwater. However, 3-point farm BHM did not show resemblance in isotopic composition to that of the Lake Naivasha. It is quite old water (about 3000years) which signifies that it consists of old groundwater or mixture of modern direct recharge and old groundwater.

The NETPATH mixing and age modelling have proven that waters in southern wells and the Olkaria wells in the study area are evolved from mixture of Lake Water and old groundwater possibly from the eastern and western flanks of the basin. The modelled ages from 8807 years to modern (27 years)

indicate modern recharge to the shallow groundwater and old recharge (long residence time) in the deep geothermal wells.

8.2 RECOMMENDATIONS

- The report has shown that there is subsurface outflow from the Lake Naivasha, which could be tapped for groundwater development. Therefore, a 'safe distance' from the Lake is needed to capture natural outflow at a specified distance. It is therefore recommended that this distance be determined using MODFLOW in future M.Sc work.
- The result of C-14 isotopic analysis was received very late from the Centrum voor IsotopenOnderzoek, Royal University of Groningen and was not used in NETPATH modelling. These new results should be incorporated in future research work, especially in NETPATH hydrodynamic modelling. This will help in knowing the spatial variations in the ages of groundwater in the study area.
- The present state of the chemical composition of the soils in Sulmac, Oserian and farms in the south of the Lake was not finalised and it recommended that it is used to re-evaluate the Exchangeable sodium ratio (ESR) and sodium absorption ratio (SAR) of the soils in subsequent studies.
- Efforts should be made to carry out standard aquifer test pumping with observation wells in the southern wells to really come out with more realistic aquifer properties that control the groundwater flow system and the hydraulic links between the shallow and deep groundwater in the study area.

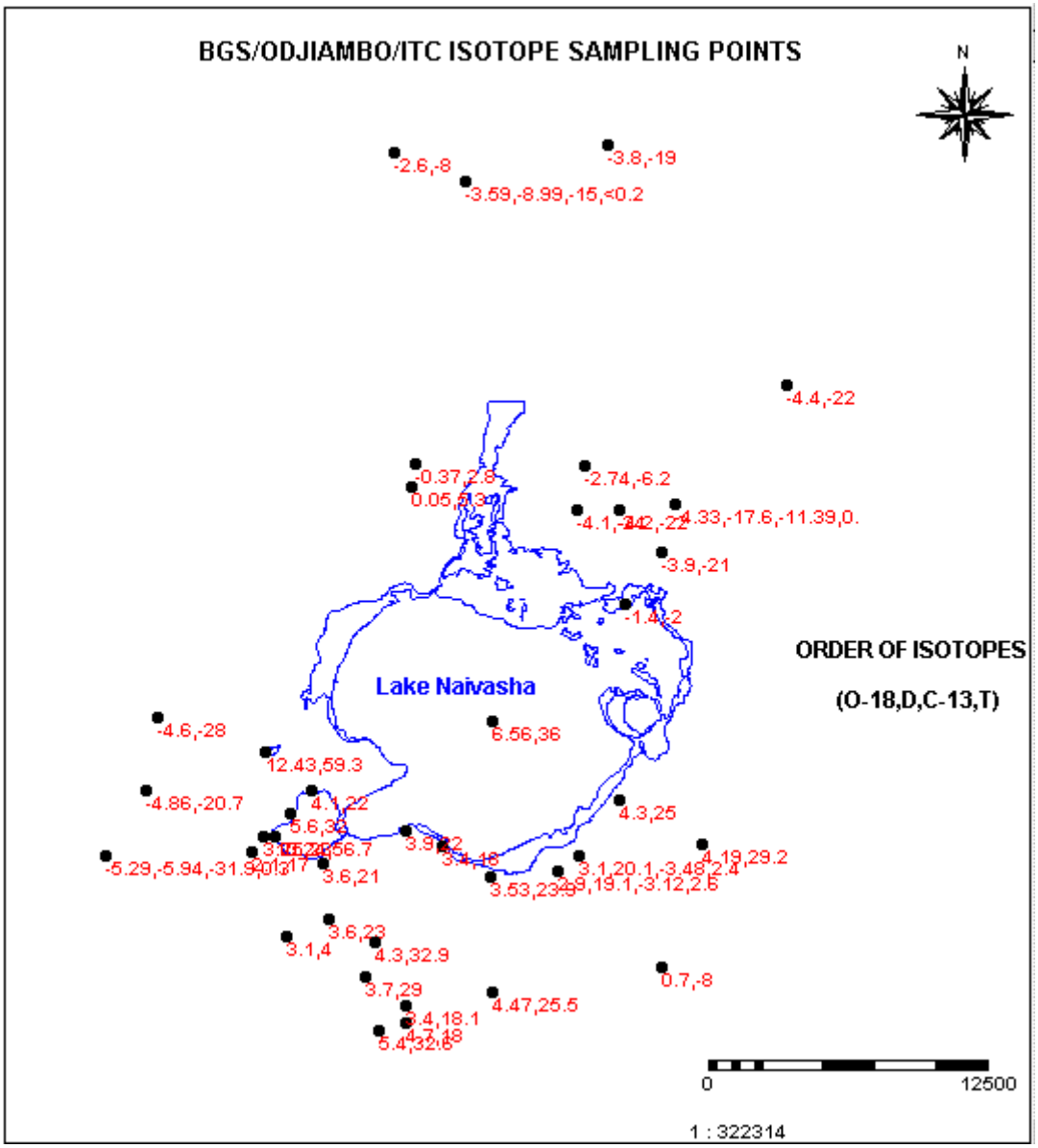

Appendix F: Compiled isotope sampling points by (BGS 1990/OJIAMBO 1992/96 AND ITC 2000) in the study area.